ENHANCING BIOCHEMICAL, STRUCTURAL, MECHANICAL PROPERTIES OF TISSUE-ENGINEERED MENISCI AND ENTHESES USING BIOCHEMICAL AND BIOMECHANICAL STIMULI

A Dissertation

Presented to the Faculty of the Graduate School

of Cornell University

In Partial Fulfillment of the Requirements for the Degree of

Doctor of Philosophy

by

Jongkil Kim

August 2022

ENHANCING BIOCHEMICAL, STRUCTURAL, MECHANICAL PROPERTIES OF TISSUE-ENGINEERED MENISCI AND ENTHESES USING BIOCHEMICAL AND BIOMECHANICAL STIMULI

Jongkil Kim, Ph. D.

Cornell University 2022

Menisci exist between the femoral condyle and tibial plateau in the knee joint and play important roles, such as load transmission, shock absorption, lubrication, and stability of the knee joint. Soft tissue-to-bone regions of menisci, called entheses, are necessary for the functions of the menisci. Menisci and entheses have distinct gradients in cell phenotypes, vascularity, collagen fiber organization, and mineral contents. The physiological functions of menisci are attributed to these gradients. Meniscal injuries are one of the most common causes for the knee surgeries in the United States and often result in osteoarthritis. Treatment options for meniscal injuries are limited, especially for tears in the avascular region of the meniscus. Currently, meniscus allograft transplantation is the sole option after total meniscectomy. Thus, there has been a great amount of attention towards tissue-engineered menisci. Thus, the overall goal of this study is to develop tissue-engineered menisci with native tissue-like gradients to enhance the mechanics.

Collagen is the major extracellular matrix molecule of the meniscus and thus has been widely used a scaffold material due to its excellent biocompatibility. However, weak mechanical properties of collagen-based scaffolds have been considered as a critical limitation for clinical use. Furthermore, many previous studies mostly focus on

the main body of menisci, and thus meniscal entheses are often overlooked in the design of tissue-engineered menisci. Recapitulating gradients in meniscal entheses still remains challenging.

In order to create a tissue-engineered meniscus with desired features, it is important to understand the structure and functions of native meniscus and previous tissue-engineering approaches (Chapter 1). Collagen fiber structure of native menisci gives rise to mechanical properties of native tissue. Moreover, the enhancement of collagen fiber organization in collagen-based scaffolds has shown to increase mechanical properties of the scaffolds. Glucose and transforming growth factor-β1 affect collagen fiber structure of collagen-based scaffolds; however, their combinational effects have not yet been studied. Thus, the effects of glucose and transforming growth factor-β1 in the presence of mechanical anchoring on collagen fiber structure and mechanical properties of tissue-engineered were investigated (Chapter 2). The incorporation of meniscal entheses into the design of tissue-engineered menisci needs to be taken into account to generate a full-sized replacement. Before combining these two components, creation of a functional tissue-engineered enthesis should be addressed. Therefore, recapitulating native enthesis-like collagen fiber structure with mineral gradients was investigated (Chapter 3). Collagen gel properties are dependent on fabrication parameters including gelation pH. Gelation pH has been studied with regard to initial properties of collagen gel, often without cells. The short- and long-term effects of gelation pH on fibrochondrocyte-seeded tissue-engineered menisci were evaluated (Chapter 4).

In conclusion, this dissertation demonstrates that native collagen fiber structure

of a meniscal body can be recapitulated within tissue-engineered meniscal constructs by regulating glucose media concentration, transforming growth factor-β1 media concentration, and mechanical boundary conditions (Chapter 2). Further, this strategy can also be utilized to mimic bio-compositional and mechanical gradients, seen in native tissue, within tissue-engineered enthesis constructs (Chapter 3). Lastly, this thesis work also shows that gelation pH significantly influences cellular metabolic activity, collagen fiber structure, and mechanical properties of collagen-based constructs in both short- and long-terms (Chapter 4).

BIOGRAPHICAL SKETCH

Jongkil Kim was born and grew up in South Korea. He attended Hanyang University, where he graduated *Summa Cum Laude* with a Bachelor of Science degree in Bioengineering in 2013. During his undergraduate career, he also served as a combat medic for 21 months from 2008 to 2010 in the Republic of Korea Army.

At the beginning of his senior year, Jongkil began his academic research career with Dr. Sang-Kyung Lee at Hanyang University. He worked on purification of a single chain antibody targeting the pan-T cell receptor and synthesis of nanoparticles encapsulating anti-cancer reagents for cancer therapy, which got him interested in a graduate degree. In the spring of 2013, he began his master's program at Hanyang University where he participated in a variety of projects, ranging from synthesizing nanoparticles for cancer therapy to developing gene delivery vehicles for siRNA and DNA.

In the fall of 2016, Jongkil went on to pursue a doctoral degree in Biomedical Engineering at Cornell University. He joined the laboratory of Dr. Lawrence Bonassar to expand his research career in the field of tissue engineering, particularly tissue engineering functional menisci and entheses. He spent the summer of 2017 shadowing Dr. John G. Kennedy at the Hospital for Special Surgery (HSS) as a part of Biomedical Engineering Clinical Immersion Program. Jongkil was awarded the Kwanjeong Educational Foundation Scholarship which supported him for his master's and doctoral degrees.

Jongkil is excited to begin a postdoctoral research fellow at Harvard Medical School under Dr. Andrew Lassar.

This dissertation is dedicated to my loving family and friends who always support me.

ACKNOWLEDGMENTS

I would first like to thank my advisor, Dr. Lawrence Bonassar, for the continuous support throughout my time at Cornell. I would also like to thank Drs. Lara Estroff and Lisa Fortier for their excellent guidance and expertise as my special committee and Drs. John G. Kennedy and Jason Spector for providing me with an unforgettable clinical perspective during my immersion term and in my academic work.

I would like to thank all the past and current members of the Bonassar group including Mary Clare McCorry, Jorge Mojica Santiago, Ben Cohen, Chris DiDomenico, Alex Boys, Jill Middendorf, Nicole Diamantides, Sierra Cook, Stephen Sloan, Liz Feeney, Rebecca Irwin, Marianne Lintz, Steven Ayala, Rachel Yerden, Sean Kim, Leigh Slyker, Karan Vishwanath, Sera Lopez, Eric Yoon, Caroline Thompson, Alikhan Fidai, and Alicia Matavosian for their insights and being not only my great colleagues but also friends. I would like to specially thank all the past and current members of Team Meniscus again including Hao Zhou, Tianyu Gao, Leyin Zheng, Roland Babmatee, and Sohum Kulkarni. Beyond the Bonassar lab, I want to thank Adrian Shimpi, Patrick Muljadi, Carolyn Chlebek, Matt Tan, Jason Chang, Alexandre Cheng, Moni Chatterjee, Regan Stephenson, Zhexun Sun, and many others for supporting me and being great classmates. I also want to express special thanks to Chi Yong Eom, Sung Ji Ahn, and Jiahn Choi for giving me great advice and help as senior BME people.

I also want to acknowledge my other friends outside of Weill Hall, especially my soulmates in Korea, for their encouragement and always having incredible time together. We do not get to see each other as often as we used to, but I never feel we drift apart. I really thank you all for making every vacation full of fun.

Lastly, I would like to thank my world best parents, Jumsook Moon and Gyeonghwan Kim, for their unconditional love and sacrifice. My brother, Jongam Kim, who always is supportive and a friend, which I cannot thank enough for. I especially thank my wife, Woori Bae, for always being by my side. I am very excited for our next chapters.

Funding for this work was provided by NIH, NYSTAR, and the Kwanjeong Educational Foundation.

TABLE OF CONTENTS

LIST OF FIGURES

LIST OF TABLES

LIST OF ABBREVIATIONS

AI - alignment index

ANOVA - analysis of variance

BMP - bone morphogenetic proteins

CMI - collagen meniscus implant

CTGF - connective tissue growth factor

DMEM - Dulbecco's modified Eagle's medium

DMMB - dimethylmethylene blue

DNA - deoxyribonucleic acid

DTAF - dichlorotriazinyl aminofluorescein

DW - dry weight

EC - effective concentration

ECM - extracellular matrix

EDTA - ethylenediaminetetraacetic acid

EGF - epithelial growth factor

FBS - fetal bovine serum

FFT - fast Fourier transforms

GAG - glycosaminoglycan

HEPES - hydroxyethyl piperazineethanesulfonic acid

HSD - Tukey's Honestly Significant Difference

Hypro - hydroxyproline

IGF - insulin-like growth factor

IL - interleukin

MMP – matrix metalloproteinase

MSC - mesenchymal stem cell

PBS - phosphate buffered saline

PCL - poly (ε-caprolactone)

PDGF - platelet-derived growth factor

PLGA - poly(lactic-co-glycolic acid)

PU - polyurethane

SDS - sodium dodecyl sulfate

SEM - scanning electron microscopy

SHG - second harmonic generation

SMA – smooth muscle actin

TGF - transforming growth factor

TIMPS - inhibitors of metalloproteases

UTS - ultimate tensile stress

CHAPTER 1

INTRODUCTION

Menisci are crescent-shaped fibrocartilaginous tissues that are triangular on cross section and found in the knee joint between the femoral condyle and tibia plateau[1]. Menisci are anchored to the underlying subchondral bone via soft-to-hard interfaces, called meniscal entheses[2]. Menisci have gained much attention due to their important roles in the knee joint, although they were once considered as a vestigial, functionless tissue. Menisci cover most of the articular surface of the tibial plateau and play a role in load transmission, shock absorption, lubrication, nutrition, and stability of the knee joint[3]. Menisci are composed mainly of water, collagen, and glycosaminoglycans (GAGs)[4]. Type I collagen is the major component of the outer region of the meniscus while type II collagen is predominant in the inner region of the meniscus. Circumferentially aligned collagen fibers tied with radial collagen fibers are responsible for transferring applied axial forces in the knee joint into hoop stresses, further transmitted to the tibial plateau. Negatively charged GAGs attract water molecules, giving rise to compressive resistance of the meniscus. Menisci also have a variation in cell phenotypes, ranging from rounded cells to oval-like cells, depending on the regions[3,4]. Meniscal entheses significantly contribute to the physiological functions of the meniscus, particularly load transmission[2,5]. Native entheses also have variations, such as cell phenotypes, collagen fiber orientation, mineral gradients[6,7]. The enthesis can be classified into four distinct regions, which are ligamentous region, uncalcified fibrocartilage region, calcified fibrocartilage region, and bone. The ligamentous region

is composed of ligament-like aligned type I collagen fibers with fibroblast-like cells and connected to the uncalcified fibrocartilage region. The uncalcified fibrocartilage region contains unaligned types I and II collagen fibers and proteoglycans with fibrochondrocytes, which is separated by tidemark from the calcified fibrocartilage region. The calcified fibrocartilage region consists of types II and X collagen and hypertrophic fibrochondrocytes, further transitioning into bone mainly composed of mineralized type I collagen with osteoblasts, osteoclasts, and osteocytes.

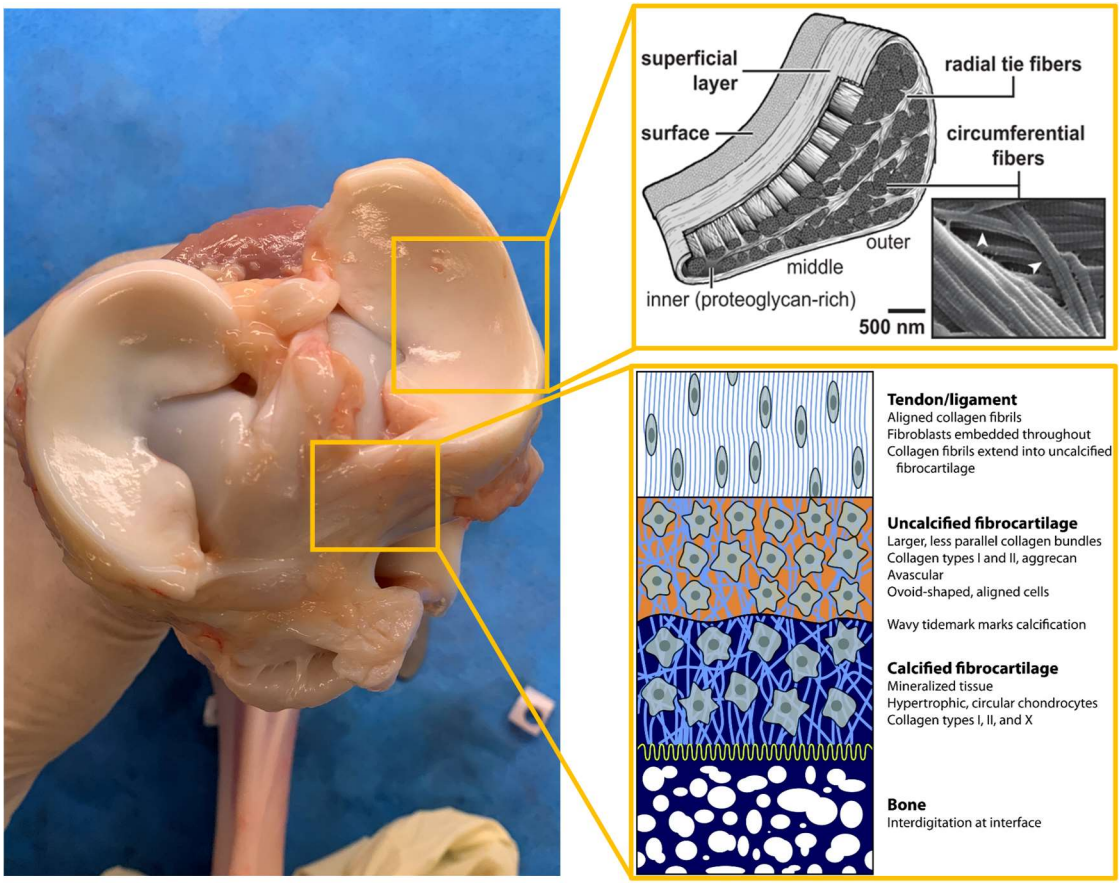

Figure 1.1. Photograph of native bovine menisci (left). Native collagen fiber structure in a meniscal body (upper right)[8]. Native cellular and compositional gradients found in an enthesis (bottom right)[9].

Meniscus Injuries and Treatment Options

Injuries to menisci are one of the most common causes of orthopedic surgeries in the United States[10]. As menisci are critical for increasing contact area and reducing contact stresses in the knee joint, meniscal injuries are strongly correlated with the development of osteoarthritis[1,3]. Additionally, meniscus root tears have shown to be closely associated with meniscus extrusion and thus increase contact stresses of the knee joint surfaces, leading to articular cartilage degeneration[11]. Treatment options for meniscal injuries including enthesis tears can vary depending on the location and pattern of tears. Due to the limited healing capacity resulting from the lack of vascularity, surgical interventions, such as partial or total meniscectomy, are often performed. As many studies have shown, total meniscectomy leads to the femoral condyle flattening and the joint space narrowing over time, eventually inducing osteoarthritis. Thus, allograft transplantation is usually performed following total meniscectomy to restore meniscal functions and prevent the initiation of osteoarthritis. Allograft transplantation has shown promising outcomes with good patient satisfaction and high survival rates of grafts[12,13]. However, allograft transplantation has several drawbacks, such as limited supply, graft preservation, disease transmission, anatomical mismatching, and immune rejection. As such, these drawbacks necessitate the development of tissue-engineered constructs to replace the damaged menisci after total meniscectomy.

Tissue-Engineered Menisci – Biomaterials

Tissue engineering menisci encompasses three core components, scaffold materials, biochemical and biomechanical stimuli, and cells. With regard to scaffold

materials, various biomaterials have been used to create tissue-engineered menisci. They can be classified into two types, synthetic and natural polymers. Poly(lactic-co-glycolic acid) (PLGA), polyurethane (PU), and poly (ε-caprolactone) (PCL) have been widely used as scaffold materials. In a previous study, PLGA was seeded with allogenic fibrochondrocytes and implanted in a leporine model after 1 week of in vitro culture[14]. Although regenerated neo-menisci were observed, the scaffold did not prevent cartilage degeneration. A composite of PCL and hyaluronic acid was used as an acellular scaffold to treat partial and total meniscal defects in an ovine model. This scaffold displayed great tissue ingrowth but was extruded into the joint space by graft compression[15]. Another acellular meniscal scaffold composite composed of PU and PCL, Actifit, has been clinically investigated. The Actifit implant showed excellent tissue ingrowth and integration with native tissue 3 months and 12 months after implantation[16,17]. Natural polymers, such as silk[18], cellulose[19], and collagen[20,21], have also been used to generate tissue-engineered menisci. Silks are fibrous proteins and have superior biocompatibility and biomechanical properties. Multilayered silk scaffolds were seeded with human primary fibroblasts outside and chondrocytes inside. After 4 weeks of culture, the constructs showed increases in cellularity, collagen, and GAG content[18]. Collagen has been widely used as a construct biomaterial as collagen is a major component of diverse connective tissues, including menisci, and has great biocompatibility compared to synthetic materials. Collagen-based scaffolds have shown promising results as replacement options. The collagen meniscus implant (CMI) was implanted in patients with chronic meniscal injuries. Compared to a control group, the CMI implanted group showed enhanced integration with surrounding native tissues, resulting in better

mobility and fewer reoperation rates[20].

Tissue-Engineered Menisci – Biochemical Stimuli

Native meniscus arises from dense mesenchymal condensates and further develops complex structural features with multiple series of biochemical and mechanical stimuli. This implies that biochemical, structural, and biomechanical properties of fabricated tissue-engineered constructs can be further enhanced by implementing biochemical and biomechanical stimuli to affect the development of native meniscus. Biochemical stimulation is mostly applied via growth factors, which influence anabolic and catabolic activities of fibrochondrocytes. Thus, many growth factors, such as transforming growth factor (TGF)-β superfamily or insulin-like growth factors (IGFs), have been used to enhance biochemical component production and cell proliferation. The TGF-β superfamily includes TGF-β1, TGF-β2, TGF-β3, activins, and bone morphogenetic proteins (BMPs). Previous studies have shown that TGF-β1 treatment increases collagen and GAG deposition[22], α-smooth muscle actin expression[23], inhibitors of metalloproteases (TIMPs) production[24]. BMPs have a profound effect on not only bone formation but also cartilage formation and meniscal regeneration. Meniscal defects in an avascular region of ovine menisci were filled with bovine bone collagen mixed with BMP-7 to investigate the therapeutic effects of BMP-7 on meniscal regeneration. After 12 weeks of implantation, the supplementation of BMP-7 showed enhanced tissue regeneration filling the defects compared to a control group[25].

Tissue-Engineered Menisci – Biomechanical Stimuli

Biomechanical stimulation is as critical as biochemical stimulation for the development and maintenance of native menisci. In absence of appropriate mechanical stimulation, the joint development including menisci is impaired[26–28]. Joint immobilization has also shown to reduce aggrecan gene expression and mechanical properties of the meniscus[29]. These findings suggest that the mechanical microenvironment affects both biochemical and mechanical properties of the native meniscus and thus should be taken into account to enhance the biochemical and biomechanical properties of tissue-engineered menisci. A variety of loading regimes, such as static, dynamic, compressive, and tensile loadings, have been studied and shown to be closely related to cellular activities within tissue-engineered constructs and tissue explants. Native tissue-like collagen fiber structure including circumferential and radial collagen fibers were observed in tissue-engineered meniscal constructs subjected to static compression after 8 weeks of culture with mechanical anchoring at the extensions of the constructs. Furthermore, static compression enhanced collagen accumulation in the statically compressed constructs[21]. The effects of dynamic compression are quite complex given amplitudes, frequencies, and duration of the stimuli all modulate the potential outcomes of dynamic compression. 10% dynamic compression on porcine meniscal explants significantly enhanced gene expression of aggrecan while 20% dynamic compression significantly increased gene expression of matrix metalloproteinase (MMP)-1, MMP-3, and MMP-13[30]. Additionally, compared to static compression, dynamic compression resulted in enhanced collagen production, collagen fiber formation, and equilibrium modulus[31]. These enhancements were further improved

with a prolonged duration of loading. Tensile loading has also been investigated as it is one of the dominant loading regimes on native menisci. Tensile loading has been shown to reduce Interleukin (IL)-1β induced pro-inflammatory cytokine upregulation of fibrochondrocytes[32]. Additionally, tensile loading increased collagen production within mesenchymal stem cell (MSC)-seeded PCL scaffolds[33].

Although the individual effects of either biochemical or mechanical stimuli on fibrochondrocytes have been widely investigated, little is known about the combined effects of these stimuli on collagen fiber structure and subsequent mechanical properties of tissue-engineered meniscal constructs. Furthermore, most previous studies employing biochemical and mechanical stimuli focused on improving the meniscal body of meniscal constructs, overlooking the interface. Therefore, there is a need for developing strategies to recapitulate distinct gradients of native entheses into tissue-engineered meniscal constructs.

Research Objectives

Collagen is an attractive biomaterial for use in tissue-engineered scaffolds considering 1) collagen is a major component of many connective tissues, 2) collagen fiber structure can be remodeled by cells, 3) collagen gel properties can be easily tuned by regulating gelation parameters. These characteristics of collagen imply that mechanical properties of collagen-based scaffolds can be further enhanced by cell-mediated remodeling or optimizing gelation parameters while achieving superior biocompatibility. The goal of the research presented in this dissertation is to investigate the effects of biochemical and biomechanical stimuli on biological activity of

fibrochondrocytes and cell-mediated collagen remodeling to generate native tissue-like structure and mechanics of tissue-engineered menisci and entheses and to assess the potential of gelation pH as an alternative approach to improve mechanical properties of tissue-engineered menisci. Specifically, we will address the following scientific questions: (a) do glucose and TGF-β1 in combination with mechanical boundary conditions have synergistic effects on tissue-engineered menisci, (b) can these effects be utilized in developing tissue-engineering enthesis, (c) is there an alternative, simple approach to enhance structural and mechanical properties of tissue-engineered menisci?

Specific Aim 1 (Chapter 2)

Rationale 1: Menisci exhibit a distinct collagen fiber orientation, giving rise to its mechanical functions[34,35]. Therefore, it is important to mimic the native meniscal fiber structure in tissue-engineered meniscal constructs. It has been reported that transforming growth factor-β1 increases the contractile forces of fibrochondrocytes and glycosaminoglycan deposition[23,36]. Previously, we have noted that fiber formation is enhanced by cellular traction forces[21,37] but weakened by GAG deposition[38]. Interestingly, TGF-β1 applied to fibrochondrocytes increases both cellular traction forces and GAG synthesis. The net effect of TGF-β1 at different concentrations in conjunction with other biochemical and biomechanical stimuli on collagen fiber formation within tissue-engineered meniscus is unknown.

Hypothesis 1: Regulation of TGF-β1, glucose, and mechanical boundary conditions will promote cell-mediated remodeling of collagen fiber structure while minimizing the negative effect of GAG on fiber structure, which will lead to increased mechanical

properties of tissue-engineered menisci.

Specific Aim 1: Elucidate the effects of TGF-β1 on fiber formation and alignment in tissue-engineered meniscal constructs along with glucose and mechanical boundary conditions.

Specific Aim 2 (Chapter 3)

Rationale 2: Meniscal entheses have a complex collagen fiber structure, including highly aligned collagen fibers in the soft tissue region and dense, unaligned collagen fibers at the interface between the soft tissue and boney regions[5,7]. This distinct fiber structure results in mechanical functions, such as connecting two regions with multiple orders of magnitude changes in stiffness while minimizing stress concentrations[6]. However, mimicking the native collagen fiber structure within tissue-engineered entheses remains challenging. In specific aim 1, we demonstrate that hyper-physiological levels of glucose (4500 mg/L) and TGF-β1 (5 ng/ml) lead to a compact and unaligned collagen fiber network, while relatively lower concentrations of glucose (500 mg/L) and TGF-β1 (0.5 ng/ml) result in aligned collagen fiber structure[39]. Our group has developed a custom bioreactor capable of generating a biochemical gradient at the soft tissue-bone interface, where different types of media can be individually applied to either bony or soft tissue portions of tissue-engineered entheses[40].

Hypothesis 2: Gradients in media will drive native enthesis-like collagen fiber structure within tissue-engineered entheses and will lead to native tissue-like mechanics.

Specific Aim 2: Investigate the combinational effects of glucose, TGF-β1, and mechanical anchoring using a tri-chamber bioreactor on collagen fiber organization and

local strain distribution of tissue-engineered soft tissue-to-bone interfaces.

Specific Aim 3 (Chapter 4)

Rationale 3: Collagen-based scaffolds have shown promising outcomes; however, matching native mechanical properties remains challenging. To overcome this limitation, various approaches have been made by controlling several gelation factors, such as pH, temperature, ionic strength of buffer, collagen concentration or crosslinking[41–44]. Previous studies demonstrated that gelation pH affects kinetics of fibrillogenesis, microstructure of collagen constructs and resultant mechanical properties[41,42]. Our group has shown that mechanical properties of collagen constructs increase with increasing collagen concentration[44]. However, most studies were performed with relatively low collagen concentrations (up to 4 mg/ml), and thus the influence of gelation pH on high-density collagen constructs (20 mg/ml) has not yet been elucidated. Moreover, it is unclear whether gelation pH also affects the cellular activity of fibrochondrocytes seeded in tissue-engineered menisci during extended culture.

Hypothesis 3: Gelation pH regulates biochemical, structural, and mechanical properties of tissue-engineered menisci, and that there exists an optimal gelation pH that leads to both enhanced extracellular matrix deposition and increased mechanical properties of tissue-engineered menisci after an extended period of culture.

Specific Aim 3: Assess the biochemical and biomechanical effects of gelation pH on high-density collagen constructs seeded with fibrochondrocytes.

References

(1) Fox, A. J. S.; Bedi, A.; Rodeo, S. A. The Basic Science of Human Knee Menisci: Structure, Composition, and Function. *Sports Health* 2012, *4* (4), 340–351.

(2) Hino, T.; Furumatsu, T.; Miyazawa, S.; Fujii, M.; Kodama, Y.; Kamatsuki, Y.; Okazaki, Y.; Masuda, S.; Okazaki, Y.; Ozaki, T. A Histological Study of the Medial Meniscus Posterior Root Tibial Insertion. *Connect. Tissue Res.* 2020, *61* (6), 546–553.

(3) Fox, A. J. S.; Wanivenhaus, F.; Burge, A. J.; Warren, R. F.; Rodeo, S. A. The Human Meniscus: A Review of Anatomy, Function, Injury, and Advances in Treatment. *Clin. Anat.* 2015, *28* (2), 269–287.

(4) Gee, S. M.; Posner, M. Meniscus Anatomy and Basic Science. *Sports Med. Arthrosc.* 2021, *29* (3), E18–E23.

(5) Haut Donahue, T. L.; Pauly, H. M. Osteoarthritic Meniscal Entheses Exhibit Altered Collagen Fiber Orientation. *Connect. Tissue Res.* 2022, *63* (2), 151–155.

(6) Abraham, A. C.; Haut Donahue, T. L. From Meniscus to Bone: A Quantitative Evaluation of Structure and Function of the Human Meniscal Attachments. *Acta Biomater.* 2013, *9* (5), 6322–6329.

(7) Boys, A. J.; McCorry, M. C.; Rodeo, S.; Bonassar, L. J.; Estroff, L. A. Next Generation Tissue Engineering of Orthopedic Soft Tissue-to-Bone Interfaces. *MRS Commun.* 2017, *7* (3), 289–308.

(8) Li, Q.; Qu, F.; Han, B.; Wang, C.; Li, H.; Mauck, R. L.; Han, L. Micromechanical Anisotropy and Heterogeneity of the Meniscus Extracellular Matrix. *Acta Biomater.* 2017, *54*, 356–366.

(9) Yang, P. J.; Temenoff, J. S. Engineering Orthopedic Tissue Interfaces. *Tissue Eng. Part B Rev.* 2009, *15* (2), 127–141.

(10) Lee, D. R.; Reinholz, A. K.; Till, S. E.; Lu, Y.; Camp, C. L.; Deberardino, T. M.; Stuart, M. J.; Krych, A. J.; Stuart, M. J. Current Reviews in Musculoskeletal Medicine : Current Controversies for Treatment of Meniscus Root Tears. *Curr. Rev. Musculoskelet. Med.* 2022, 1–13.

(11) Ozeki, N.; Koga, H.; Sekiya, I. Degenerative Meniscus in Knee Osteoarthritis : From Pathology to Treatment. *Life* 2022, *12* (4), 603–616.

(12) Shelton, W. R. Meniscus Allograft Transplantation. *Oper. Tech. Sports Med.* 2007, *26* (3), 189–204.

(13) De Bruycker, M.; Verdonk, P. C. M.; Verdonk, R. C. Meniscal Allograft Transplantation: A Meta-Analysis. *Sicot-J* 2017, *3*.

(14) Kang, S.-W.; Son, S.-M.; Lee, J.-S.; Lee, E.-S.; Lee, K.-Y.; Park, S.-G.; Park, J.-H.; Kim, B.-S. Regeneration of Whole Meniscus Using Meniscal Cells and Polymer Scaffolds in a Rabbit Total Meniscectomy Model. *J. Biomed. Mater. Res. Part A* 2006, *77* (4), 659–671.

(15) Chiari, C.; Koller, U.; Dorotka, R.; Eder, C.; Plasenzotti, R.; Lang, S.; Ambrosio, L.; Tognana, E.; Kon, E.; Salter, D.; Nehrer, S. A Tissue Engineering Approach to Meniscus Regeneration in a Sheep Model. *Osteoarthr. Cartil.* 2006, *14* (10), 1056–1065.

(16) Baynat, C.; Andro, C.; Vincent, J. P.; Schiele, P.; Buisson, P.; Dubrana, F.; Gunepin, F. X. Actifit® Synthetic Meniscal Substitute: Experience with 18 Patients in Brest, France. *Orthop. Traumatol. Surg. Res.* 2014, *100* (8), S385–

S389.

(17) Verdonk, R.; Verdonk, P.; Huysse, W.; Forsyth, R.; Heinrichs, E. L. Tissue Ingrowth after Implantation of a Novel, Biodegradable Polyurethane Scaffold for Treatment of Partial Meniscal Lesions. *Am. J. Sports Med.* 2011, *39* (4), 774–782.

(18) Mandal, B. B.; Park, S. H.; Gil, E. S.; Kaplan, D. L. Multilayered Silk Scaffolds for Meniscus Tissue Engineering. *Biomaterials* 2011, *32* (2), 639–651.

(19) Martínez, H.; Brackmann, C.; Enejder, A.; Gatenholm, P. Mechanical Stimulation of Fibroblasts in Micro-Channeled Bacterial Cellulose Scaffolds Enhances Production of Oriented Collagen Fibers. *J. Biomed. Mater. Res. - Part A* 2012, *100* (4), 948–957.

(20) Rodkey, W. G.; DeHaven, K. E.; Montgomery, W. H.; Baker, C. L.; Beck, C. L.; Hormel, S. E.; Steadman, J. R.; Cole, B. J.; Briggs, K. K. Comparison of the Collagen Meniscus Implant with Partial Meniscectomy: A Prospective Randomized Trial. *J. Bone Jt. Surg. - Ser. A* 2008, *90* (7), 1413–1426.

(21) Puetzer, J. L.; Koo, E.; Bonassar, L. J. Induction of Fiber Alignment and Mechanical Anisotropy in Tissue Engineered Menisci with Mechanical Anchoring. *J. Biomech.* 2015, *48* (8), 1436–1443.

(22) Pangborn, C. A.; Athanasiou, K. A. Effects of Growth Factors on Meniscal Fibrochondrocytes. *Tissue Eng.* 2005, *11* (7–8), 1141–1148.

(23) Zaleskas, J. M.; Kinner, B.; Freyman, T. M.; Yannas, I. V.; Gibson, L. J.; Spector, M. Growth Factor Regulation of Smooth Muscle Actin Expression and Contraction of Human Articular Chondrocytes and Meniscal Cells in a Collagen-

GAG Matrix. *Exp. Cell Res.* 2001, *270* (1), 21–31.

(24) Hui, W.; Rowan, A. D.; Cawston, T. Modulation of the Expression of Matrix Metalloproteinase and Tissue Inhibitors of Metalloproteinases by TGF-B1 and IGF-1 in Primary Human Articular and Bovine Nasal Chondrocytes Stimulated with TNF-α. *Cytokine* 2001, *16* (1), 31–35.

(25) Forriol, F.; Ripalda, P.; Duart, J.; Esparza, R.; Gortazar, A. R. Meniscal Repair Possibilities Using Bone Morphogenetic Protein-7. *Injury* 2014, *45* (S4), S15–S21.

(26) Mikic, B.; Johnson, Tiffany, L.; Chhabra, A. B.; Schalet, B. J.; Wong, M.; Hunziker, E. B. Differential Effects of Embryonic Immobilization on the Development of Fibrocartilaginous Skeletal Elements. *J. Rehabil. Res. Dev.* 2000, *37* (2), 127–134.

(27) Galloway, M. T.; Lalley, A. L.; Shearn, J. T. The Role of Mechanical Loading in Tendon Development, Maintenance, Injury, and Repair. *J. Bone Jt. Surg. - Ser. A* 2013, *95* (17), 1620–1628.

(28) McNulty, A. L.; Guilak, F. Mechanobiology of the Meniscus. *J. Biomech.* 2015, *48* (8), 1469–1478.

(29) Djurasovic, M.; Aldridge, J. W.; Grumbles, R.; Rosenwasser, M. P.; Howell, D.; Ratcliffe, A. Knee Joint Immobilization Decreases Aggrecan Gene Expression in the Meniscus. *Am. J. Sports Med.* 1998, *26* (3), 460–466.

(30) Zielinska, B.; Killian, M.; Kadmiel, M.; Nelsen, M.; Haut Donahue, T. L. Meniscal Tissue Explants Response Depends on Level of Dynamic Compressive Strain. *Osteoarthr. Cartil.* 2009, *17* (6), 754–760.

(31) Puetzer, J. L.; Ballyns, J. J.; Bonassar, L. J. The Effect of the Duration of Mechanical Stimulation and Post-Stimulation Culture on the Structure and Properties of Dynamically Compressed Tissue-Engineered Menisci. *Tissue Eng. - Part A* 2012, *18* (13–14), 1365–1375.

(32) Ferretti, M.; Madhavan, S.; Deschner, J.; Rath-Deschner, B.; Wypasek, E.; Agarwal, S. Dynamic Biophysical Strain Modulates Proinflammatory Gene Induction in Meniscal Fibrochondrocytes. *Am. J. Physiol. - Cell Physiol.* 2006, *290* (6), 1610–1615.

(33) Nerurkar, N. L.; Sen, S.; Baker, B. M.; Elliott, D. M.; Mauck, R. L. Dynamic Culture Enhances Stem Cell Infiltration and Modulates Extracellular Matrix Production on Aligned Electrospun Nanofibrous Scaffolds. *Acta Biomater.* 2011, *7* (2), 485–491.

(34) Andrews, S. H. J.; Rattner, J. B.; Abusara, Z.; Adesida, A.; Shrive, N. G.; Ronsky, J. L. Tie-Fibre Structure and Organization in the Knee Menisci. *J. Anat.* 2014, *224* (5), 531–537.

(35) Li, Q.; Doyran, B.; Gamer, L. W.; Lu, X. L.; Qin, L.; Ortiz, C.; Grodzinsky, A. J.; Rosen, V.; Han, L. Biomechanical Properties of Murine Meniscus Surface via AFM-Based Nanoindentation. *J. Biomech.* 2015, *48* (8), 1364–1370.

(36) Sweigart, M. A.; Athanasiou, K. A. Toward Tissue Engineering of the Knee Meniscus. *Tissue Eng.* 2001, *7* (2), 111–129.

(37) Mueller, S. M.; Shortkroff, S.; Schneider, T. O.; Breinan, H. A.; Yannas, I. V.; Spector, M. Meniscus Cells Seeded in Type I and Type II Collagen-GAG Matrices in Vitro. *Biomaterials* 1999, *20* (8), 701–709.

(38) McCorry, M. C.; Puetzer, J. L.; Bonassar, L. J. Characterization of Mesenchymal Stem Cells and Fibrochondrocytes in Three-Dimensional Co-Culture: Analysis of Cell Shape, Matrix Production, and Mechanical Performance. *Stem Cell Res. Ther.* 2016, *7* (1), 1–10.

(39) Kim, J.; Boys, A. J.; Estroff, L. A.; Bonassar, L. J. Combining TGF-B1 and Mechanical Anchoring to Enhance Collagen Fiber Formation and Alignment in Tissue-Engineered Menisci. *ACS Biomater. Sci. Eng.* 2021, *7* (4), 1608–1620.

(40) Iannucci, L. E.; Boys, A. J.; Mccorry, M. C.; Estroff, L. A.; Bonassar, L. J. Cellular and Chemical Gradients to Engineer the Meniscus-to-Bone Insertion. *Adv. Healthc. Mater.* 2018, *1800806*, 1–10.

(41) Jiang, F.; Hörber, H.; Howard, J.; Müller, D. J. Assembly of Collagen into Microribbons: Effects of PH and Electrolytes. *J. Struct. Biol.* 2004, *148* (3), 268–278.

(42) Li, Y.; Asadi, A.; Monroe, M. R.; Douglas, E. P. PH Effects on Collagen Fibrillogenesis in Vitro: Electrostatic Interactions and Phosphate Binding. *Mater. Sci. Eng. C* 2009, *29* (5), 1643–1649.

(43) Ibusuki, S.; Halbesma, G. J.; Randolph, M. A.; Redmond, R. W.; Kochevar, I. E.; Gill, T. J. Photochemically Cross-Linked Collagen Gels as Three-Dimensional Scaffolds for Tissue Engineering. *Tissue Eng.* 2007, *13* (8), 1995–2001.

(44) Diamantides, N.; Wang, L.; Pruiksma, T.; Siemiatkoski, J.; Dugopolski, C.; Shortkroff, S.; Kennedy, S.; Bonassar, L. J. Correlating Rheological Properties and Printability of Collagen Bioinks: The Effects of Riboflavin

Photocrosslinking and PH. *Biofabrication* 2017, *9* (3).

CHAPTER 2

Combining TGF-β1 and Mechanical Anchoring to Enhance Collagen Fiber Formation and Alignment in Tissue-Engineered Menisci

Abstract

Recapitulating the collagen fiber structure of native menisci is one of the major challenges in the development of tissue-engineered menisci. Native collagen fibers are developed by the complex interplay of biochemical and biomechanical signals. In this study, we optimized glucose and transforming growth factor-β1 (TGF-β1) concentrations in combination with mechanical anchoring to balance contributions of proteoglycan synthesis and contractile behavior in collagen fiber assembly. Glucose had a profound effect on the final dimensions of collagen-based constructs. TGF-β1 influenced construct contraction rate and glycosaminoglycan (GAG) production with two half-maximal effective concentration (EC_{50}) ranges, which are 0.23 to 0.28 and 0.53 to 1.71 ng/mL, respectively. At concentrations less than the EC_{50}, for the GAG production and contraction rate, TGF-β1 treatment resulted in less organized collagen fibers. At concentrations greater than the EC_{50}, TGF-β1 led to dense, disorganized collagen fibers. Between the two EC_{50} values, collagen fiber diameter and length increased. The effects of TGF-β1 on fiber development were enhanced by mechanical anchoring, leading to peaks in fiber diameter, length, and alignment index. Fiber diameter and length increased from 7.9 ± 1.4 and 148.7 ± 16.4 to 17.5 ± 2.1 and 262.0 ± 13.0 μm, respectively. The alignment index reached 1.31, comparable to that of native tissue, 1.40. These enhancements in fiber architecture resulted in significant increases in tensile modulus and ultimate tensile stress (UTS) by 1.6- and 1.4-fold. Correlation

analysis showed that tensile modulus and UTS strongly correlated with collagen fiber length, diameter, and alignment, while compressive modulus correlated with GAG content. These outcomes highlight the need for optimization of both biochemical and biomechanical cues in the culture environment for enhancing fiber development within tissue-engineered constructs.

Kim, J., Boys, A. J., Estroff, L. A., & Bonassar, L. J. (2021). Combining TGF-β1 and Mechanical Anchoring to Enhance Collagen Fiber Formation and Alignment in Tissue-Engineered Menisci. ACS Biomaterials Science & Engineering, 7(4), 1608-1620.

Introduction

Meniscal injury is one of the major causes of knee surgery in the United States with over one million cases per year[1]. Depending on the site and type of the meniscal injury, treatment can range from nonoperative to partial or total meniscectomy[2]. Due to the limited healing capacity of the menisci, partial or total meniscectomy is commonly performed, followed by meniscal implantation or allograft transplantation. For total meniscectomy, meniscal allograft transplantation is considered as the only treatment option[3]. Although meniscal allograft transplantation has shown promising outcomes, several limitations, such as limited supply, disease transmission, and immune rejection, necessitate the development of tissue-engineered menisci[4]. Here, we combine biochemical and biomechanical cues to improve the collagen organization in tissue-engineered meniscal replacements.

The primary roles of the menisci are biomechanical functions including load transmission, shock absorption, and stabilization of the knee joint[5]. A majority of previous studies on tissue-engineered menisci have focused on enhancing construct mechanical properties to match those of the native menisci. A persistent challenge in matching the mechanical properties of the native meniscus is rooted in an inability to mimic the native fiber structure[6–9]. Since the native fiber structure contributes to not only the mechanical properties but also the mechanical anisotropy of native menisci, which is directly related to the biomechanical functions in vivo, replicating the native meniscal fiber structure is critical for the development of tissue-engineered menisci.

Considerable effort has been directed at mimicking the native fiber structure using various techniques involving synthetic or natural polymers with prealigned

structure or mechanical boundary conditions[7,10–13]. Recently, we demonstrated a negative correlation between glycosaminoglycan (GAG) deposition and fiber alignment[13]. As such, collagen fiber development can be regulated by controlling the proteoglycans involved in collagen fibrillogenesis using different concentrations of glucose in media[14]. Furthermore, multiple studies have demonstrated that cellular traction force is a major contributor to cell-mediated collagen fiber organization[12,14,15]. These findings suggest that collagen fibers are not merely organized by a single factor and thus recapitulating native collagen fiber structure within tissue-engineered menisci requires a deep understanding of the interactions among multiple biochemical and biomechanical factors.

Transforming growth factor-betas (TGF-βs) have been widely used in tissue engineering as growth factors to enhance proliferation of fibrochondrocytes and production of extracellular matrix (ECM) components[8,16–18]. Compared to other growth factors, TGF-βs have shown superior fibrochondrogenic effects on meniscus tissue engineering approaches[17,19]. Additionally, these effects are subject to additional biochemical and biomechanical factors[20–23], indicating the importance of optimizing a culture condition. Furthermore, among TGF-βs, TGF-β1 has been shown to increase cellular traction forces by enhancing α-smooth muscle actin (α-SMA) expression of fibrochondrocytes[24]. Interestingly, TGF-β1 stimulates two competing factors that regulate collagen fiber organization: proteoglycan synthesis[22,25,26], which inhibits fiber formation[14,27], and cellular traction forces[24], which enhance fiber formation[24,28–30]. As such, while TGF-β1 has been used to enhance proteoglycan production in tissue-engineered menisci, the effects of TGF-β1 on collagen fiber formation and alignment in

combination with additional biochemical and biomechanical cues have not been investigated. We hypothesize that the effects of TGF-β1 on cellular contractile behavior and proteoglycan synthesis lead to optimal fiber formation at intermediate concentrations of TGF-β1 and that these effects are mediated by media glucose and mechanical anchoring. To test this hypothesis, we investigated collagen fiber formation and alignment in tissue-engineered menisci using TGF-β1 in combination with variations in media glucose concentrations and mechanical boundary conditions. The first aim of this study was to examine the influence of TGF-β1 under two different glucose concentrations, 4500 mg/L, which is commonly used in cartilage culture as it promotes proteoglycan synthesis[31,32], and 500 mg/L, which we previously found to be the most effective at enhancing collagen organization[14]. The second aim was to assess the influence of TGF-β1 in combination with mechanical anchoring, which we have also previously shown to promote collagen organization[12,15,33]. These results are useful for developing an optimal culture condition for fiber organization in tissue-engineered menisci and facilitating the transition of tissue-engineered menisci to clinical use.

Materials and Methods

Cell Preparation. Fibrochondrocytes were harvested from a total of 8 juvenile bovine menisci as previously described for each experimental set[6,34]. Briefly, menisci were diced and subsequently digested using a 0.3% (wt/vol) collagenase (Worthington Biochemical Corporation, Lakewood, NJ) in Dulbecco's modified Eagle medium (DMEM) with 100 μg/mL penicillin and 100 μg/mL streptomycin for 18 h, followed by filtering through a 100 μm cell strainer. Prior to seeding in collagen scaffolds, the cells

pooled from all 8 menisci were rinsed with phosphate-buffered saline (PBS) and suspended to a concentration of 150×10^6 cells/mL.

Collagen and Meniscal Construct Preparation. Type I collagen was extracted from Sprague-Dawley rat tails (Pel-Freez Biologicals, Rogers, AZ), lyophilized, and reconstituted in 0.1% (vol/vol) acetic acid at 30 mg/mL concentration as previously described[29,34,35]. The reconstituted collagen solution was mixed with a working solution composed of 1 N NaOH, 10× PBS, and 1× PBS to initiate the gelation at pH 7 using a syringe stopcock. Then, isolated fibrochondrocytes were homogeneously mixed with the collagen solution to obtain a final concentration of 25×10^6 cells/mL and 20 mg/mL collagen gel. The mixture of collagen and cells was immediately injected either between two glass plates to create a sheet gel 2 mm thick or into meniscal molds and allowed to gel for 30 min at 37 °C[12,36]. Using sheet gels, 8 mm-diameter disc constructs were obtained using biopsy punches (n = 12 per condition). Each meniscal construct, 1 to 3.5 mm in height from the inner to outer region at 65° slope across 5.4 mm width, was clamped into a poly(sulfone) disc at the meniscal extensions using a stainless-steel mesh and bar to mimic native mechanical boundary conditions (n = 4-5 per condition)[12,13]. Constructs were cultured in DMEM at 500 or 4500 mg/L glucose concentrations without or with TGF-β1 at concentrations ranging from 0 to 10 ng/mL (MilliporeSigma, St. Louis, MO), 10% (vol/vol) fetal bovine serum, 100 μg/mL penicillin, 100 μg/mL streptomycin, 0.1 mM nonessential amino acids, 50 μg/mL ascorbic acid, and 0.4 mM L-proline at 37 °C and 5% CO_2 for up to 30 days. Culture media were collected and replenished every third day. Photographs of each construct were obtained at each medium change and imported into ImageJ software (NIH, Bethesda, MD) to calculate

contraction of each construct.

Biochemical Analysis. After 30 days of culture, portions of each construct were harvested and weighed to measure wet weight (ww) and then frozen and lyophilized to measure dry weight (dw). Lyophilized samples were digested in 1.25 mg/mL papain digestion solution (Sigma-Aldrich, MO, USA) and analyzed for DNA via a Hoechst DNA assay[37], GAG via a modified 1,9-dimethylmethylene blue (DMMB) assay[38], and collagen via a hydroxyproline (Hypro) assay[39]. Media from each sample were collected at each medium change and analyzed by the DMMB assay.

Multiphoton Microscopy. At the end of each culture period, cross sections of disc constructs and meniscal constructs were fixed in 10% (vol/vol) buffered formalin for 48 h, followed by storage in 70% (vol/vol) ethanol. A Zeiss LSM 880 confocal/multiphoton inverted microscope using a 40×/1.2 C-Apochromat water immersion objective was used to image circumferential collagen fibers using second harmonic generation (SHG) and autofluorescence in a two-dimensional manner[14]. Cellular autofluorescence was captured between 495 and 580 nm. Collagen fibers with noticeable boundaries were considered as individual fibers (Figure 2.S1). Subsequently, average fiber diameter and length were manually measured using ImageJ software (NIH, Bethesda, MD). A total of 3 SHG images per sample were taken, blindly analyzed, and averaged. The fiber alignment index (AI) was calculated using a custom MATLAB code[40]. Briefly, this code divides a representative image of the orientation for a construct into a 4 × 4 set of panes to examine maximum orientation for each pane. The resultant panes are converted into two-dimensional fast Fourier transforms (FFTs) of the original image pane. This FFT is then rotated in increments of 10° around the

central axis. At each angle, the center line of the FFT is averaged to determine the angle at which the maximum signal for the FFT occurs. This value is then divided by the value at the orthogonal angle, thus creating an AI. The average AI was then calculated for each pane and averaged for all panes to create an AI each image. As such, samples with completely unorganized fibers have an AI of 1, and samples with perfectly aligned fibers have an AI of infinity.

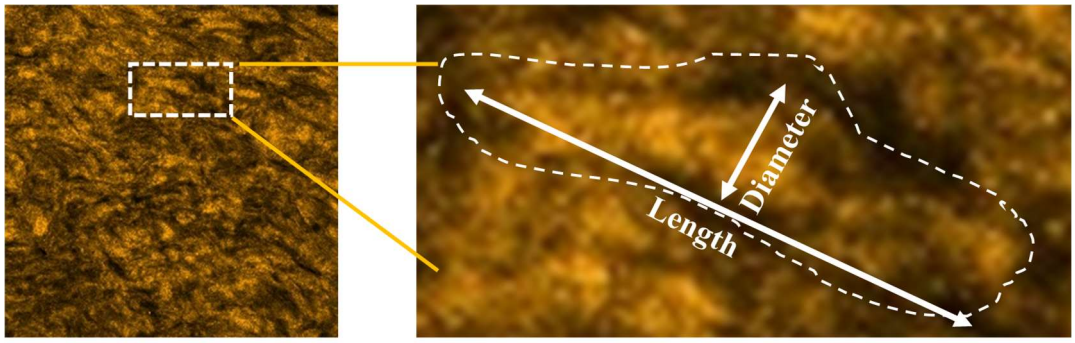

Figure 2.S1. The measurements of collagen fiber diameter and length. Collagen fibers with noticeable boundary (dashed line) were considered as individual collagen fiber. Each double-sided arrow indicates either collagen fiber diameter or length.

Histology and Immunohistochemistry. Cross-sectioned samples were dehydrated, embedded in paraffin blocks, and sectioned. Sections were stained with picrosirius red, followed by imaging under brightfield and under polarized light to assess fiber organization. Immunohistochemistry was performed to assess collagen and α-SMA expression using antibodies for type I collagen (Abcam, Cambridge, MA), type II collagen (Chondrex, Redmond, WA), and α-SMA (Abcam, Cambridge, MA). As a negative control, sections were treated without primary antibodies. All slides were counterstained with Weigert's hematoxylin. Images were captured with a Nikon Eclipse TE2000-S microscope (Nikon Instruments, Melville, NY) with a SPOT RT camera

(Diagnostic Instruments, Sterling Heights, MI).

Mechanical Analysis. Tensile and confined compression stress relaxation tests were performed using an Enduratec ElectroForce 3200 System (Bose, Eden Prairie, MN) as previously reported[15,34]. The tensile testing was performed at a quasistatic strain rate of 0.75%/s. The tensile modulus was calculated as the slope of the linear elastic portion of the stress-strain curve. The ultimate tensile stress (UTS) was determined as the maximum stress before construct failure. The stress relaxation test was performed by imposing 6 steps of 5% compression each, with 10 min between steps to allow for full stress relaxation. The resulting loads were fitted to a poroelastic model using a custom MATLAB program to measure the equilibrium modulus[34].

Statistical Analysis. All values were reported as mean ± standard deviation. Data were tested for normality using Shapiro-Wilk's test and analyzed using one-way or two-way analysis of variance with Tukey's honestly significant difference post hoc tests where $p < 0.05$ was considered to be significant. Total GAG production and time required to reach half of the total contraction were fit to a four-parameter logistic curve to calculate half-maximal effective concentration (EC_{50}) according to the following equations:

$$\mathrm{Y} = \mathrm{bottom} + \frac{\mathrm{X}^{\mathrm{HillSlope}} * (\mathrm{top} - \mathrm{bottom})}{(\mathrm{X}^{\mathrm{HillSlope}} + \mathrm{EC_{50}}^{\mathrm{HillSlope}})} \quad (1)$$

$$\mathrm{Y} = \mathrm{bottom} + \frac{(\mathrm{top} - \mathrm{bottom})}{(1 + (\mathrm{EC_{50}}/\mathrm{X})^{\mathrm{HillSlope}})} \quad (2)$$

Where X represents the concentration of TGF-β1, Y represents either of corresponding total GAG production (eq 1) or time required to reach half of total contraction (eq 2), HillSlope is the slope, and bottom and top represent the minimum and maximum values,

respectively. EC_{50} was calculated as the inflection point of the sigmoid. The correlation analysis between all the measured variables was performed using a least-square fit and Pearson correlation. All statistical analysis was performed using GraphPad Prism (GraphPad Prism Software Inc., San Diego, CA).

Results

Disc Construct Contraction. To observe the combined effect of TGF-β1 and glucose on cellular contractile behavior, we assessed construct contraction over 30 days. Final construct size after 30 days in culture was similar for all TGF-β1 concentrations and was uniformly smaller at 4500 mg/L glucose compared to 500 mg/L ($p < 0.05$) (Figure 2.1a,b). Disc constructs cultured in 4500 mg/L glucose concentration medium contracted to ~20-30% of their initial size while disc constructs in 500 mg/L glucose concentration medium contracted to ~50-60% of their initial size (Figure 2.1b). There was no significant difference in the final size between the groups cultured in 500 mg/L glucose, but 4500 mg/L glucose medium-cultured groups showed a decreasing trend in the final size with the increasing TGF-β1 concentration up to a 1 ng/ mL of TGF-β1. Interestingly, this decreasing trend was not observed in a 10 ng/mL TGF-β1-treated group, which showed a slight and gradual increase in the size after 15 days of culture and the comparable size to the 0 ng/mL TGF-β1 control group (Figure 2.1b,c). Notably, the rate of contraction appeared to vary with TGF-β1 treatment although TGF-β1 treatment did not affect the final sizes of the disc constructs cultured in 500 mg/L glucose. To assess the contraction rate, we calculated the time at which half-maximal contraction occurred for all groups. Increasing TGF-β1 concentration resulted in shorter

time to reach half of the total contraction in both glucose concentrations. This effect was clearly dose-dependent with an EC_{50} at 0.23 ng/mL ($R^2 = 0.9232$) for 4500 mg/L glucose in medium and at 0.27 ng/mL ($R^2 = 0.8586$) for 500 mg/L glucose in medium (Figure 2.1d). The 95% confidence intervals for EC_{50} are 0.15 to 0.41 for the 4500 mg/L glucose and 0.19 to 0.36 for the 500 mg/L glucose.

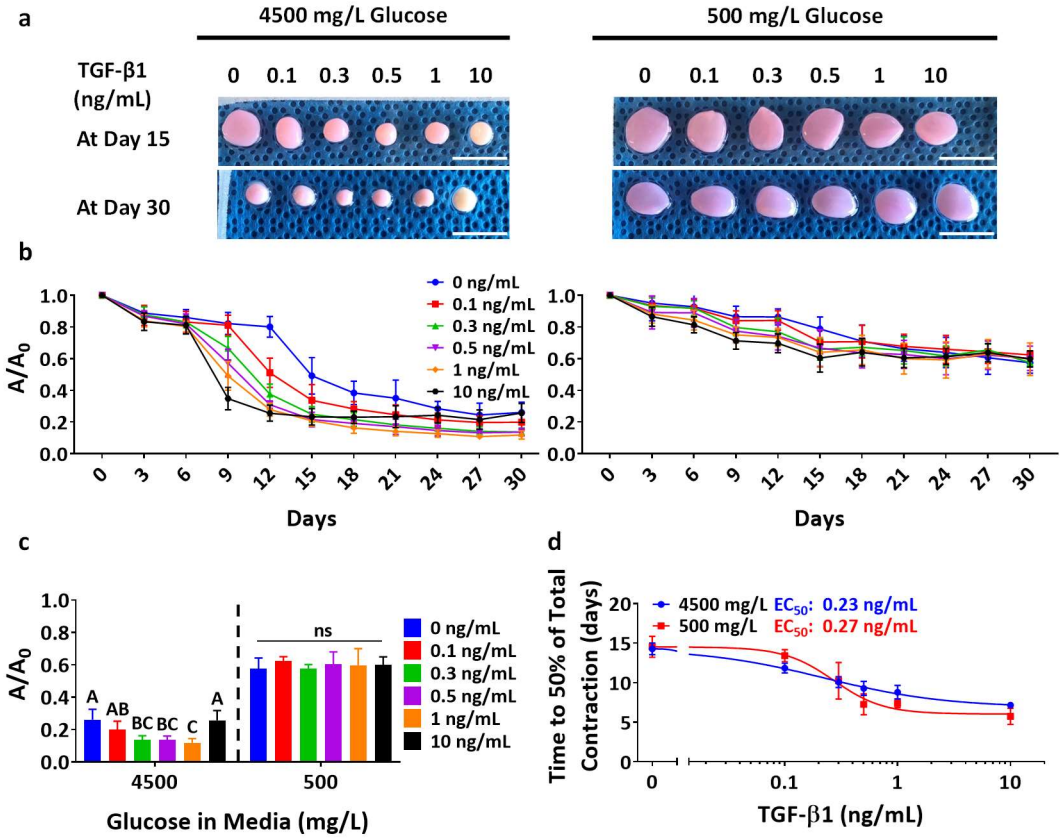

Figure 2.1. Contraction of disc constructs over 30 days of culture. (a) Photographs of disc constructs after 15 and 30 days of culture in media containing 4500 mg/L (left panels) and 500 mg/L (right panels) glucose with indicated TGF-β1 concentrations. (b) Ratio of projected disc construct area over initial projected area throughout culture (n = 6-12). (c) Ratio of projected area over initial projected area at day 30 (n = 6). Different letters represent statistical significance between groups ($p < 0.05$; ns, non-significant).

No comparison was done between groups cultured in different medium glucose concentrations. (d) Time required for half-maximal contraction as a function of TGF-β1 concentrations (n = 6). Scale bars are 1 cm.

Disc Construct GAG Production. To assess whether glucose and TGF-β1 are associated with GAG production by fibrochondrocytes, the amount of GAG in disc constructs and media was measured over 30 days. All TGF-β1-treated groups cultured in 4500 mg/L glucose showed a significant increase in GAG content standardized to ww compared to the control group. Constructs in 500 mg/L glucose, however, showed a significant increase in only 1 and 10 ng/mL TGF-β1-treated groups (Figure 2.2a). Total GAG production as a function of TGF-β1 concentration showed a dose-dependent response with an EC_{50} at 1.71 ng/mL (R^2 = 0.9717) for the 4500 mg/L medium glucose concentration and at 1.34 ng/mL (R^2 = 0.9793) for the 500 mg/L medium glucose concentration. The 95% confidence intervals for EC_{50} are 1.43 to 2.24 for the 4500 mg/L glucose concentration and 1.17 to 1.54 for the 500 mg/L glucose concentration. Glucose, however, did not appear to affect the total GAG production under the same TGF-β1 treatments (Figure 2.2b). Interestingly, DNA content per construct significantly increased only when cultured at 4500 mg/L glucose and 10 ng/mL TGF-β1 concentrations (Figure 2.S2). Furthermore, only 10 ng/mL of TGF-β1 treatment led to a significant increase in GAGs/DNA by 2.4-fold in 4500 mg/L glucose media and 2.8-fold in 500 mg/L glucose media groups (Figure 2.S3). However, while there was a small increase in hydroxyproline content at 10 ng/mL of TGF-β1-treated groups, there was no significant difference in hydroxyproline content between groups (Figure 2.S4).

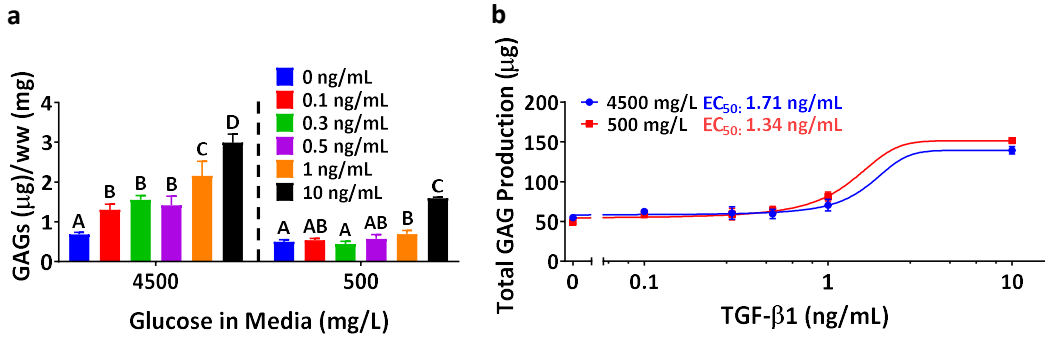

Figure 2.2. GAG content in disc constructs and total GAG production throughout 30 days of culture analyzed by the DMMB assay. (a) GAG content in disc constructs normalized to wet weight (n = 3). (b) Total GAG production as a function of TGF-β1 concentration (n = 3). Total GAG production is calculated as a sum of GAG in the disc construct and GAG released to the media. Different letters represent statistical significance between groups ($p < 0.05$). No comparison was done between groups cultured in different medium glucose concentrations.

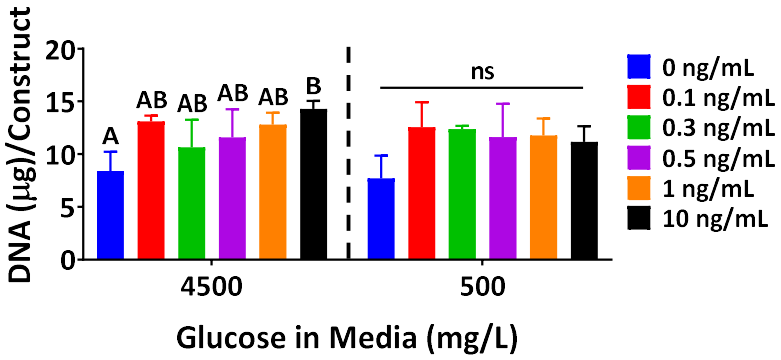

Figure 2.S2. DNA content in each disc construct after 30 days of culture analyzed by the DNA Hoechst assay. Different letters represent statistical significance between groups ($p < 0.05$; ns, non-significant; n = 3). No comparison was done between groups cultured in different medium glucose concentrations.

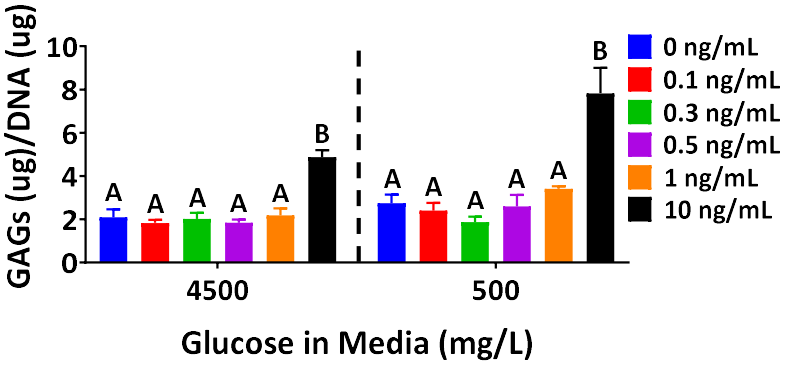

Figure 2.S3. GAG content normalized to DNA content after 30 days of culture analyzed by the DMMB assay. Different letters represent statistical significance between groups ($p < 0.05$; $n = 3$). No comparison was done between groups cultured in different medium glucose concentrations.

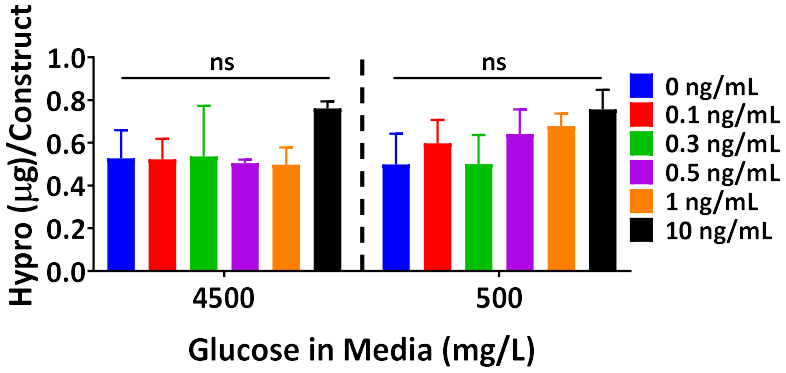

Figure 2.S4. Collagen content per disc construct after 30 days of culture analyzed by the hydroxyproline assay (ns, non-significant; $n = 3$). No comparison was done between groups cultured in different medium glucose concentrations.

Fiber Alignment Analysis on Disc Constructs via SHG Microscopy. In order to investigate how these differences in the construct contraction and GAG production influence collagen fiber formation within the construct, SHG images of each construct were taken. For 500 mg/L glucose, robust and aligned collagen fiber organization was

observed in the 0.5 ng/ mL of the TGF-β1-treated group and to a lesser extent in the 0.3 ng/mL of the TGF-β1-treated group (Figure 2.3a and Table 2.S1). This organization is characterized by the presence of continuous fibers greater than 10 μm in diameter and 100 μm in length. Constructs cultured in 4500 mg/L glucose displayed denser SHG signals with characteristic features smaller than 10 μm with minimal spatial organization and did not show any significant difference in fiber diameter and length in response to TGF-β1 treatment. In contrast, constructs cultured in 500 mg/L glucose showed differing development depending on concentrations of TGF-β1. The average fiber diameter and length peaked at 0.5 ng/mL TGF-β1 with 11.3 ± 2.2 and 223.6 ± 15.8 μm, respectively (Figure 2.3b,c). However, fiber analysis of AI revealed that all doses of TGF-β1 resulted in AI ranging from 1.17 to 1.24 with no statistical difference between groups (Figure 2.S5). Notably, all constructs cultured in the 500 mg/L glucose had a similar final size, indicating that TGF-β1 influences remodeling of the collagen network in a manner independent of the level of construct contraction (see Figure 2.S6 for representative high, median, and low fiber organization of each group). Based on these observations, meniscal constructs with mechanical anchoring were cultured in 500 mg/L glucose to maximize collagen organization.

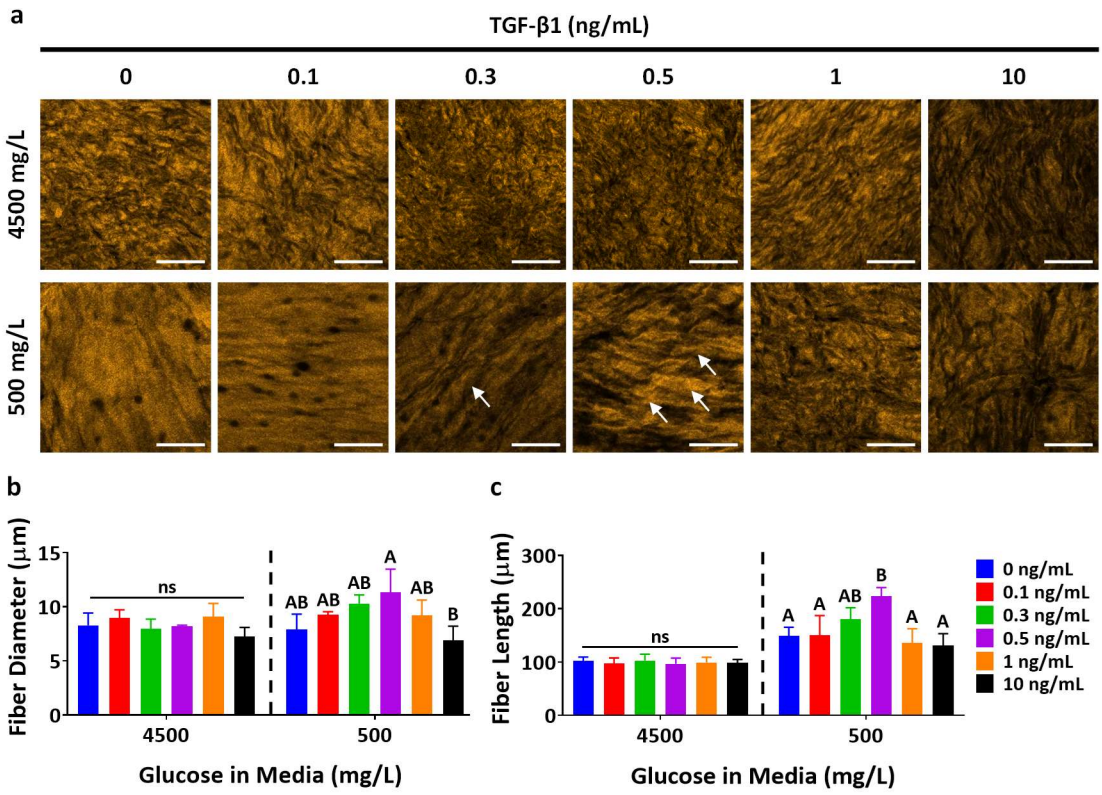

Figure 2.3. Fiber organization of disc constructs after 30 days of culture. (a) Representative SHG images of disc constructs cultured in 4500 mg/L glucose (top) and in 500 mg/L glucose (bottom) at indicated TGF-β1 concentrations. Representative areas with aligned collagen fibers are indicated by white arrows. Scale bars are 100 μm. Average collagen fiber (b) diameter and (c) length (n = 3). Different letters represent statistical significance between groups ($p < 0.05$). No comparison was done between groups cultured in different medium glucose concentrations.

	TGF-β1 (ng/mL)					
	0	0.1	0.3	0.5	1	10
4500 mg/L	1.16	1.13	1.11	1.13	1.27	1.24
500 mg/L	1.08	1.21	1.22	1.24	1.13	1.21

Table 2.S1. Alignment index of representative SHG images of disc constructs in Figure 3a.

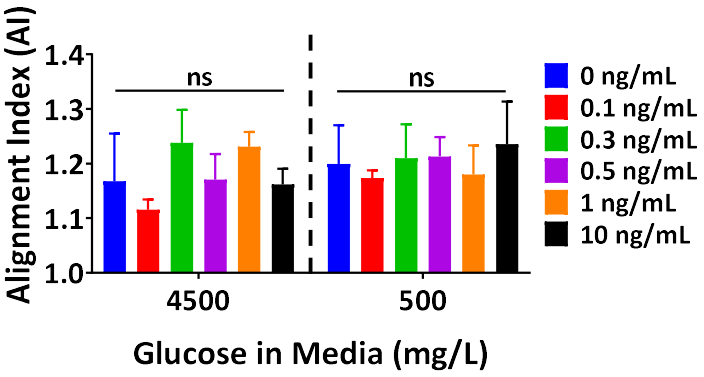

Figure 2.S5. Fiber analysis of disc constructs after 30 days of culture in 4500 mg/L and 500 mg/L glucose as a function of TGF-β1 dose. (ns, non-significant; n = 3). No comparison was done between groups cultured in different medium glucose concentrations.

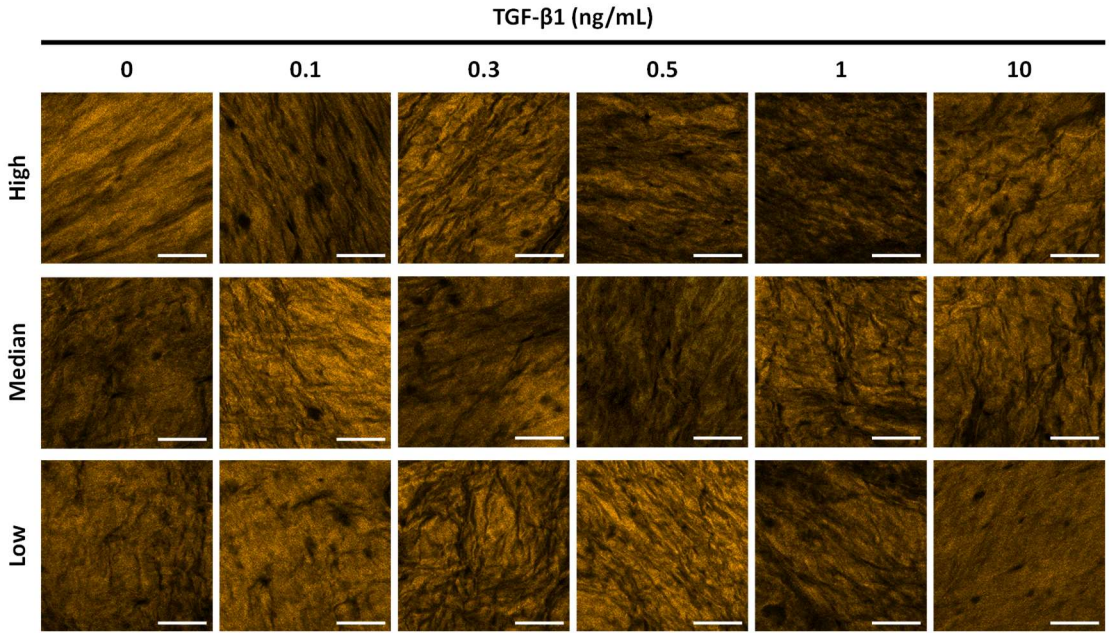

Figure 2.S6. Selected SHG images representing high, median, and low fiber organization of disc constructs cultured in 500 mg/L glucose after 30 days of culture. Each representative image shows high (top), median (middle), and low (bottom) fiber

organization within disc constructs at indicated TGF-β1 concentrations. Scale bars are 100 μm.

Meniscal Construct Contraction. It has been shown that static mechanical boundary conditions can contribute to native-tissue-like fiber organization within collagen-based meniscal constructs[12,13]. To evaluate how TGF-β1 treatment affects collagen fiber formation in combination with mechanical anchoring, meniscal constructs were fabricated and clamped at the extensions, as previously described[12,14]. Subsequently, meniscal constructs were cultured in 500 mg/ L glucose along with 6 different concentrations of TGF-β1 ranging from 0 to 10 ng/mL. Meniscal constructs maintained around 80% of their original size over time in culture except for 5 and 10 ng/mL of TGF-β1-treated groups which showed a greater contraction to ~60% of their initial size (Figure 2.4a-c). Moreover, the meniscal constructs, which were mechanically anchored, appeared to contract less than the unconstraint disc constructs when relatively low concentrations of TGF-β1 were used. Additionally, the contraction rate of the meniscal constructs also showed a dose-dependent response with EC_{50} at 0.28 ng/mL ($R^2 = 0.7145$), which is similar to that of the disc constructs (Figure 2.4d).

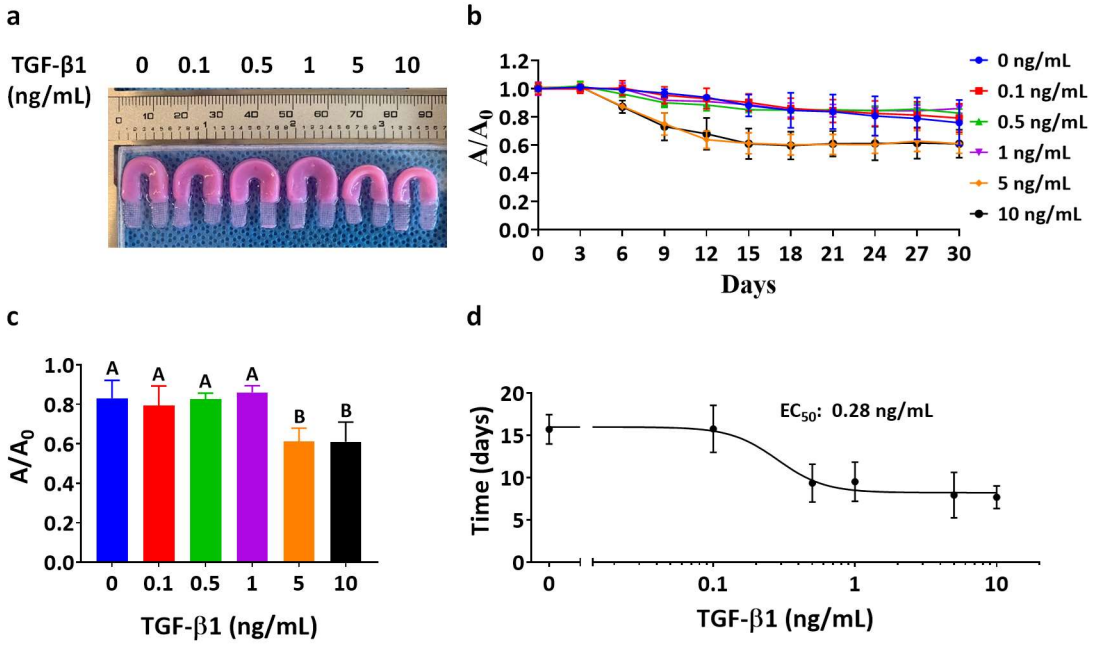

Figure 2.4. Contraction of meniscal constructs over 30 days of culture. (a) Photographs of meniscal constructs after 30 days of culture in 500 mg/L glucose and indicated TGF-β1 concentrations. (b) Ratio of projected meniscal construct area to initial projected area over time in culture measured in the same fashion (n = 4-5). (c) Ratio of projected area over initial projected area at day 30 (n = 4-5). (d) Time required for half-maximal contraction as a function of TGF-β1 concentrations. Different letters represent statistical significance between groups ($p < 0.05$).

Meniscal Construct GAG Production. The amount of GAG deposited in meniscal constructs and released to media was measured to reveal the cumulative effects of TGF-β1 and mechanical anchoring on GAG production by fibrochondrocytes. The GAGs/ww significantly increased in only 5 and 10 ng/mL of TGF-β1-treated groups by ~250% and ~280%, respectively, compared to the untreated group (Figure 2.5a). Additionally, the total GAG production showed a dose-dependent increase with EC_{50} at

0.53 ng/mL (R^2 = 0.892) (Figure 2.5b). The DNA content, however, showed a decreasing trend up to 5 ng/mL of TGF-β1 but recovered at 10 ng/mL TGF-β1 (Figure 2.S7, left). Intriguingly, the GAG content normalized to the DNA content gradually increased up to 5 ng/mL TGF-β1 but showed a nominal decrease at 10 ng/mL TGF-β1 compared to 5 ng/mL TGF-β1 (Figure 2.S7, right). Similar to the disc constructs, hydroxyproline content per meniscal construct did not show any significant difference between groups (Figure 2.S8, left). However, the Hypro/ww slightly decreased with increasing TGF-β1 concentrations up to 1 ng/mL and recovered at 5 and 10 ng/mL TGF-β1 (Figure 2.S8, right).

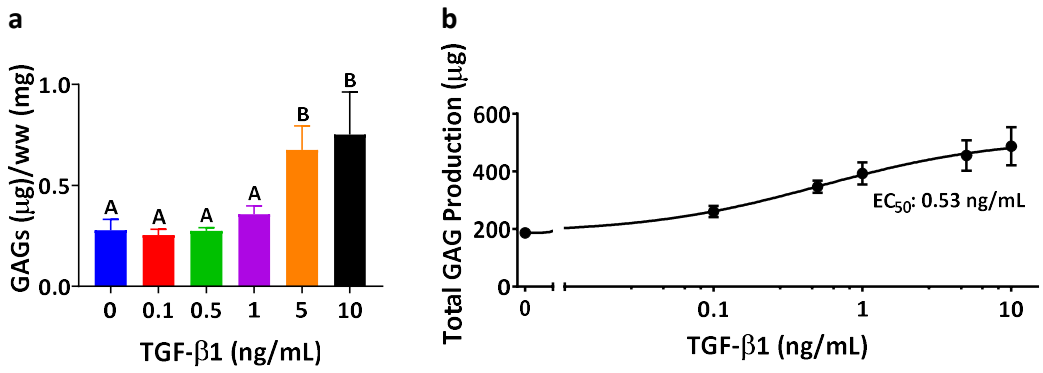

Figure 2.5. GAG content in meniscal constructs with mechanical anchoring and total GAG production throughout 30 days of culture analyzed by the DMMB assay. (a) GAG content in meniscal constructs normalized to wet weight (n = 4-5). (b) Total GAG production (calculated the same as in Figure 2b) as a function of TGF-β1 concentration. Different letters represent statistical significance between groups ($p < 0.05$).

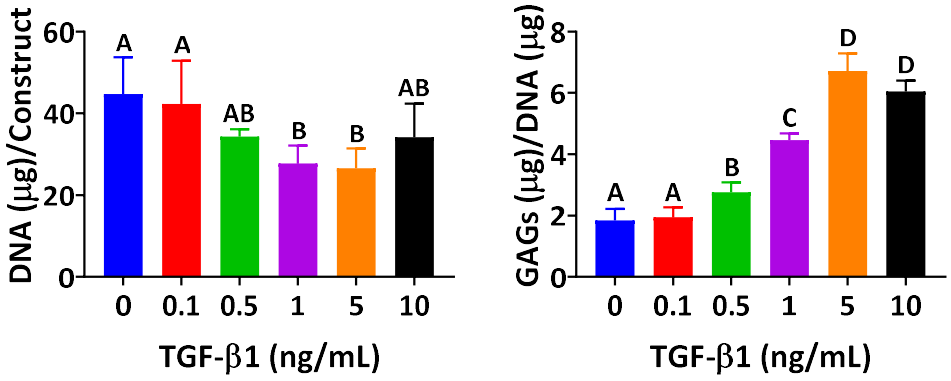

Figure 2.S7. DNA content (left) and total GAG production standardized to DNA content (right) in each meniscal construct after 30 days of culture analyzed by the DNA Hoechst assay and the DMMB assay. Different letters represent statistical significance between groups ($p < 0.05$ and $n = 4$-5).

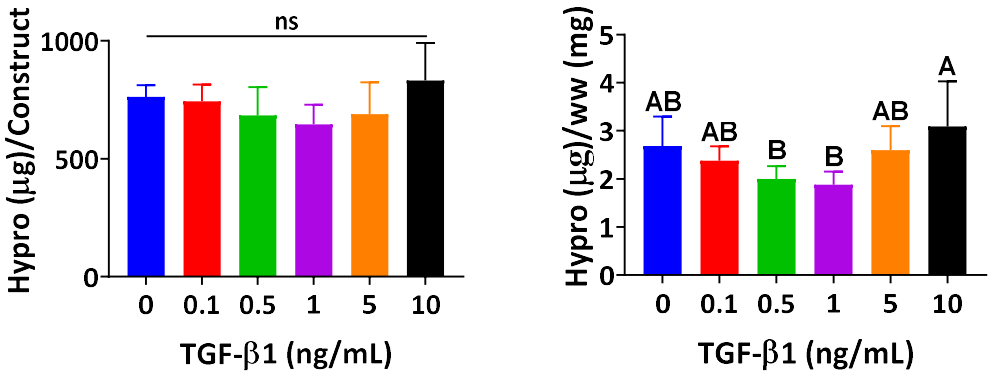

Figure 2.S8. Hydroxyproline content per meniscal construct (left) and normalized to wet weight (right) after 30 days of culture analyzed by the hydroxyproline assay. Different letters represent statistical significance between groups (ns, non-significant; $p < 0.05$; $n = 4$-5).

Fiber Alignment Analysis on Meniscal Constructs via SHG Imaging and Picrosirius Red Staining. As observed in the disc constructs cultured in 500 mg/L glucose (Figure 2.3a, bottom), meniscal constructs also showed different fiber

development in response to TGF-β1 (Figure 2.6a). Thin but long collagen fibers, smaller than 10 μm in diameter and greater than 150 μm in length, were observed in control and 0.1 ng/mL TGF-β1-treated groups along with relatively evenly dispersed fibrochondrocytes. The meniscal constructs treated with 0.5 ng/mL of TGF-β1 exhibited significantly larger collagen fibers. The mean fiber diameter and length were 17.5 ± 2.1 and 262.0 ± 13.0 μm, approaching native tissue levels averaging around 35 μm in diameter and greater than hundreds of microns in length (Figure 2.6b,c)[12,13,41]. Furthermore, the 0.5 ng/mL of the TGF-β1-treated group showed the highest AI, comparable to that of native tissue (Figure 2.6d). In addition, laterally joined collagen fibers (indicated by white arrows in Figure 2.6a, top) were observed. Fibrochondrocytes were also found to be aligned with the collagen fibers (shown in the boxed area in Figure 2.6a, top and Figure 2.S9). The 1, 5, and 10 ng/mL of TGF-β1-treated groups showed more compact and disorganized collagen fibers, resulting in significant decreases in fiber diameter, length, and AI compared to the 0.5 ng/mL of the TGF-β1-treated group. Picrosirius red stained images were consistent with the SHG images. Picrosirius red staining highlights large fibers in yellow or orange. Notably, the 0.5 ng/mL TGF-β1 group showed large and continuous fibers while the other groups displayed small or discontinuous fibers in a random direction (Figure 2.6a, middle and bottom).

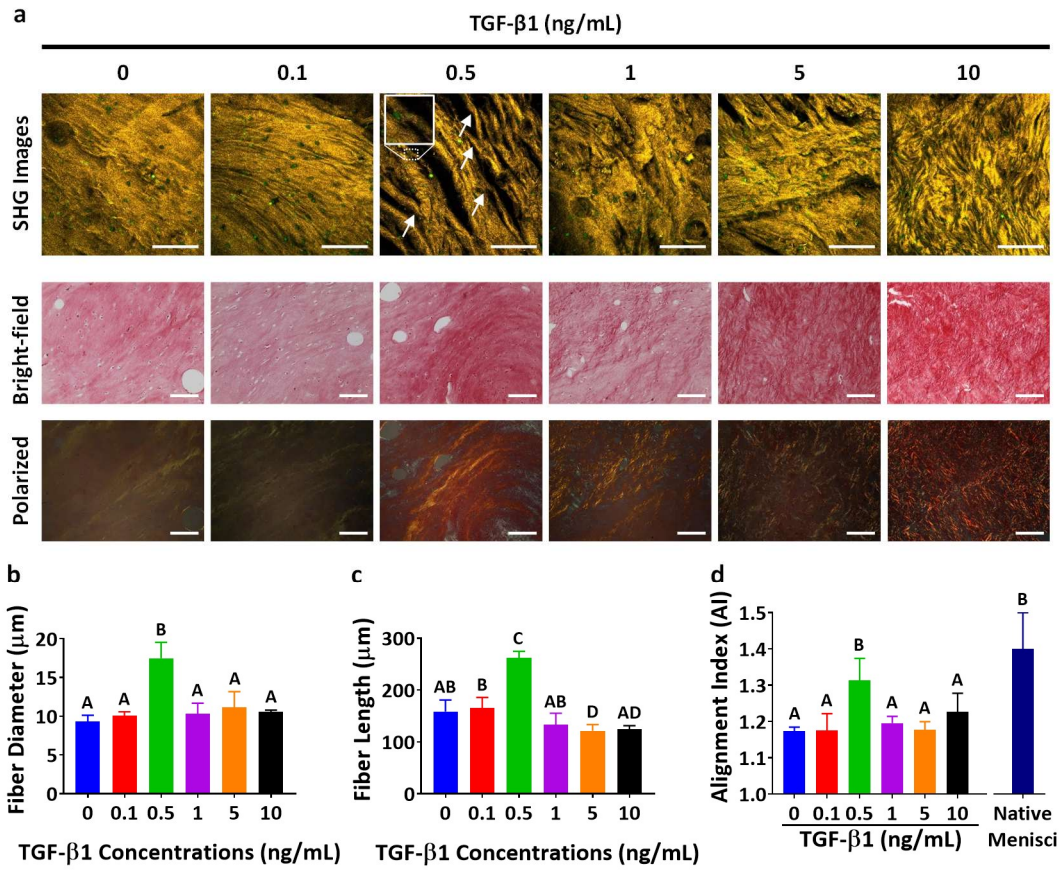

Figure 2.6. Fiber organization of meniscal constructs after 30 days of culture as a function of TGF-β1 dose. (a) Representative SHG (top), picrosirius red staining under bright-field (middle) and polarized (bottom) light images. Cellular autofluorescence is shown in green (top). Scale bars are 100 μm. Quantitative analysis of collagen fiber (b) diameter, (c) length, and (d) alignment index (n = 4-5). Different letters represent statistical significance between groups ($p < 0.05$).

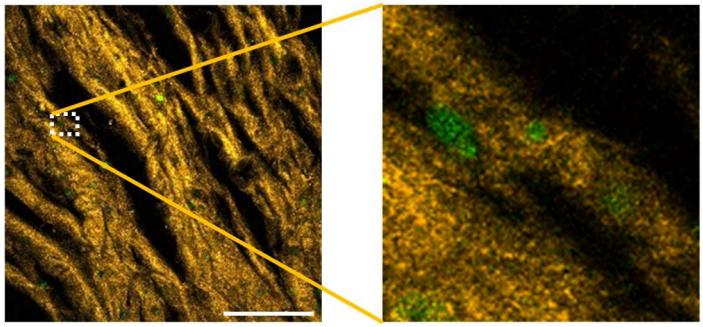

Figure 2.S9. Fibrochondrocyte distribution in the 0.5 ng/mL TGF-β1 treated meniscal construct. The magnified boxed area is shown on the right. Fibrochondrocytes (green) were found along with collagen fibers (yellow).

Collagen Production and α-SMA Expression. TGF-β1 is known to promote a chondrogenic phenotype and enhance cellular contractility[24,25,42,43]. To assess both phenotype and contractile behavior of fibrochondrocytes, we performed immunohistochemical staining for types I and II collagen as well as α-SMA. As meniscal constructs were formed from a type I collagen gel, all meniscal constructs exhibited the presence of type I collagen. However, the staining intensity of type I collagen appeared to decrease with increasing TGF-β1 concentrations (Figure 2.7, top). Type II collagen was also detected in all groups, but the staining was more intense at 5 and 10 ng/mL TGF-β1 (Figure 2.7, middle). All groups stained positive for α-SMA without a noticeable difference between the groups, as is supported by a quantitative analysis of cells exhibiting α-SMA staining (Figure 2.7, bottom and Figure 2.S10). Negative controls did not show any staining (Figure 2.S11).

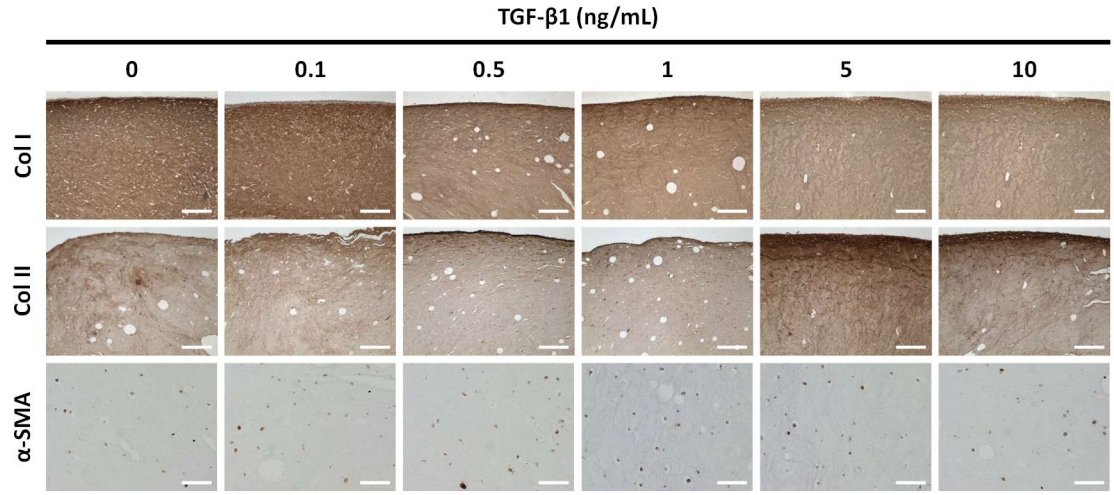

Figure 2.7. Immunohistochemical staining (DAB, brown) for type I collagen (top), type II collagen (middle), and intracellular α-SMA (bottom) of the meniscal constructs after 30 days of culture. Scale bars are 200 μm.

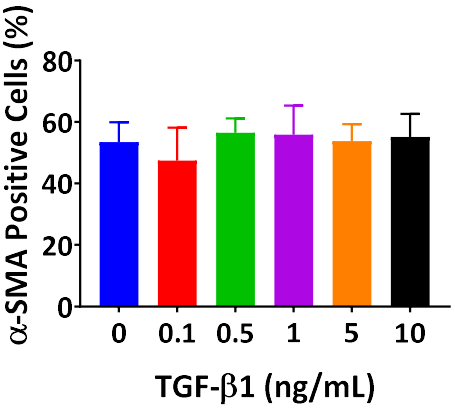

Figure 2.S10. The percentage of α-SMA positive cells (no statistical difference detected between groups, $p < 0.05$, $n = 4$-5).

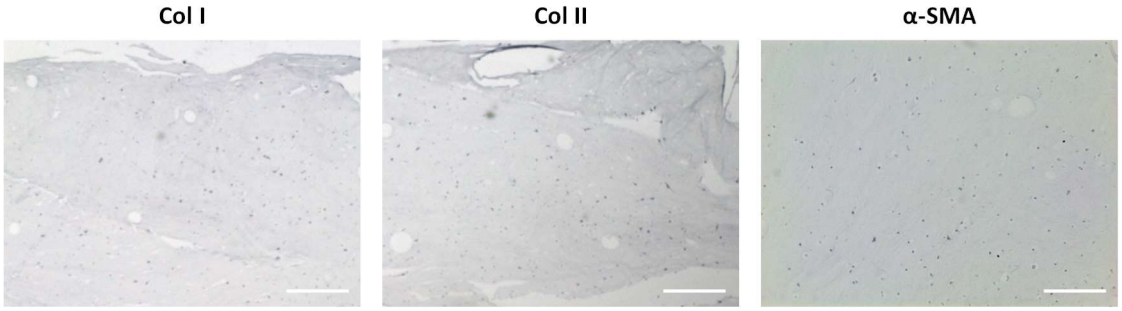

Figure 2.S11. Representative negative controls of immunohistochemical staining for collagen type I (left), collagen type II (middle), and intracellular α-SMA (right) of the meniscal constructs after 30 days of culture. Scale bars are 200 μm.

Construct Mechanical Properties. In order to investigate how these compositional and structural differences affect the functionality of tissue-engineered menisci, we performed tensile and compression testing on the tissue-engineered menisci. Tensile analysis demonstrated that only the samples treated with 0.5 ng/mL of TGF-β1 showed significantly enhanced tensile modulus and UTS compared to the control group by 1.7- and 2.0-fold, respectively (Figure 2.8a). Samples treated with 1 ng/mL of the TGF-β1-treated group showed a 2.3-fold increase in an equilibrium compressive modulus ($p < 0.05$), and those treated with 5 and 10 ng of TGF-β1 were similar to the 1 ng/mL of TGF-β1 ($p > 0.85$) (Figure 2.8b). Furthermore, we performed a correlation analysis to examine the relationship between these measured parameters and biochemical and structural measurements (Figure 2.S12). Mechanical properties (tensile modulus, UTS, and equilibrium modulus) were compared with other biochemical and structural properties. Tensile modulus was strongly correlated with fiber diameter ($R^2 = 0.96$ and $p < 0.01$) and fiber length ($R^2 = 0.86$ and $p < 0.01$), while moderately correlated with AI ($R^2 = 0.69$ and $p = 0.04$). UTS was strongly correlated

with fiber diameter ($R^2 = 0.96$ and $p < 0.01$), fiber length ($R^2 = 0.79$ and $p = 0.02$), and AI ($R^2 = 0.74$ and $p = 0.03$). Equilibrium modulus was moderately correlated with total GAG content per construct ($R^2 = 0.46$ and $p = 0.14$) (Figures 2.S12 and 2.S13).

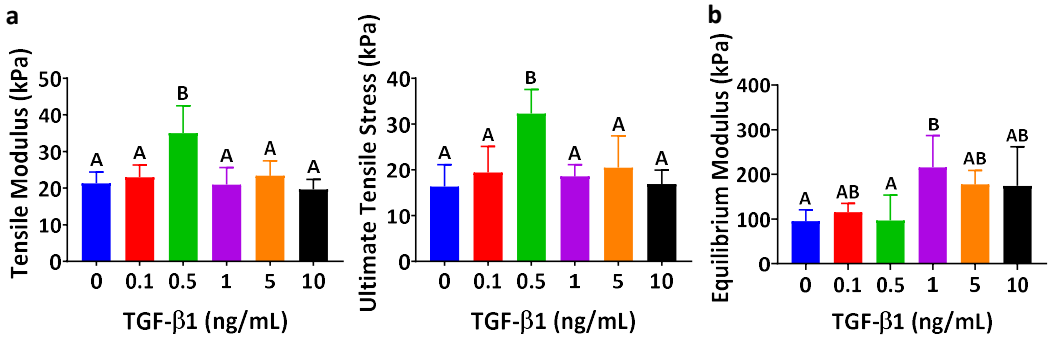

Figure 2.8. Mechanical properties of tissue engineered meniscal constructs after 30 days of culture. (a) Tensile modulus and ultimate tensile stress (UTS) (n = 4-5). (b) Equilibrium modulus (n = 4-5). Different letters represent statistical significance between groups ($p < 0.05$).

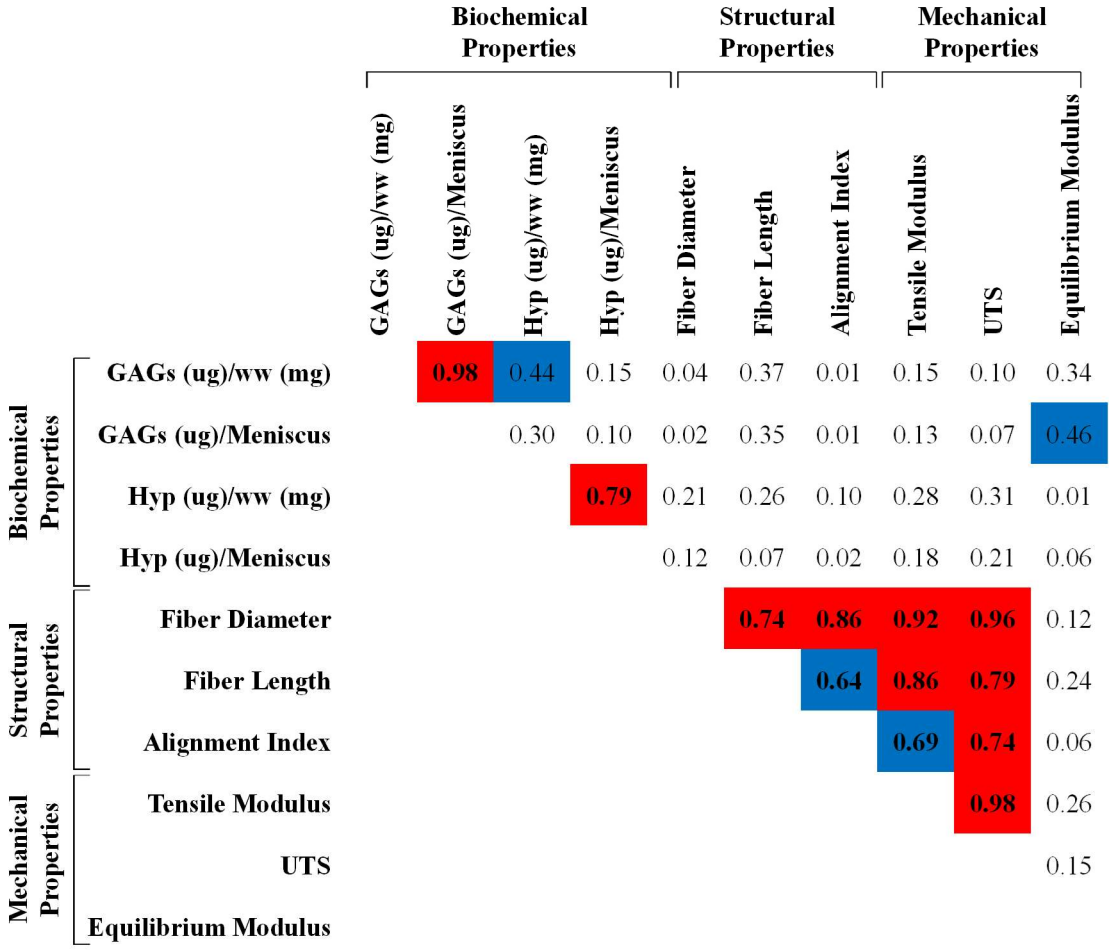

Figure 2.S12. Correlation analysis (R^2) between biochemical, structural, and mechanical properties. Red indicates strong correlations ($R^2 \geq 0.7$), and blue indicates moderate correlations ($R^2 < 0.7$ and $R^2 \geq 0.4$). Bolded values indicate significant correlations with $p < 0.05$.

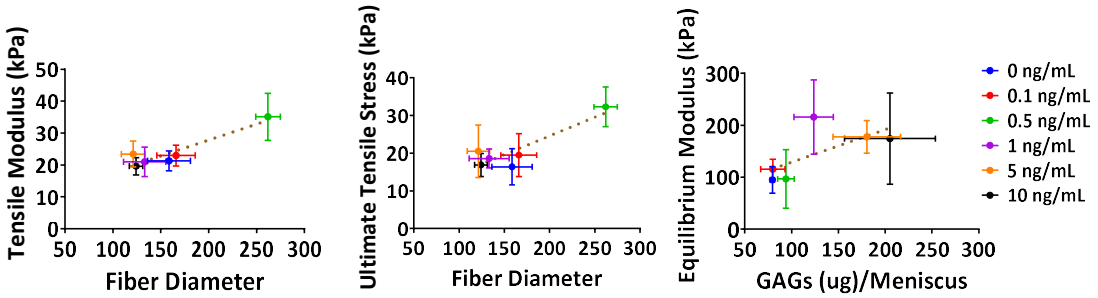

Figure 2.S13. Representative correlation analysis of tensile modulus, ultimate tensile

stress, and equilibrium modulus. Each data point indicates the TGF-β1 concentration of each group.

Discussion

The objective of this study was to investigate the combined effects of TGF-β1, glucose, and mechanical anchoring on collagen fiber architecture of tissue-engineered menisci. Previously, we assessed the role of glucose and mechanical anchoring independently[12,14]. In this work, we examined how biochemical and biomechanical factors interact to optimize fiber formation and alignment in meniscal constructs. We found that the optimal fiber formation, as assessed by fiber diameter, length, and AI, occurred in media with 500 mg/L glucose, 0.5 ng/mL TGF-β1, and mechanical anchoring. Interestingly, these concentrations of glucose and TGF-β1 are both lower than those conventionally used in tissue engineering of cartilage and fibrocartilage[31,32].

This study demonstrated that TGF-β1 enhanced the rate of construct contraction with an EC_{50} ranging from 0.23 to 0.28 ng/mL and the synthesis of proteoglycans with an EC_{50} ranging from 0.53 to 1.71 ng/mL. Interestingly, collagen fiber organization was most effectively enhanced at intermediate concentrations of TGF-β1 (0.3 and 0.5 ng/mL). Moreover, the effect of TGF-β1 on fiber formation was most prominent in media with 500 mg/L glucose and in samples that were mechanically anchored. As such, these data indicate that considerable interplay of biochemical and biomechanical stimuli relates to overall collagen fiber development in tissue-engineered constructs.

Contraction of collagen-based constructs is considered indicative of cell-mediated collagen remodeling. Furthermore, cell-mediated contraction with mechanical

anchoring enhances matrix organization and mechanical properties of scaffolds[44–47]. Dramatic contraction of tissue-engineered constructs, however, potentially imposes a significant clinical problem since anatomical matching to defect size is critical to prevent meniscal replacements from extruding or degenerating after implantation[48]. Disc contraction data revealed that glucose has a profound effect on the final level of contraction while TGF-β1 facilitates construct contraction. It has been shown that glucose increases expression of integrins in fibroblasts, glomerular epithelial cells, and podocytes[49–51]. In particular, enhanced expression of α1β1 integrin in fibroblasts resulted in increased contraction of the collagen matrix, indicating that glucose enhances cell-ECM interaction[51]. Thus, the significant contraction observed in the disc constructs cultured in 4500 mg/L glucose media might result from higher activation of integrins in fibrochondrocytes. Furthermore, we previously demonstrated that mechanical anchoring helps reduce the isotropic nature of contraction of collagen-based scaffolds and thus prevents dramatic contraction[12,33]. In this context, the use of relatively low glucose media and mechanical anchoring is beneficial for culturing collagen-based scaffolds seeded with fibrochondrocytes. Furthermore, dramatic contraction could potentially limit space for cells to remodel the surrounding ECM, which might lead to inferior matrix organization and mechanical performance.

Glycosaminoglycans are one of the major components of the native meniscus and play a key role in mechanical properties, especially resistance to compressive load. Additionally, proteoglycans consisting of core proteins and glycosaminoglycan chains also have been shown to interact with collagen fibrils and subsequently play a role in fibrillogenesis[14,27,52–55]. Studies on the development of fibrocartilage tissues, for

example, ligament and meniscus, revealed that collagen fiber growth, by fusion of adjacent collagen fibrils, initiates when proteoglycan contents decrease[27,56]. Furthermore, collagen fiber architecture is actively developed during pre- and neonatal phases while GAG deposition occurs with advancing age[13,57–59]. These data indicate the importance of temporal variation in GAG content over the culture period in order to establish fiber networks with similarities to native menisci. For example, we showed that reducing GAG content during collagen fiber development before increasing GAG deposition results in the establishment of a fiber network that is similar to native menisci[14]. Biochemical analysis of the disc constructs showed that total GAG production did not significantly change in response to glucose concentrations in medium, but the amount of GAG accumulating in constructs (GAGs/ww) was affected by TGF-β1. This difference in GAG accumulation may result from both the chondrogenic effects of TGF-β1 as well as enhanced contraction. Uncontrolled and dramatic construct contraction can lead to an undesirable increase in the local concentration of glycosaminoglycans involved in collagen fibrillogenesis. The increased concentration might give rise to an excessive interaction between glycosaminoglycans and collagen fibrils, leading to the impairment of fiber organization, consistent with previous studies showing that the excess amount of proteoglycans resulted in a decreased fiber diameter and organization[13,53,60].

Comparison of disc and meniscal constructs suggests that mechanical anchoring not only reduces the contraction of collagen-based constructs by providing mechanical supports but also enhances cellular responses induced by TGF-β1. We previously demonstrated that when clamped at the extension mimicking a native meniscal horn,

constructs contract less and exhibit more aligned fibers[12], which was also shown in this study. The reduction of construct contraction resulting from mechanical anchoring is likely to be beneficial for clinical applications in preventing size mismatching particularly when contraction-inducing growth factors are used. Furthermore, a significant increase in AI as well as fiber diameter and length was only seen when both mechanical anchoring and 0.5 ng/mL of TGF-β1 were applied. These data indicate a critical interaction mechanical anchoring and TGF-β1 on collagen fiber development.

Interestingly, mechanical anchoring also appeared to enhance the sensitivity of fibrochondrocytes to TGF-β1, as indicated by a 2.5-fold lower EC_{50} for total GAG production in the anchored constructs compared to the disc constructs (0.53 ng/mL vs 1.34 ng/mL, respectively). Additionally, the effect of TGF-β1 on cell proliferation was dependent on mechanical anchoring. Without mechanical anchoring, all disc constructs cultured in 500 mg/L glucose showed no significant difference in the DNA content. However, with mechanical anchoring, only the 10 ng/mL of the TGF-β1 treatment group showed comparable cell proliferation to the nontreated group while the other TGF-β1 treatment groups exhibited decreasing trends in proliferation. Conversely, GAG production showed a significant increase with the increasing TGF-β1 concentrations, and the GAG production normalized to DNA content peaked at the 5 ng/mL TGF-β1 concentration where the lowest DNA content was detected. On the contrary, without mechanical anchoring, only the 10 ng/mL of TGF-β1 treatment resulted in a significant increase in the GAGs/DNA in both glucose groups. These data indicate that the effects of TGF-β1 on GAG production and cell proliferation of fibrochondrocytes are not only biomechanical stimulus-dependent but also

concentration-dependent. It can be surmised that when TGF-β1 concentrations reach a certain threshold in media, the TGF-β1 takes on roles in both these mechanisms. The detailed mechanism of this transition is not clear, but we can speculate that in the presence of mechanical anchoring, TGFβ1 initiates higher production of GAGs rather than cell proliferation at relatively low concentrations while at relatively high concentrations, TGF-β1 promotes both GAG production and cell proliferation. This observation is consistent with other studies showing that the effects of growth factors including TGF-β1 can vary depending on concentrations and the presence of mechanical stimuli, although fibrochondrocytes were from different sources[23,42,61–63].

TGF-β1 is one of the most commonly used growth factors in cartilage and meniscus tissue engineering due to its well-known ability to enhance GAG and collagen production, two major biochemical components of articular cartilage and meniscus[64]. Thus, most studies using TGF-β1 mainly focused on achieving the highest GAG production in monolayer or explant cultures of human, bovine, ovine, porcine, and leporine menisci[17,25,26,43,65]. The concentrations of TGF-β1 used in these studies are frequently higher than EC_{50} for the construct contraction rate and the GAG production. In our study, we show that an optimal concentration range of TGF-β1 exists for promoting collagen fiber organization. This concentration range, between 0.27 and 0.53 ng/mL TGF-β1 as indicated by the EC_{50} for the contraction rate and GAG production, seeks a balance between cell-mediated remodeling and GAG production. Consequently, we observed the most robust and aligned fiber organization in the 0.5 ng/mL TGF-β1-treated group. Moreover, gene expressions of Lox and Dpt, modulators of TGF-β1, have been shown to be present in an early embryonic meniscus development, and their

expression levels increase with age[66]. These observations support the idea that at the early stage of fiber development, fiber alignment and/or growth precede GAG deposition in conjunction with an appropriate concentration of TGF-β1. Therefore, the choice of TGF-β1 concentrations should be taken into consideration regarding the purpose of the use of TGF-β1, such as fiber organization or GAG production.

Native menisci display regional variations in ECM components and cellular phenotypes. Type I collagen is a primary component of the ECM, but type II collagen is also present within the native meniscus. Aside from recapitulating fiber organization, mimicking biochemical distribution is also essential for tissue engineering a whole meniscal construct. Immunohistochemical staining showed that type I collagen staining decreased while type II collagen staining increased with the increasing TGF-β1 concentrations, demonstrating that TGF-β1 can drive fibrochondrocytes toward more chondrogenic behavior. This observation is consistent with the previous literature showing that TGF-β1 increases a ratio of type II collagen to total collagen produced by chondrocytes[67]. Interestingly, type II collagen appeared to be more concentrated to the outer layer of the tissue-engineered meniscus where most contraction occurred, which might lead to accumulation of newly synthesized type II collagen. In addition, the outer layer is likely to be directly exposed to TGF-β1, resulting in more production of type II collagen than other areas. This distribution is opposite to that of native tissue and thus should be addressed in future studies.

Cells expressing α-SMA are involved in the reparative process of fibrous tissues due to their increased proficiency at remodeling surrounding collagen networks[68–70]. Fibrochondrocytes have been shown to express α-SMA, and the expression of α-SMA

in fibrochondrocytes can be enhanced by TGF-β1, leading to an enhanced contraction of the collagen-GAG matrix[24,28]. We observed no significant difference in α-SMA staining between groups, but all groups were stained positive for α-SMA to some extent. One possible explanation might be that an increase in α-SMA production occurred when meniscal construct contraction actively took place, which was from day 3 to 15. Once the contraction plateaued, the effect of TGF-β1 on α-SMA may have diminished. This explanation is supported by a study showing a rapid turnover of α-SMA, where pretreatment with TGF-β1 did not affect the contractile behavior of fibrochondrocytes[24]. Another possible explanation could be that fibrochondrocytes might not actively express α-SMA under the 500 mg/L media glucose concentration where glucose supply is limited.

Histology and immunohistochemistry images displayed several holes, which are presumably air bubbles trapped in the collagen matrix during construct fabrication. Interestingly, fewer holes were found in the 5 and 10 ng/mL of TGF-β1- treated groups, which showed significant contraction compared to the other groups. This observation indicates that cell-mediated collagen remodeling is unlikely influenced by these holes. Considering the fact that the meniscal constructs were created on the same day and randomly divided into the groups and that the 0.5 ng/mL of the TGF-β1-treated group showed the enhanced structural features, these holes appear to have minimal effects on the collagen alignment.

Controlling structural and compositional properties is essential for the enhancement in mechanical performance of tissue-engineered menisci. In this study, these properties were successfully regulated using mechanical and biochemical stimuli,

subsequently leading to increases in both tensile modulus and UTS of the tissue-engineered menisci. The optimal condition for collagen fiber organization resulted in the enhanced tensile modulus and UTS. Furthermore, correlation analysis demonstrated that tensile modulus and UTS are strongly correlated with structural properties while GAG content per construct is the best predictor for the equilibrium modulus (Figure 2.S12). These findings are consistent with many previous studies showing that the native collagen fiber structure is responsible for tensile properties while glycosaminoglycans for compressive resistance[64,71–73]. These observations indicate the importance of appropriate tuning of the culture environment including mechanical anchoring and media compositions for better mechanical performance.

One of the limitations of this study is that the GAG content our meniscal constructs contained is an order of magnitude lower than native tissue. A possible solution to increase GAG production in our tissue-engineered constructs is the use of dynamic mechanical loading. Compared to static compression, dynamic compressive loading systems lead to a significant increase in the production of ECM components[74–76]. Furthermore, this increase in ECM production occurs over long culture time periods[76]. Therefore, applying dynamic mechanical stimulation, longer culture times, or temporal control over media regimens utilizing a lower TGF-β1 concentration for fiber alignment and a higher TGF-β1 concentration for GAG production may drive these constructs toward native tissue compositions. Furthermore, native tissue has ~30 Hypro/ww (μg/mg) with tensile modulus, UTS, and elastic modulus ranging from approximately 13-26 MPa, 4-19 MPa, and 110-500 kPa, respectively[77–79]. While the meniscal constructs showed the elastic modulus comparable to native tissue in this

study, the hydroxyproline content and tensile properties did not reach the native tissue levels. Given that collagen organization is a key factor for tensile properties of the meniscal constructs[80,81], future studies will pay more attention to establishing native tissue-like collagen content and fiber structure. Aforementioned approaches for enhancing GAG content within the meniscal constructs can also be utilized to improve collagen content and mechanical properties.

Another limitation of this study is that direct comparisons between disc and meniscal constructs with regard to the effects of mechanical anchoring might be difficult due to the dissimilar dimensions of disc and meniscal constructs. This dissimilarity can also contribute to different diffusion kinetics of biological molecules including glucose and TGF-β1 and to contraction forces generated over the culture period. In addition, in this study, fibrochondrocytes from juvenile bovine menisci were employed. It has been demonstrated that fibrochondrocytes from adult bovids show a higher ratio of collagen type I to II gene expression compared to those cells from juvenile bovids[82]. The effects of growth factors on fibrochondrocytes from either juvenile or adult bovids also vary[19]. With regard to the zonal difference, it has been shown that cells from the inner zone produce more proteoglycans than those cells from the outer zone[43]. As such, further validation depending on construct geometry and cell sources might be required. Moreover, collagen fiber organization was investigated using SHG and histological microscopy. These techniques have a limited capability of capturing the fibril-level structure. As such, assessing nanoscale tissue-engineered meniscus structure using scanning or transmission electron microscopy or atomic force microscopy will provide a better understanding of how biochemical and biomechanical stimuli affect the

collagen fibril structure in tissue-engineered menisci[80,83]. Finally, the optimal concentrations of glucose and TGF-β1 for enhancing collagen fiber organization can vary depending on other parameters related to initial properties of collagen constructs, such as initial collagen density, gelation pH, cell seeding density, or sizes of constructs. Therefore, the optimal concentrations of glucose and TGF-β1 may be different for different collagen gel formulations, and thus, optimization of glucose and TGF-β1 concentrations should be performed on other systems as needed.

The heterogeneity of the native meniscus should be carefully considered in future studies. The native meniscus exhibits distinct spatial distribution of biological components including collagen and GAGs, regional structure patterns of collagen fibers, and anisotropic mechanical properties[83]. A potential approach to incorporate these characteristics of native tissue into tissue-engineered menisci might be the use of a multi-chamber bioreactor. Recent work from our laboratory demonstrated that the use of the tri-chamber bioreactor allows for spatial application of different types of media to tissue-engineered constructs[15]. Thus, our current culture system can be further modified to include multiple chambers. With the new system, 4500 mg/L glucose and 10 ng/mL TGF-β1 containing media can be applied to the inner zone of the meniscal construct for higher GAG production and randomly organized collagen fibers while 500 mg/L glucose and 0.5 ng/ mL TGF-β1 media to the middle/outer zone of the meniscal construct for less GAG production and highly aligned collagen fibers. Furthermore, seeding fibrochondrocytes from different regions of menisci into the corresponding regions of tissue-engineered menisci might help generate tissue-engineered menisci with enhanced structural and compositional similarities to native tissue[43].

A significant amount of effort has been devoted to tissue engineering menisci using various techniques and materials. Due to differences in properties such as stiffness or cell adhesion, meniscal constructs made of materials other than collagen are unlikely to have contraction behavior similar to the constructs in the current work. Therefore, the findings from this study with regard to construct contraction might not be relevant to other studies, particularly any constructs fabricated using synthetic polymers. However, since collagen is a major component of native menisci and its structure is essential for mechanical properties of menisci, the majority of studies on tissue engineering menisci are presumably going to focus on producing bundles of large, organized collagen fibers. In this context, our findings regarding the combinational effects of glucose, TGF-β1, and mechanical anchoring on collagen fiber organization can be utilized in a wider range of studies.

Conclusions

We have demonstrated that biochemical and mechanical environments of tissue-engineered meniscal constructs can be manipulated to optimize collagen fiber formation. Notably, fiber formation was optimal at 500 mg/L glucose and 0.5 ng/ mL TGF-β1 in mechanically anchored constructs. The concentration of TGF-β1 that was optimal for fiber formation was between the two EC_{50} for construct contraction and proteoglycan production. Furthermore, the enhanced collagen fiber formation resulted in improved tensile modulus and UTS, suggesting the importance of interaction between these two factors. Collectively, these data point to the need for optimization of culture environments specifically geared toward enhancing collagen fiber formation and

organization.

References

(1) Hasan, J., Fisher, J. & Ingham, E. Current strategies in meniscal regeneration. *J. Biomed. Mater. Res. - Part B Appl. Biomater.* 102, 619–634 (2014).

(2) Mordecai, S. C. Treatment of meniscal tears: An evidence based approach. *World J. Orthop.* 5, 233 (2014).

(3) Fox, A. J. S., Wanivenhaus, F., Burge, A. J., Warren, R. F. & Rodeo, S. A. The human meniscus: A review of anatomy, function, injury, and advances in treatment. *Clin. Anat.* 28, 269–287 (2015).

(4) Sherman, S. L., Thomas, D. M., Gulbrandsen, T. R. & Farr, J. Meniscus Allograft Transplantation. *Oper. Tech. Sports Med.* 26, 189–204 (2018).

(5) Chevrier, A., Nelea, M., Hurtig, M. B., Hoemann, C. D. & Buschmann, M. D. Meniscus structure in human, sheep, and rabbit for animal models of meniscus repair. *J. Orthop. Res.* 27, 1197–1203 (2009).

(6) Ballyns, J. J., Wright, T. M. & Bonassar, L. J. Effect of media mixing on ECM assembly and mechanical properties of anatomically-shaped tissue engineered meniscus. *Biomaterials* 31, 6756–6763 (2010).

(7) Balint, E., Gatt, C. J. & Dunn, M. G. Design and mechanical evaluation of a novel fiber-reinforced scaffold for meniscus replacement. *J. Biomed. Mater. Res. - Part A* 100 A, 195–202 (2012).

(8) Huey, D. J. & Athanasiou, K. A. Maturational growth of self-assembled, functional menisci as a result of TGF-β1 and enzymatic chondroitinase-ABC

stimulation. *Biomaterials* 32, 2052–2058 (2011).

(9) Higashioka, M. M., Chen, J. A., Hu, J. C. & Athanasiou, K. A. Building an anisotropic meniscus with zonal variations. *Tissue Eng. - Part A* 20, 294–302 (2014).

(10) Patel, J. M., Merriam, A. R., Culp, B. M., Gatt, C. J. & Dunn, M. G. One-Year Outcomes of Total Meniscus Reconstruction Using a Novel Fiber-Reinforced Scaffold in an Ovine Model. *Am. J. Sports Med.* 44, 898–907 (2015).

(11) Lee, C. H. *et al.* Protein-releasing polymeric scaffolds induce fibrochondrocytic differentiation of endogenous cells for knee meniscus regeneration in sheep. *Sci. Transl. Med.* 6, (2014).

(12) Puetzer, J. L., Koo, E. & Bonassar, L. J. Induction of fiber alignment and mechanical anisotropy in tissue engineered menisci with mechanical anchoring. *J. Biomech.* 48, 1436–1443 (2015).

(13) McCorry, M. C. & Bonassar, L. J. Fiber development and matrix production in tissue-engineered menisci using bovine mesenchymal stem cells and fibrochondrocytes. *Connect. Tissue Res.* 58, 329–341 (2017).

(14) McCorry, M. C. *et al.* Regulation of proteoglycan production by varying glucose concentrations controls fiber formation in tissue engineered menisci. *Acta Biomater.* 100, 173–183 (2019).

(15) Iannucci, L. E., Boys, A. J., Mccorry, M. C., Estroff, L. A. & Bonassar, L. J. Cellular and Chemical Gradients to Engineer the Meniscus-to-Bone Insertion. *Adv. Healthc. Mater.* 1800806, 1–10 (2018).

(16) Ignotz, R. A. & Massagué, J. Transforming growth factor-beta stimulates the

expression of fibronectin and collagen and their incorporation into the extracellular matrix. *J. Biol. Chem.* 261, 4337–45 (1986).

(17) Pangborn, C. A. & Athanasiou, K. A. Effects of Growth Factors on Meniscal Fibrochondrocytes. *Tissue Eng.* 11, 1141–1148 (2005).

(18) Poniatowski, L. A., Wojdasiewicz, P., Gasik, R. & Szukiewicz, D. Transforming growth factor beta family: Insight into the role of growth factors in regulation of fracture healing biology and potential clinical applications. *Mediators Inflamm.* 2015, (2015).

(19) Ionescu, L. C., Lee, G. C., Huang, K. L. & Mauck, R. L. Growth factor supplementation improves native and engineered meniscus repair in vitro. *Acta Biomater.* 8, 3687–3694 (2012).

(20) Hidalgo Perea, S., Lyons, L. P., Nishimuta, J. F., Weinberg, J. B. & McNulty, A. L. Evaluation of culture conditions for in vitro meniscus repair model systems using bone marrow-derived mesenchymal stem cells. *Connect. Tissue Res.* 61, 322–337 (2020).

(21) Tessaro, I. *et al.* Characterization of different in vitro culture conditions to induce a fibro-chondrogenic differentiation of swine adipose-derived stem cells. *J. Biol. Regul. Homeost. Agents* 32, 97–103 (2018).

(22) Imler, S. M., Doshi, A. N. & Levenston, M. E. Combined effects of growth factors and static mechanical compression on meniscus explant biosynthesis. *Osteoarthr. Cartil.* 12, 736–744 (2004).

(23) Gunja, N. J., Uthamanthil, R. K. & Athanasiou, K. A. Effects of TGF-β1 and hydrostatic pressure on meniscus cell-seeded scaffolds. *Biomaterials* 30, 565–

573 (2009).

(24) Zaleskas, J. M. *et al.* Growth factor regulation of smooth muscle actin expression and contraction of human articular chondrocytes and meniscal cells in a collagen-GAG matrix. *Exp. Cell Res.* 270, 21–31 (2001).

(25) Collier, S. & Ghosh. Effects of transforming growth factor beta on proteoglycan synthesis by cell and explant cultures derived from the knee joint meniscus. *Osteoarthr. Cartil.* 3, 127–138 (1995).

(26) Lietman, S. A., Hobbs, W., Inoue, N. & Reddi, A. H. Effects of selected growth factors on porcine meniscus in chemically defined medium. *Orthopedics* 26, 799–803 (2003).

(27) Chen, S. & Birk, D. E. The regulatory roles of small leucine-rich proteoglycans in extracellular matrix assembly. *FEBS J.* 280, 2120–2137 (2013).

(28) Mueller, S. M., Schneider, T. O., Shortkroff, S., Breinan, H. A. & Spector, M. α-Smooth muscle actin and contractile behavior of bovine meniscus cells seeded in type I and type II collagen-GAG matrices. *Biomaterials* 45, 157–166 (1999).

(29) Bowles, R. D., Williams, R. M., Zipfel, W. R. & Bonassar, L. J. Self-Assembly of Aligned Tissue-Engineered Annulus Fibrosus and Intervertebral Disc Composite Via Collagen Gel Contraction. *Tissue Eng. Part A* 16, 1339–1348 (2010).

(30) Checa, S., Rausch, M. K., Petersen, A., Kuhl, E. & Duda, G. N. The emergence of extracellular matrix mechanics and cell traction forces as important regulators of cellular self-organization. *Biomech. Model. Mechanobiol.* 14, 1–13 (2015).

(31) Freed, L. E., Marquis, J. C., Langer, R. & Vunjak-Novakovic, G. Kinetics of

chondrocyte growth in cell-polymer implants. *Biotechnol. Bioeng.* 43, 597–604 (1994).

(32) Ragetly, G. R. *et al.* Effect of chitosan scaffold microstructure on mesenchymal stem cell chondrogenesis. *Acta Biomater.* 6, 1430–1436 (2010).

(33) McCorry, M. C. *et al.* A model system for developing a tissue engineered meniscal enthesis. *Acta Biomater.* 56, 110–117 (2017).

(34) Puetzer, J. L. & Bonassar, L. J. High density type I collagen gels for tissue engineering of whole menisci. *Acta Biomater.* 9, 7787–7795 (2013).

(35) Cross, V. L. *et al.* Dense type I collagen matrices that support cellular remodeling and microfabrication for studies of tumor angiogenesis and vasculogenesis in vitro. *Biomaterials* 31, 8596–8607 (2010).

(36) McCorry, M. C., Puetzer, J. L. & Bonassar, L. J. Characterization of mesenchymal stem cells and fibrochondrocytes in three-dimensional co-culture: Analysis of cell shape, matrix production, and mechanical performance. *Stem Cell Res. Ther.* 7, 1–10 (2016).

(37) Kim, Y.-J., Sah, R. L. Y., Doong, J.-Y. H. & Grodzinsky, A. J. Fluorometric assay of DNA in cartilage explants using Hoechst 33258. *Anal. Biochem.* 174, 168–176 (1988).

(38) Enobakhare, B. O., Bader, D. L. & Lee, D. A. Quantification of Sulfated Glycosaminoglycans in Chondrocyte/Alginate Cultures, by Use of 1,9-Dimethylmethylene Blue. *Anal. Biochem.* 243, 189–191 (1996).

(39) Neuman, R. E. & Logan, M. A. The Determination of Collagen and Elastin in Tissues. *J. Biol. Chem.* 186, 549–556 (1950).

(40) Boys, A. J. *et al.* Understanding the Stiff-to-Compliant Transition of the Meniscal Attachments by Spatial Correlation of Composition, Structure, and Mechanics. *ACS Appl. Mater. Interfaces* 11, 26559–26570 (2019).

(41) Jiang, D. *et al.* The Radiated Deep-frozen Xenogenic Meniscal Tissue Regenerated the Total Meniscus with Chondroprotection. *Sci. Rep.* 8, 1–12 (2018).

(42) Imler SM, Doshi, A. N. & Levenston, M. E. Effects of anabolic cytokines and static compression on meniscus tissue explants. *Trans Orthop Res Soc* 50, 633 (2004).

(43) Tanaka, T., Fujii, K. & Kumagae, Y. Comparison of biochemical characteristics of cultured fibrochondrocytes isolated from the inner and outer regions of human meniscus. *Knee Surgery, Sport. Traumatol. Arthrosc.* 7, 75–80 (1999).

(44) Nirmalanandhan, V. S. *et al.* Effect of scaffold material, construct length and mechanical stimulation on the in vitro stiffness of the engineered tendon construct. *J. Biomech.* 41, 822–828 (2008).

(45) Krishnan, L. *et al.* Effect of mechanical boundary conditions on orientation of angiogenic microvessels. *Cardiovasc. Res.* 78, 324–332 (2008).

(46) Evans, M. C. & Barocas, V. H. The modulus of fibroblast-populated collagen gels is not determined by final collagen and cell concentration: Experiments and an inclusion-based model. *J. Biomech. Eng.* 131, 1–7 (2009).

(47) Morin, K. T., Smith, A. O., Davis, G. E. & Tranquillo, R. T. Aligned human microvessels formed in 3D fibrin gel by constraint of gel contraction. *Microvasc. Res.* 90, 12–22 (2013).

(48) Brophy, R. H. & Matava, M. J. Surgical options for meniscal replacement. *J. Am. Acad. Orthop. Surg.* 20, 265–272 (2012).

(49) Kitsiou, P. V. *et al.* Glucose-induced changes in integrins and matrix-related functions in cultured human glomerular epithelial cells. *Am. J. Physiol. - Ren. Physiol.* 284, 671–679 (2003).

(50) Han, S. Y. *et al.* High glucose and angiotensin II increase β1 integrin and integrin-linked kinase synthesis in cultured mouse podocytes. *Cell Tissue Res.* 323, 321–332 (2006).

(51) Zhang, X. *et al.* Effects of elevated glucose levels on interactions of cardiac fibroblasts with the extracellular matrix. *Vitr. Cell. Dev. Biol. - Anim.* 43, 297–305 (2007).

(52) Oldberg, A. & Ruoslahti, E. Interactions between chondroitin sulfate proteoglycan, fibronectin, and collagen. *J. Biol. Chem.* 257, 4859–4863 (1982).

(53) Vogel, K. G. & Trotter, J. A. The Effect of Proteoglycans on the Morphology of Collagen Fibrils Formed In Vitro. *Top. Catal.* 7, 105–114 (1987).

(54) Scott, J. E. Proteoglycan-fibrillar collagen interactions. *Biochem. J.* 252, 313–23 (1988).

(55) Kalamajski, S. & Oldberg, A. The role of small leucine-rich proteoglycans in collagen fibrillogenesis. *Matrix Biol.* 29, 248–253 (2010).

(56) Fukazawa, I., Hatta, T., Uchio, Y. & Otani, H. Development of the meniscus of the knee joint in human fetuses. *Congenit. Anom. (Kyoto).* 49, 27–32 (2009).

(57) Clark, C. R. & Ogden, J. A. Prenatal and Postnatal Development of Human Knee Joint Menisci. *Iowa Orthop. J.* 1, 20 (1981).

(58) McNicol, D. & Roughley, P. J. Extraction and characterization of proteoglycan from human meniscus. *Biochem. J.* 185, 705–713 (1980).

(59) Peters, T. J. & Smillie, E. S. Studies on the chemical composition of the menisci of the knee joint with special reference to the horizontal cleavage lesion. *Clin. Orthop. Relat. Res.* 86, 245–252 (1972).

(60) Raspanti, M. *et al.* Glycosaminoglycans show a specific periodic interaction with type I collagen fibrils. *J. Struct. Biol.* 164, 134–139 (2008).

(61) Pangborn, C. A. & Athanasiou, K. A. Growth factors and fibrochondrocytes in scaffolds. *J. Orthop. Res.* 23, 1184–1190 (2005).

(62) Kasemkijwattana, C. *et al.* The use of growth factors, gene therapy and tissue engineering to improve meniscal healing. *Mater. Sci. Eng. C* 13, 19–28 (2000).

(63) Detamore, M. S. & Athanasiou, K. A. Effects of growth factors on temporomandibular joint disc cells. *Arch. Oral Biol.* 49, 577–583 (2004).

(64) Makris, E. A., Hadidi, P. & Athanasiou, K. A. The knee meniscus: Structure-function, pathophysiology, current repair techniques, and prospects for regeneration. *Biomaterials* 32, 7411–7431 (2011).

(65) Gruber, H. E. *et al.* Three-dimensional culture of human meniscal cells: Extracellular matrix and proteoglycan production. *BMC Biotechnol.* 8, 1–7 (2008).

(66) Pazin, D. E., Gamer, L. W., Capelo, L. P., Cox, K. A. & Rosen, V. Gene signature of the embryonic meniscus. *J. Orthop. Res.* 32, 46–53 (2014).

(67) Blunk, T. *et al.* Differential effects of growth factors on tissue-engineered cartilage. *Tissue Eng.* 8, 73–84 (2002).

(68) Postacchini, F., Accinni, L., Natali, P. G., Ippolito, E. & DeMartino, C. Regeneration of rabbit calcaneal tendon - A morphological and immunochemical study. *Cell Tissue Res.* 195, 81–97 (1978).

(69) Faryniarz, D. A., Chaponnier, C., Gabbiani, G., Yannas, I. V. & Spector, M. Myofibroblasts in the healing lapine medial collateral ligament: Possible mechanisms of contraction. *J. Orthop. Res.* 14, 228–237 (1996).

(70) Kambic, H. E., Futani, H. & Mcdevitt, C. A. Cell, matrix changes and alpha-smooth muscle actin expression in repair of the canine meniscus. *Wound Repair Regen.* 8, 554–561 (2000).

(71) Skaggs, D. L., Warden, W. H. & Mow, V. C. Radial tie fibers influence the tensile properties of the bovine medial meniscus. *J. Orthop. Res.* 12, 176–185 (1994).

(72) Melrose, J., Smith, S., Cake, M., Read, R. & Whitelock, J. Comparative spatial and temporal localisation of perlecan, aggrecan and type I, II and IV collagen in the ovine meniscus: An ageing study. *Histochem. Cell Biol.* 124, 225–235 (2005).

(73) Nakano, T., Dodd, C. M. & Scott, P. G. Glycosaminoglycans and proteoglycans from different zones of the porcine knee meniscus. *J. Orthop. Res.* 15, 213–220 (1997).

(74) Gupta, T., Zielinska, B., McHenry, J., Kadmiel, M. & Haut Donahue, T. L. IL-1 and iNOS gene expression and NO synthesis in the superior region of meniscal explants are dependent on the magnitude of compressive strains. *Osteoarthr. Cartil.* 16, 1213–1219 (2008).

75) Zielinska, B., Killian, M., Kadmiel, M., Nelsen, M. & Haut Donahue, T. L. Meniscal tissue explants response depends on level of dynamic compressive

strain. *Osteoarthr. Cartil.* 17, 754–760 (2009).

(76) Puetzer, J. L., Ballyns, J. J. & Bonassar, L. J. The effect of the duration of mechanical stimulation and post-stimulation culture on the structure and properties of dynamically compressed tissue-engineered menisci. *Tissue Eng. - Part A* 18, 1365–1375 (2012).

(77) Eleswarapu, S. V., Responte, D. J. & Athanasiou, K. A. Tensile properties, collagen content, and crosslinks in connective tissues of the immature knee joint. *PLoS One* 6, 1–7 (2011).

(78) Tissakht, M. & Ahmed, A. M. Tensile stress-strain characteristics of the human meniscal material. *J. Biomech.* 28, 411–422 (1995).

(79) Sweigart, M. A. *et al.* Intraspecies and interspecies comparison of the compressive properties of the medial meniscus. *Ann. Biomed. Eng.* 32, 1569–1579 (2004).

(80) Puetzer, J. L., Ma, T., Sallent, I., Gelmi, A. & Stevens, M. M. Driving Hierarchical Collagen Fiber Formation for Functional Tendon, Ligament, and Meniscus Replacement. *Biomaterials* 120527 (2020).

(81) MacBarb, R. F., Makris, E. A., Hu, J. C. & Athanasiou, K. A. A chondroitinase-ABC and TGF-β1 treatment regimen for enhancing the mechanical properties of tissue-engineered fibrocartilage. *Acta Biomater.* 9, 4626–4634 (2013).

(82) Son, M. S. & Levenston, M. E. Quantitative tracking of passage and 3D culture effects on chondrocyte and fibrochondrocyte gene expression. *J. Tissue Eng. Regen. Med.* 11, 1185–1194 (2017).

(83) Li, Q. *et al.* Micromechanical anisotropy and heterogeneity of the meniscus

extracellular matrix. *Acta Biomater.* 54, 356–366 (2017).

CHAPTER 3

Recapitulating Native Structural and Biochemical Gradients to Enhance Mechanics of Tissue-Engineered Entheses

Abstract

The incorporation of entheses into the design of tissue-engineered menisci is critical for its clinical application. Recapitulating gradients in collagen fiber organization and mineral contents of meniscal entheses for native tissue-like mechanics remains challenging. In this study, a simplified enthesis construct containing a fibrochondrocyte-seeded cylinder of type I collagen gel with bone plugs on both ends was utilized as a tissue-engineered enthesis model. With this model, we employed spatially controlled biochemical and biomechanical stimuli using a tri-chamber bioreactor. Moreover, partially demineralized bone plugs were used to mimic the mineral gradient of the native meniscal entheses. The application of spatially controlled biochemical and biomechanical stimuli during culture of these constructs generated native-like hierarchy and gradients in biochemical composition and collagen fiber structure of native entheses within tissue-engineered enthesis constructs. There was a smoother local strain distribution with a less concentrated peak strain in samples cultured in a tri-chamber bioreactor compared to those cultured in a single chamber bioreactor, which is likely due to the enhancement in collagen fiber organization in this group. To further improve the robustness of the collagen-bone plug interface, we introduced partially demineralized bone plugs to the constructs. When tested in uniaxial tension, these constructs had smoother local strain distributions and significant increases in toughness and strain at failure, as compared to constructs made using fully

mineralized bone plugs. Overall, these findings highlight the importance of zone-specific biochemical and biomechanical stimuli as well as a choice of biomimetic scaffold material.

Kim, J., Boys, A. J., Babmatee, R., Estroff, L. A., and Bonassar, L. J. Recapitulating Native Structural and Biochemical Gradients to Enhance Mechanics of Tissue-Engineered Entheses. In preparation.

Introduction

Soft-to-hard tissue interfaces, including ligament-to-bone, tendon-to-bone, or meniscus-to-bone, are critical for physiological functions of diverse tissues. They specialize in transmitting applied loads from the soft tissue to their underlying bone[1]. Meniscus-to-bone interfaces, known as meniscal entheses, transfer axial loads in the knee joint to the underlying subchondral bone with smooth local strain distributions while mitigating stress concentrations at the interfaces between mechanically dissimilar tissues[2]. These distinct functions of soft tissue-to-bone interfaces are attributed to their unique characteristics, such as gradients in cell phenotypes, collagen fiber organization, and mineral contents[3,4]. Given the importance of the gradients of native entheses, the recapitulation of these native tissue-like gradients within tissue-engineered constructs remains a persistent challenge in the field of enthesis tissue engineering.

Incidences of injuries at interfaces often occur via wear and tear, especially among the population over the age of 60[5]. Autografts and allografts are commonly employed to replace a damaged tissue. However, autografts do not possess compositional and structural gradients matching native entheses, as each enthesis has different microstructure in response to anatomical locations. Allografts also have several limitations, such as limited supply, risk of immune rejection, and variations in mechanics[6]. These drawbacks lead to high failure rates, mostly at the interfaces. As such, interface tissue engineering has gained a significant amount of attention as a promising means to generate functional replacements[7]. Clinical outcomes have demonstrated that bone fixation of allografts is superior to soft tissue fixation, indicated by enhanced integration and mechanical functions[8]. Furthermore, injuries to the main

body of menisci often require total meniscectomy due to their poor healing capacity. As a full-scale meniscus replacement, allograft transplantation is currently the sole clinical option. Thus, there is a significant need for tissue engineering menisci that include meniscus-to-bone regions.

Previous strategies to create a native-like soft tissue-to-bone interface with gradients utilized electrospinning[9], sequential deposition[10], freeze-drying[11], or composite layers[12] to incorporate structural and compositional gradients of native entheses. These strategies showed promising outcomes; however, they failed to produce native tissue-like structural or mechanical gradients or solely focused on recapitulating mature organization without considering early postnatal enthesis development, which lack continuity. Tissue engineering functional structures with these continuous gradients has been a large, persistent challenge and is at the forefront of interface tissue engineering[13]. Moreover, these approaches mostly focused on tendon- or ligament-to-bone interfaces, using primary tenocytes or mesenchymal stem cells with induced tenogenic differentiation. A meniscus-to-bone interface is different from tendon- or ligament-to-bone interfaces with respect to cell phenotypes and the angle of collagen fiber interdigitation into the underlying subchondral bone. As such, little is known about strategies to generate a meniscus-to-bone interface.

To incorporate the early postnatal enthesis development to ensure production of gradients in tissue-engineered constructs, biochemical and biomechanical cues should be taken into consideration. Multiple growth factors are involved in developing the structural and compositional complexity of entheses. The transforming growth factor-β (TGF-β) superfamily including morphogenetic proteins (BMP), such as TGF-β1, TGF-

β2, TGF-β3, BMP2, or BMP4, plays an important role in the development and maintenance of tendon, ligament, bone, and meniscus and is thus widely used in tissue engineering approaches for the aforementioned connective tissues[2,14]. In addition to biochemical cues, biomechanical stimuli also have profound effects on the development of the connective tissues. In the absence of mechanical loading, mineral deposition, collagen fiber organization, and fibrocartilage formation were impeded[15,16]. These findings suggest that appropriate biochemical and biomechanical stimuli should be incorporated to induce native tissue-like development within tissue-engineered constructs. Our prior work has demonstrated that native tissue-like aligned, robust collagen fibers in a meniscus construct are induced in a sub-physiologic glucose culture media supplemented with transforming growth factor-β1[17,18]. Further, we have developed a simplified tissue-engineered enthesis construct, composed of a fibrochondrocyte-seeded cylinder-shaped collagen gel and bone plugs at both ends, which is useful to evaluate effects of biochemical and biomechanical stimuli on enthesis constructs[19]. Moreover, we have also developed a bioreactor allowing for the application of different types of media and mechanical boundary conditions to tissue-engineered enthesis constructs[20]. Lastly, we have shown that native mineral gradients can be recapitulated by partial demineralization of bone plugs[21].

Here we show that: 1) zone-specific biochemical and biomechanical stimuli recapitulate gradients in collagen fiber organization and mechanics of native entheses and that 2) this mimicked collagen fiber structure and mechanics can be further improved by the incorporation of the mineral gradient using partially demineralized bone plugs, leading to the enhanced integration and mechanical properties of tissue-

engineered enthesis constructs.

Materials and Methods

Bone Plug Decellularization and Demineralization

Trabecular bone plugs were harvested and decellularized as previously reported[19]. Briefly, bone plugs were obtained from the distal femur of 1-3 day old bovids (Gold Medal Packing, Inc., Rome, NY) using a 6 mm coring bit and cut into 10 mm long cylinders. Sectioned bone plugs were rinsed with a high velocity stream of deionized water (~140 mL/s through a 5 mm diameter nozzle) to remove cellular debris and bone marrow. Bone plugs were then soaked subsequently in 0.1 w/v% ethylenediaminetetraacetic acid (EDTA) (Sigma, St. Louis, MO) in phosphate buffered saline (PBS) (Corning, Manassas, VA) at room temperature for 3 h, hypotonic buffer (10 mM Trizma base (TCI, Tokyo, Japan), 0.1 w/v% EDTA) at 4 °C for 24 h, and detergent (10 mM Trizma base, 0.5 w/v% sodium dodecyl sulfate (SDS) (Sigma, St. Louis, MO) in PBS) at 4 °C for 24 h. Following washes, bone plugs were rinsed 7 times with PBS and frozen for later use. For partial demineralization of bone plugs, bone plugs were skewered on a surgical needle and partially submerged in a 9.5 w/v% EDTA in PBS for 4.5 hours as previously shown[21].

Construct Fabrication

Constructs were generated as previously described[19]. Collagen was extracted from Sprague-Dawley rat tails (BioIVT, Westbury, NY), dissolved in 0.1 v/v% acetic acid (Sigma, St. Louis, MO) at a concentration of 30 mg/mL, and stored at 4 °C until use. Fibrochondrocytes were isolated from the menisci of 1-3 day old bovids. Menisci

were diced and then digested in a 0.3 w/v% collagenase (Worthington Biochemical Corporation, Lakewood, NJ) in Dulbecco's Modified Eagle Medium (DMEM) with 100 μg/mL penicillin and 100 μg/mL streptomycin for 18 hours, followed by filtering through a 100-μm cell strainer. The cells were pooled, rinsed with phosphate-buffered saline (PBS), and suspended to a concentration of 150 x 10^6 cells/mL. Non-demineralized or partially demineralized bone plugs were placed 20 mm apart inside Tygon® tubing. 2 mL of collagen stock solution at a 30 mg/mL concentration was mixed with 0.5 mL of a working solution composed of 1M NaOH, 10x PBS, and 1x PBS to start the gelation at pH 7.0 and 300 mOsm using a syringe stopcock. Then, 0.5 mL of media containing harvested fibrochondrocytes at a 150 x 10^6 cells/mL concentration were subsequently mixed with the neutralized collagen solution to achieve a final concentration of 25 x 10^6 cells/mL and 20 mg/mL collagen gel. The collagen and cell mixture was immediately injected into the tubing between the bone plugs and placed in an incubator at 37 °C for 45 min to finish the gelation process. Constructs were removed from the tubing and placed either in a custom polysulfone clamping bioreactor[19] or in a custom tri-chamber polysulfone diffusion bioreactor[20]. The bony portion of constructs were clamped in both bioreactors. For a single chamber bioreactor, constructs were cultured with either 4500 mg/L glucose DMEM and 5 ng/mL TGF-β1 (High) or 500 mg/L glucose DMEM and 0.5 ng/mL TGF-β1 (Low) media supplemented with 10 v/v% fetal bovine serum (FBS), 100 μg/mL penicillin, 100 μg/mL streptomycin, 0.1 mM non-essential amino acids, 50 μg/mL ascorbic acid, and 0.4 mM L-proline at 37 °C and 5% CO_2. In the tri-chamber bioreactor (Bioreactor), High media was applied to the bony portion of constructs, and Low media was applied

to the collagen portion of constructs. All the constructs were cultured for 30 days. Gross images were taken before and after 30 days of culture to assess construct contraction.

Histology

After 30 days of culture, constructs were biaxially cut along the long axis to generate two halves containing both bony and collagen portions. One half was used for histological analysis, and the other half was used for confocal fluorescence elastography. Samples for histological analysis were fixed in 10% buffered formalin for 48 h, decalcified, dehydrated, embedded in paraffin, and sectioned. Sections of non-demineralized or partially demineralized tissue-engineered enthesis constructs were stained with picrosirius red. Immunohistochemistry was performed as previously described[17] to assess collagen content using antibodies for type II collagen (Chondrex, Redmond, WA) and type X collagen (Abcam, Cambridge, MA). Sections were stained in the same batch process and exposed to the same duration and concentration of reagents. Histological and immunohistological images were taken using a Nikon Eclipse TE2000-S microscope (Nikon Instruments, Melville, NY) and a SPOT RT camera (Diagnostic Instruments, Steriling Heights, MI) under brightfield or polarized light.

Confocal Fluorescence Elastography

To investigate local strain distributions in tissue-engineered enthesis constructs, constructs were longitudinally bisected using a cryotome, stained with 5-(4,6-Dichlorotriazinyl)aminofluorescein (5-DTAF) for 60 min, and rinsed three times with PBS. The bony portion of the bisected construct was adhered to a fixed back plate on a tissue deformation imaging stage (TDIS), and the collagen portion was glued to a loading plate[3]. Samples were then mounted onto the TDIS and submerged in PBS. The

TDIS was placed on an inverted Zeiss LSM 710 confocal microscope. 20% strain was applied to each sample at an incremental step of 1% strain. Images from each step were taken using a 10X objective and a 488 nm laser after allowing 10 minutes to ensure a complete stress relaxation. Images were then analyzed using an open-source digital imaging software in MATLAB (Ncorr) to develop spatial strain maps and quantify local strains[22].

Mechanical Testing

Uniaxial tensile testing was performed using an Enduratec ElectroForce 5500 System (Bose, Eden Prairie, MN) as previously reported[18,19]. Bony ends of whole constructs were clamped into the testing frame. Based on the distance between bone-collagen interfaces of constructs, a quasistatic strain rate of 0.75%/s was applied until construct failure. The elastic modulus, ultimate tensile stress, stain at failure were calculated from the measured stress and strain curves.

Statistics

All values were reported as mean ± standard deviation. Data were tested for normality using Shapiro-Wilk's test and analyzed using one-way or two-way analysis of variance (ANOVA) with Tukey's Honestly Significant Difference (HSD) post hoc tests where $p < 0.05$ was considered to be significant. All statistical analysis was performed using GraphPad Prism (GraphPad Prism Software Inc., San Diego, CA).

Results

Construct Contraction. Shrinkage of meniscal grafts after transplantation reduces contact area and thus impairs biomechanical properties of the graft, eventually

leading to failure. Therefore, after 30 days of culture, we first examined construct contraction. All groups, High, Low, and Bioreactor, appeared to minimally contract over the culture period, showing less than 5% contraction (Figure 3.1). No statistical difference in construct contraction was observed between the groups.

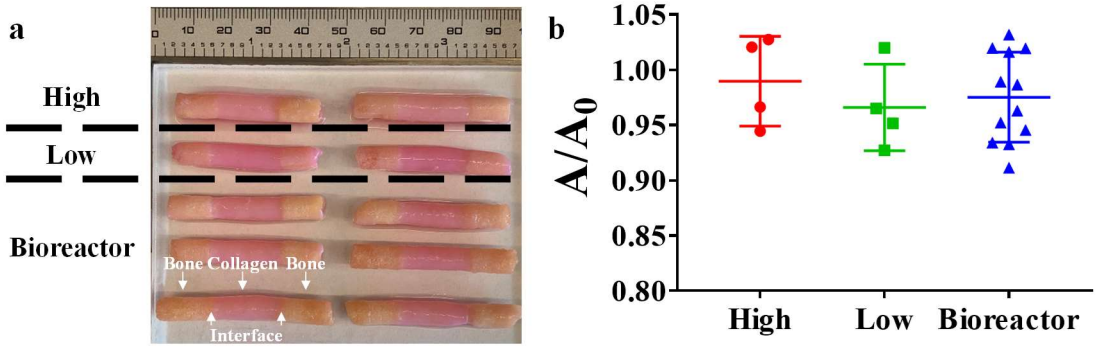

Figure 3.1. Contraction of tissue-engineered enthesis constructs over 30 days of culture. (a) Photographs of enthesis constructs after 30 days of culture in either a single chamber bioreactor (High, 4500 mg/L glucose DMEM and 5 ng/mL TGF-β1; Low, 500 mg/L glucose DMEM and 0.5 ng/mL TGF-β1) or a tri-chamber bioreactor (Bioreactor, 4500 mg/L glucose DMEM and 5 ng/mL TGF-β1 at bony regions and 500 mg/L glucose DMEM and 0.5 ng/mL TGF-β1 at a collagen region). Each construct contains three regions: bone, interface, and collagen. (b) Ratio of enthesis construct area over initial projected area (A/A_o) after 30 days of culture (n = 4-12).

Collagen Fiber Microstructure. Next, we performed picrosirius red staining to assess collagen fiber structure within the tissue-engineered enthesis constructs. Picrosirius red stained samples were imaged under cross-polarized light. The High group showed dense, more radially aligned collagen fibers across the construct while the Low group displayed dense collagen fibers at the interface and more radially aligned collagen fibers in the soft tissue region (Figure 3.2a,b). Notably, the Bioreactor group,

allowing for the application of 5 ng/mL TGF-β1 and 4500 mg/L glucose media to the bony region and 0.5 ng/mL TGF-β1 and 500 mg/L glucose media to the soft tissue region, showed a more native-like collagen fiber structure (Figure 3.2c). Nicely aligned collagen fibers that appear as birefringence in green to yellow were observed in the soft tissue region while more interconnected collagen fibers were found at the interface. This observation resembles a native enthesis collagen fiber structure although a native enthesis displayed larger, banded collagen fiber bundles which appear in red to yellow in the soft tissue region and clearly interdigitated collagen fibers into the bony region (Figure 3.2d).

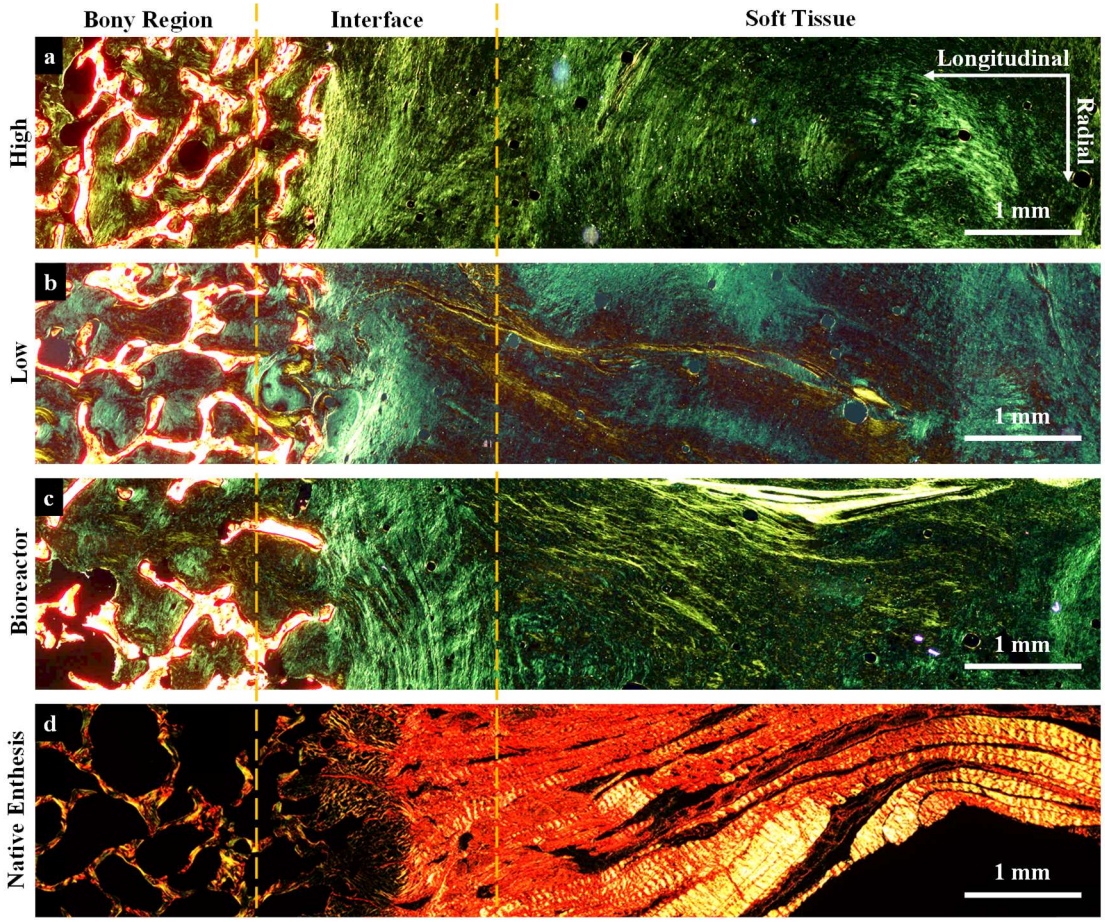

Figure 3.2. Picrosirius red staining imaged under polarized light for a) High, b) Low,

and c) Bioreactor after 30 days of culture and d) native enthesis.

Immunohistochemical analysis. In the native enthesis, different types of collagen are observed depending on the regions: Type I collagen in the ligamentous region, types I, II, and III collagen in the unmineralized fibrocartilage region, types II and X collagen in the mineralized fibrocartilage region, and mineralized type I collagen in the bony region. Therefore, immunohistochemical staining for types II and X collagen was performed to investigate how different media applications influence the production of these collagen types. Type II collagen stained positive in all three groups at the interface between the bony and collagen regions (Figure 3.3), similar to native tissue[23]. The High group exhibited a higher degree of type X collagen staining across the construct (Figure 3.4a), indicating the presence of hypertrophy. Interestingly, the Low and Bioreactor groups showed more localized type X collagen staining at the interface and the bony region to some extent (Figure 3.4b,c).

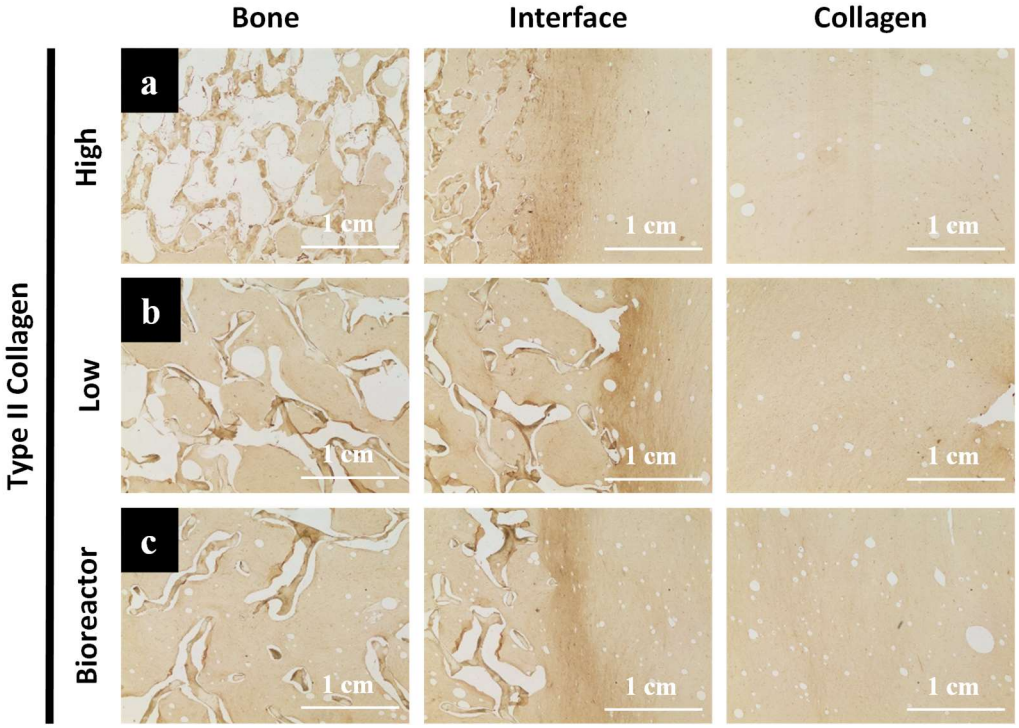

Figure 3.3. Immunohistochemical staining for type II collagen of a) High, b) Low, and c) Bioreactor at three different regions: bone, interface, and collagen.

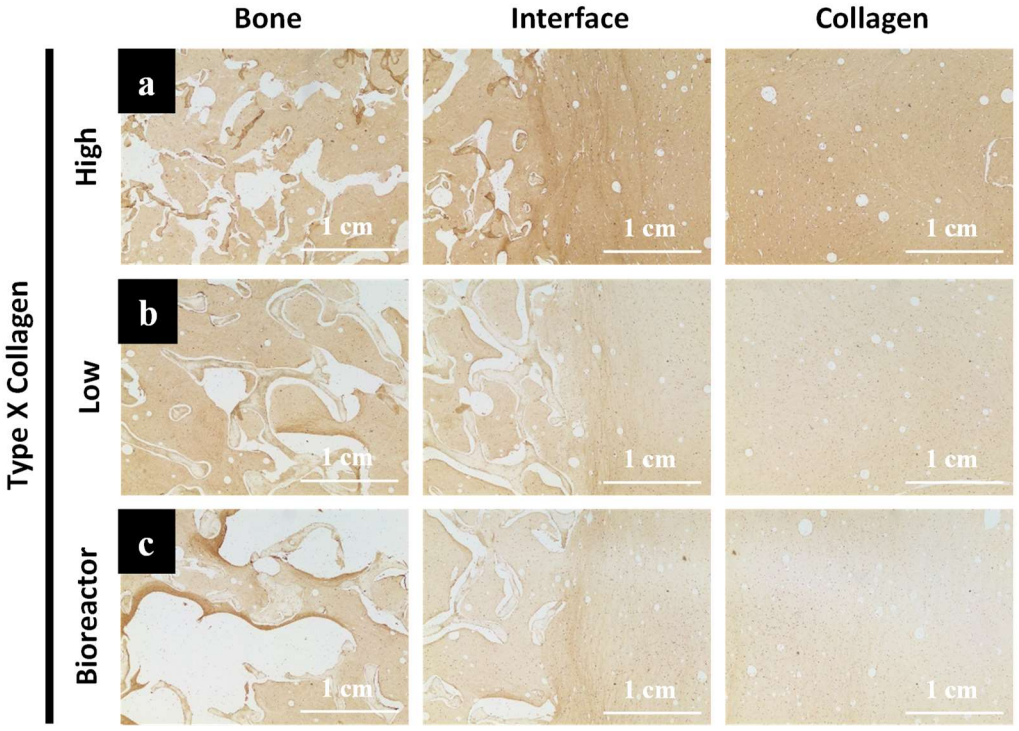

Figure 3.4. Immunohistochemical staining for type X collagen of a) High, b) Low, and c) Bioreactor at three different regions: bone, interface, and collagen.

Fluorescence elastography analysis. In order to investigate how the structural differences observed via picrosirius red staining affect the tissue-engineered enthesis constructs under tensile loading, confocal fluorescent elastography was performed[3]. At 10% bulk strain, the High group showed highly concentrated local strain, mostly at the interface between the bone plug and the soft tissue (Figure 3.5a, left). Similarly, the Low group also showed the concentrated local strain at the interface (Figure 3.5a, middle). Interestingly, the Bioreactor group showed less concentrated local strain compared to the High and Low groups (Figure 3.5a, right). Quantitative analysis of local strain maps revealed that the High and Low groups had peak strains within 2 mm from the interface and 3 to 4 times greater peak strain levels compared to the bulk strain (10%) (Figure 3.5b). Interestingly, the Bioreactor group showed a peak strain further away from the interface and a smaller peak strain level compared to the High and Low groups, indicating the Bioreactor group has a smoother local strain distribution further into the soft tissue region. This observation was consistent with lower bulk strain levels, 3% and 5% (Figure 3.S1).

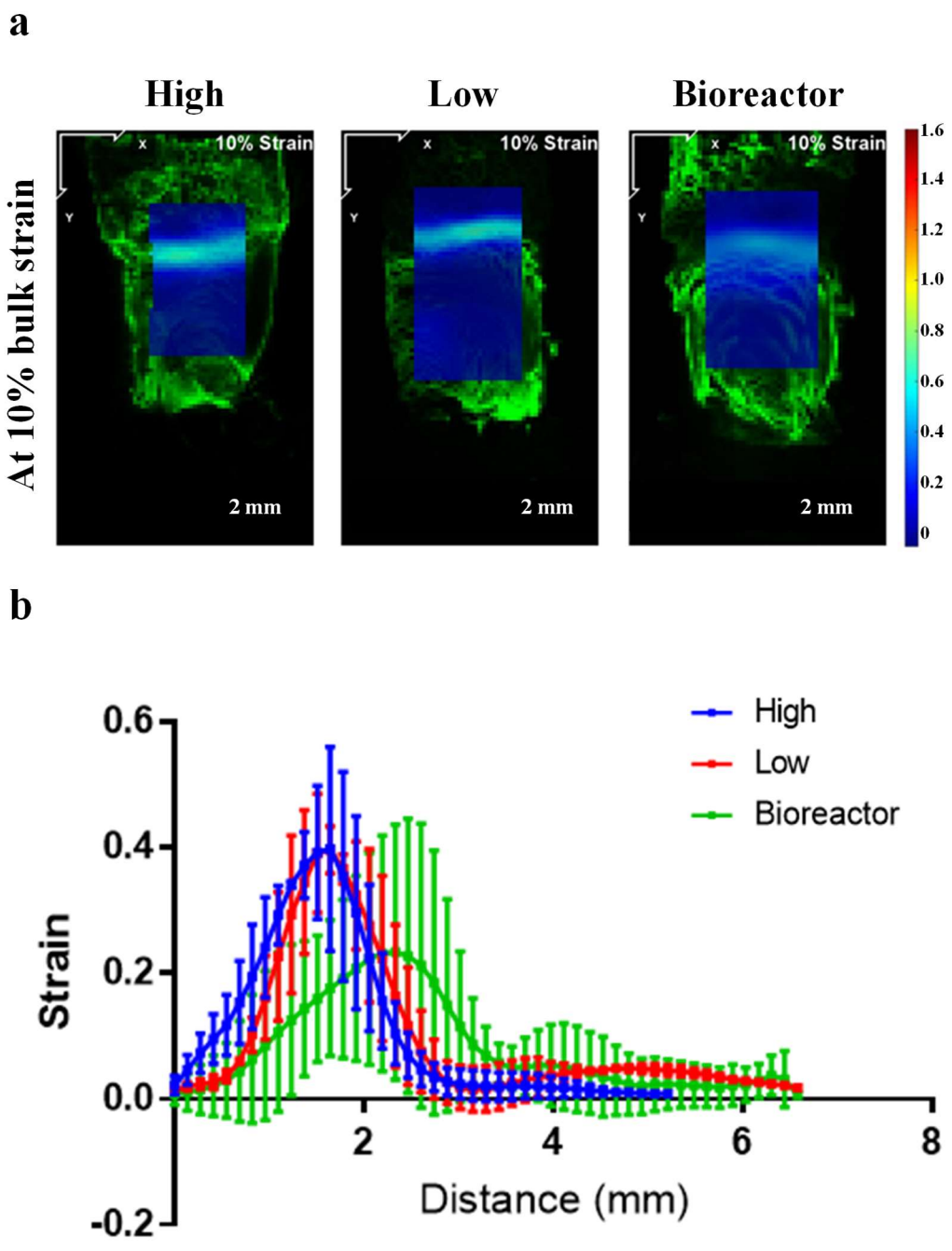

Figure 3.5. Local strain distributions of tissue-engineered enthesis constructs at 10% bulk strain. (a) Representative local strain maps of tissue-engineered constructs cultured in either a single chamber bioreactor or a multi-chamber bioreactor at 10% bulk strain. Fluorescence images were superimposed with local strain maps. (b) Averaged local

strains of tissue-engineered enthesis constructs at 10% bulk strain as a function of distance from the mineralized interface (n = 2-4).

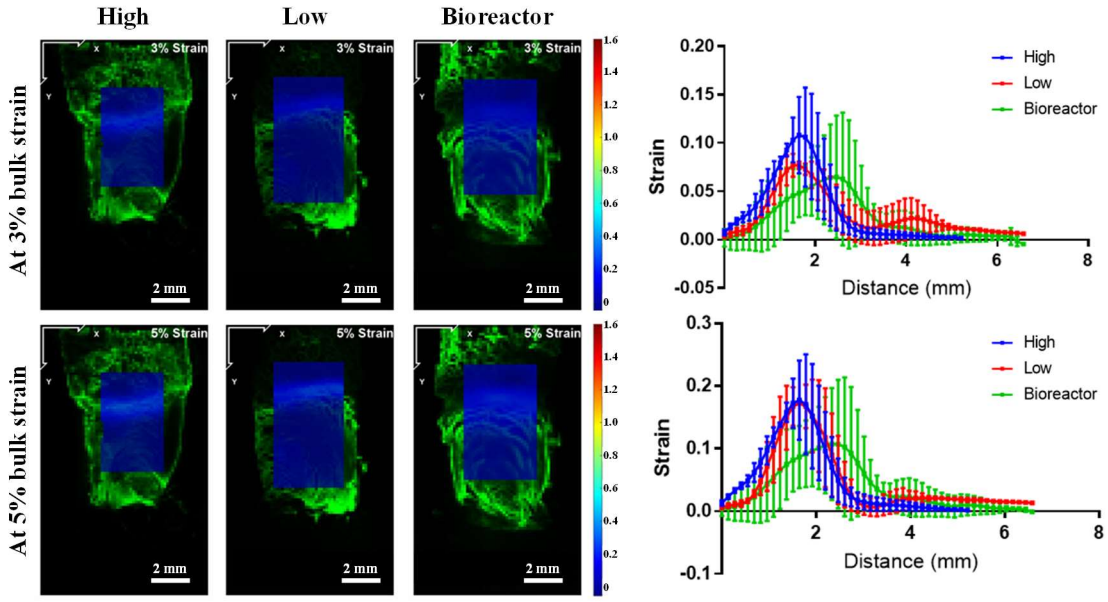

Figure 3.S1. Local strain distributions of tissue-engineered enthesis constructs at 3% and 5% bulk strain. (a) Representative local strain maps of tissue-engineered constructs cultured in either a single chamber bioreactor or a multi-chamber bioreactor at 3% (top) and 5% (bottom) bulk strains. Fluorescence images were superimposed with local strain maps. (b) Averaged local strains of tissue-engineered enthesis constructs at 3% (top) and 5% (bottom) bulk strains as a function of distance from the mineralized interface (n = 2-4).

Construct Contraction. Given that native entheses possess a gradient in mineral contents, we utilized partially demineralized bone plugs[18] to investigate how the native tissue-like mineral gradient influences tissue-engineered enthesis constructs compared to the non-demineralized bone plug. Tissue-engineered enthesis constructs with either non-demineralized bone plugs or partially demineralized bone plugs were

cultured in a tri-chamber bioreactor with High (for bony region) and Low (for collagen) media for 30 days. First, we examined construct contraction of non-demineralized and partially demineralized bone plug tissue-engineered enthesis constructs after 30 days in culture. Contraction analysis showed that both groups maintained their initial shape, ~94-95%, over time in culture (Figure 3.6). Furthermore, partial demineralization appeared to result in an increased contraction; however, the difference between the two groups was not significant.

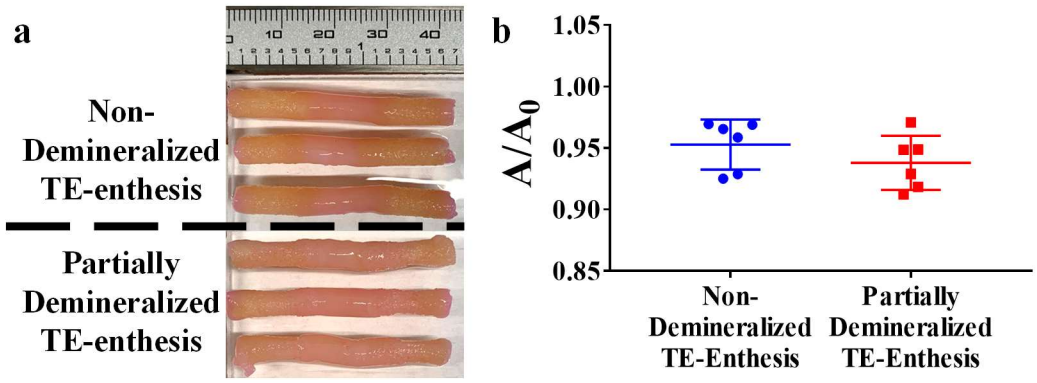

Figure 3.6. Contraction of non-demineralized and partially demineralized tissue-engineered enthesis constructs over 30 days of culture. (a) Photographs of non-demineralized and partially demineralized bone plug enthesis constructs after 30 days of culture in a multi-chamber bioreactor (b) Ratio of enthesis construct area over initial projected area (A/A_o) at day 30 ($n = 6$).

Collagen fiber development in bony regions. Next, picrosirius red staining was performed to examine the changes in collagen fiber organization depending on mineralization of bone plugs. Both groups showed that trabecular bone pores were filled with collagen to a similar extent. Notably, compared to the non-demineralized bone plugs in tissue-engineered enthesis constructs, partially demineralized bone plugs

showed more robust collagen fiber formation in the demineralized bony region (indicated by white arrows in Figure 3.7).

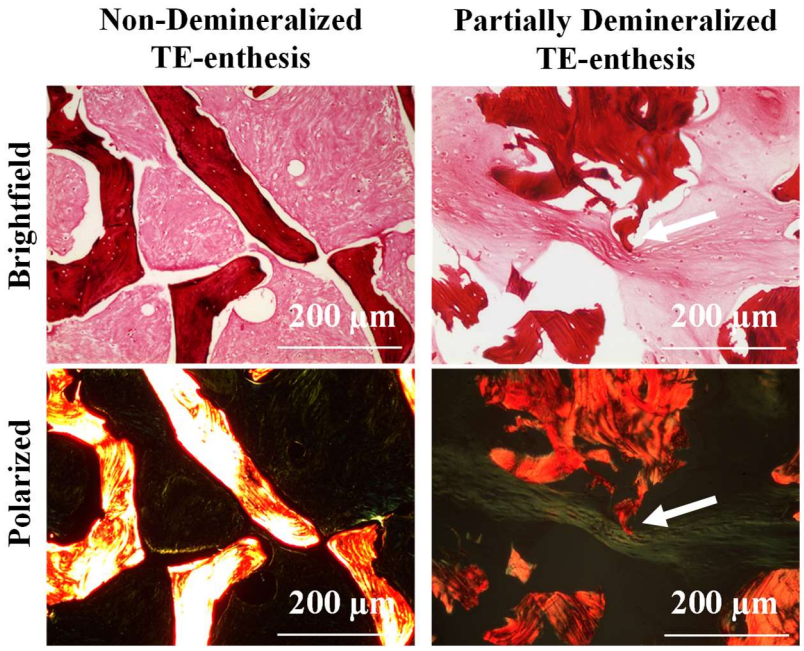

Figure 3.7. Picrosirius red staining imaged under brightfield (top) and polarized light (bottom) for the non-demineralized and partially demineralized bone plug tissue-engineered enthesis constructs after 30 days of culture. Arrows indicate regions of prominent collagen fiber formation.

Local Strain Distribution. In order to investigate how the changes in collagen fiber development in bony regions influence biomechanics of tissue-engineered enthesis constructs, confocal fluorescent elastography was performed under the same settings as Figure 3.5. At 15% bulk strain, non-demineralized enthesis constructs displayed a localized strain at the interface. In contrast, partially demineralized constructs showed a less concentrated, broader local strain distribution (Figure 3.8a). Quantitative analysis showed that significantly greater local strains were observed in the bony region of the partially demineralized bone plug enthesis constructs compared to the non-

demineralized bone plug constructs, indicating smoother, less concentrated local strain distributions across the construct (Figure 3.8b). A similar trend was also observed at 5% bulk strain (Figure 3.S2).

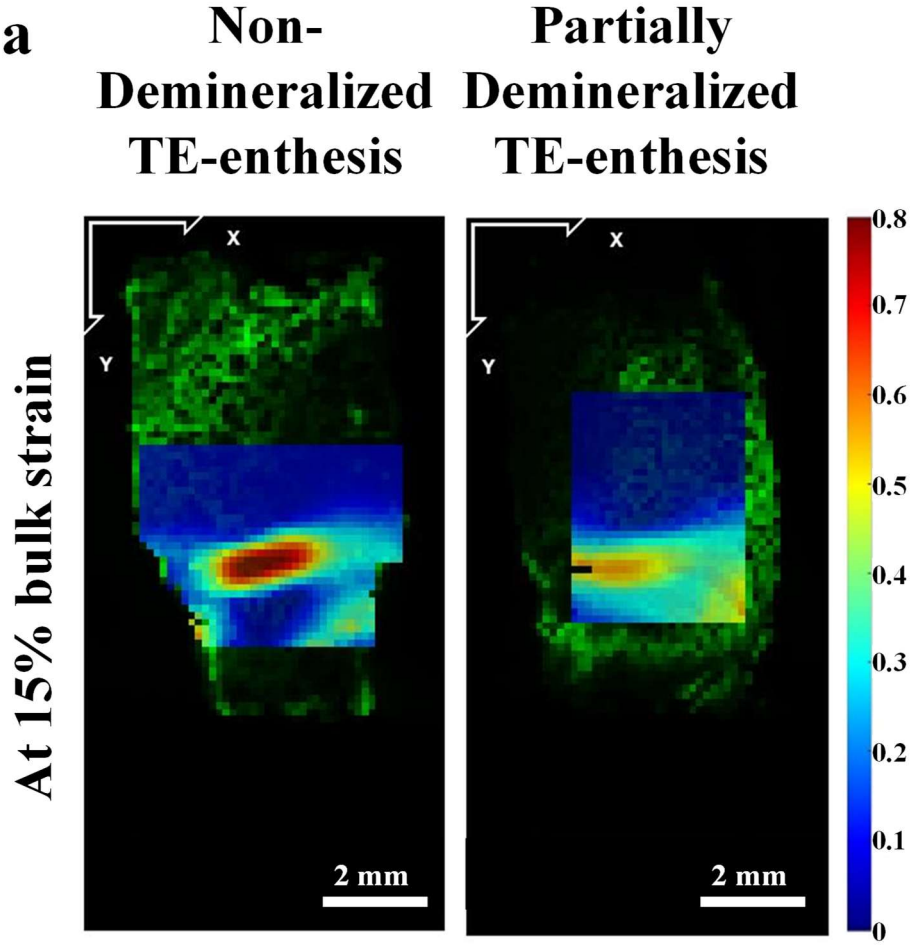

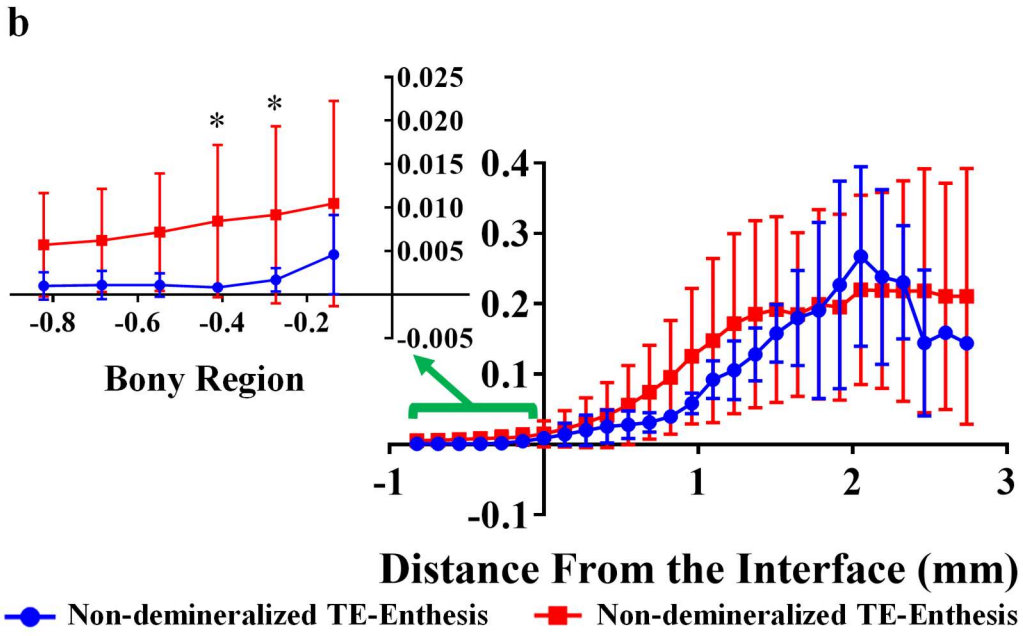

Figure 3.8. Local strain distributions of non-demineralized and partially demineralized bone plug tissue-engineered enthesis constructs at 15% bulk strain. (a) Representative local strain maps of tissue-engineered constructs cultured in a tri-chamber bioreactor at 15% bulk strain. Fluorescence images were superimposed with local strain maps. (b) Averaged local strains of tissue-engineered enthesis constructs at 15% bulk strain as a function of distance from the mineralized or demineralized interface (n = 3-6).

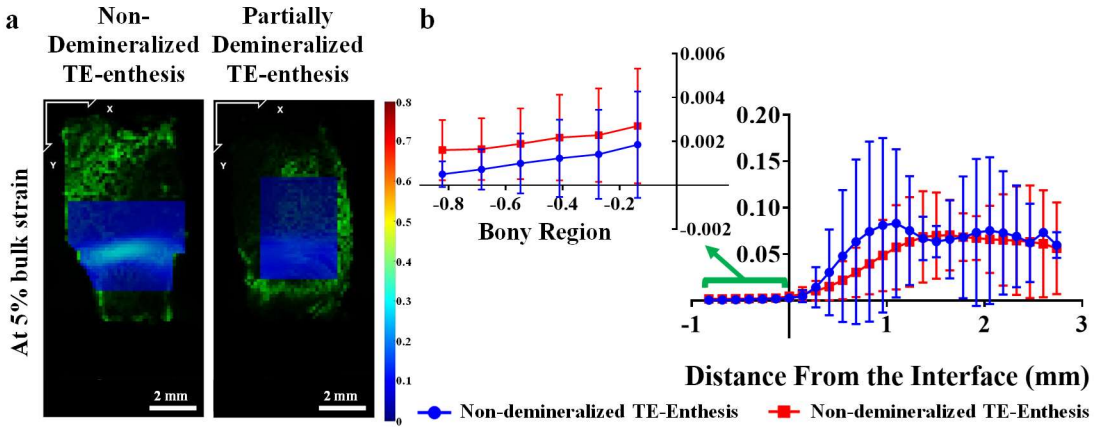

Figure 3.S2. Local strain distributions of non-demineralized and partially demineralized bone plug tissue-engineered enthesis constructs at 5% bulk strain. (a) Representative local strain maps of tissue-engineered constructs cultured in a tri-chamber bioreactor at 5% bulk strain. Fluorescence images were superimposed with local strain maps. (b) Averaged local strains of tissue-engineered enthesis constructs at 5% bulk strain as a function of distance from the mineralized or demineralized interface (n = 3-6).

Uniaxial Tensile Testing. Last, we performed uniaxial tensile tests to examine how these structural and micro-biomechanical differences affect bulk mechanical properties of tissue-engineered constructs. Although non-demineralized bone plug constructs appeared to have greater ultimate tensile stress and tensile modulus, 20.50 ± 5.91 kPa and 118.74 ± 66.04 kPa, respectively, compared to the partially demineralized bone plug constructs, 19.53 ± 7.36 kPa and 74.26 ± 31.23 kPa, respectively, there were no statistical differences between the groups (Figure 3.9a,b). Intriguingly, significantly higher toughness and strain at failure were observed in the partially demineralized bone plug enthesis constructs, 5.97 ± 2.14 J/m^3 vs. 4.03 ± 0.82 J/m^3 and 0.67 ± 0.16 vs. 0.47

± 0.11, respectively.

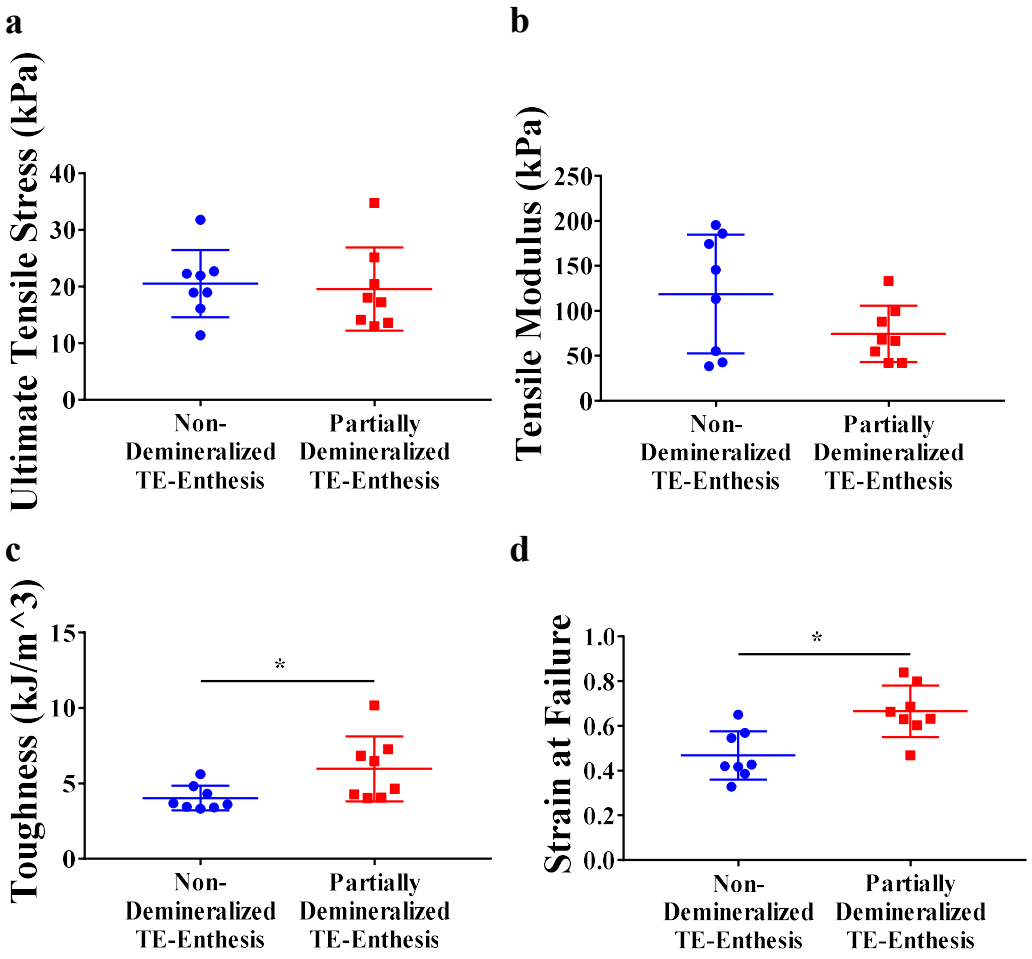

Figure 3.9. Tensile Mechanical properties of non-demineralized and partially demineralized enthesis constructs. (a) Ultimate tensile stress (n = 8). (b) Tensile modulus (n = 8). (c) Toughness (n = 8 and *, $p < 0.05$). (d) Strain to failure (n = 8 and *, $p < 0.05$).

Discussion

We have demonstrated that native enthesis-like collagen fiber structure and mechanics can be recapitulated in tissue-engineered entheses using biochemical and

biomechanical stimuli, which can be further enhanced by the incorporation of native-like mineral gradients in bone plugs. We utilized two different culture media, 1) 4500 mg/L glucose and 5 ng/mL TGF-β1 which is known to induce densely packed collagen fiber formation and 2) 500 mg/L glucose and 0.5 ng/mL TGF-β1 which is known to result in thick, nicely aligned collagen fibers[16], to mimic dense collagen fiber structure at the interface between the bone plug and collagen gel and longitudinally aligned collagen fiber structure in the soft tissue region. The spatial application of these two media in addition to mechanical anchoring was accomplished using a tri-chamber bioreactor, as previously reported[17]. These combined spatial biochemical and biomechanical stimuli resulted in gradients in collagen fiber organization within tissue-engineered enthesis constructs, resembling those of native enthesis. We show that these native tissue-like gradients in collagen fiber structure leads to native tissue-like mechanics, broad local strain distribution with alleviated local peak.

All the constructs cultured in single- or tri-chamber bioreactors showed nominal construct contraction (Figure 3.1a,b). It has been reported that anatomical accuracy of allografts is critical for clinical success and that a meniscal implant with a size tolerance of 5% should be employed[24,25]. Nominal construct contraction is likely attributed to mechanical anchoring imposed by the bioreactor, consistent with previous studies showing the mechanical boundary conditions prevent construct contraction[19,26]. The observed construct contraction in this study ranged from 1% to 6%, matching closely to the range of the graft size tolerance. This minimal contraction is likely to reduce the risk of graft failure, as larger shrinkage of grafts is associated with graft extrusion, a common issue in current graft applications.

Gradients in collagen fiber organization of native enthesis play an important role in transferring loads from the soft tissue to the underlying bone while reducing stress concentrations between these two mechanically dissimilar biomaterials[27]. Picrosirius red staining images under cross-sectional polarized light revealed that biochemical stimuli have a profound effect on collagen fiber organization within tissue-engineered constructs (Figure 3.2). Tissue-engineered constructs cultured in a single-chamber bioreactor with 4500 mg/L glucose and 5 ng/mL TGF-β1 lacked the gradients in collagen fiber organization, rather showing homogenous collagen fiber structure, parallel to the interface, across the construct. Conversely, the constructs cultured in a single chamber bioreactor with 500 mg/L glucose and 0.5 ng/mL TGF-β1 showed the less robust gradients, some interconnected collagen fibers at the interface and some longitudinally aligned collagen fibers in the soft tissue region. This observation is consistent with our previous study, showing that relatively low concentrations of glucose and TGF-β1 produce robust, aligned collagen fibers along the direction of the imposed tension while relatively high concentrations result in dense collagen fiber structure regardless of external mechanical stimuli[16]. The bioreactor-mediated gradients in biochemical stimuli appeared to augment the spatial heterogeneity of collagen fiber organization. The soft tissue-to-bone interface and collagen region exhibited their distinct regional collagen organization when region-specific biochemical stimuli were applied using a tri-chamber bioreactor, suggesting that spatially controlled biochemical stimuli is necessary to mimic native tissue-like collagen fiber structure.

Local biochemical cues and ECM components have profound effects on cellular behavior. Previous studies have shown that chondrogenic or osteogenic differentiation

of MSCs can be induced controlling composition of scaffold materials[28,29]. All the constructs showed types II and X collagen staining at the interface, which is likely due to the local environment, particularly the effects of bone plugs and TGF-β1 (Figures 3.3 and 3.4). Notably, type X collagen stained across the constructs cultured in 4500 mg/L glucose and 5 ng/mL TGF-β1, which is not observed in native entheses (Figure 3.4). This suggests that excessive biochemical stimuli could have adverse effects and thus optimization of biochemical stimuli should be performed.

The differences in the organization and spatial distribution of collagen led to changes in local strain distribution across the constructs under tensile loading. The bioreactor group showed smoother local strain distribution with the peak strain farther from the interface compared to the High and Low groups, which showed more concentrated local strain distribution with the peak strain closer the interface (Figure 3.5). Interestingly, the High and Low groups displayed similar local strain distributions although they showed different collagen fiber structures. This might suggest that the Low group is likely to contain longitudinally aligned collagen fibers in the soft tissue region but less integrated collagen fibers at the interface compared to the Bioreactor group, which showed more densely packed collagen fibers at the interface.

We also demonstrate that partial demineralization of bone plugs, mimicking the mineral gradients observed in native enthesis, enhances collagen fiber formation within the demineralized region and integration with the collagen fibers extending from the soft tissue region, eventually leading to a smoother local strain distribution. Partial demineralization appeared to slightly increase construct contraction, from 4% to 6% without statistical significance (Figure 3.6). However, partial demineralization appeared

to enhance collagen fiber formation in the partially demineralized region (Figure 3.7). The demineralized region showed more prominent, organized collagen fibers observed in both brightfield and polarized light, consistent with our previous study showing the newly deposited thicker, aligned collagen fibers in the demineralized region by MSCs but not in the mineralized region[26]. This enhancement in collagen fiber development in the demineralized region of the bone plug is likely to improve the integration between the bony region and collagen gel region. The exact mechanism by which the demineralized bony region enhances collagen fiber formation remains unclear; however, it can be speculated that 1) demineralization of bone plugs recover binding sites for collagen molecules which are otherwise blocked by minerals or 2) demineralization removes bone-residing proteoglycans which inhibit fiber formation in the surrounding environment. These speculations should be investigated in future studies.

Partially demineralized bone plug enthesis constructs exhibited a smoother local strain distribution with greater local strains in the bony region compared to the non-demineralized constructs (Figure 3.8). Just as mineralization increases the stiffness of collagen, partial demineralization reduces the stiffness of the demineralized bony region. This partially decreased stiffness in the bony region likely allows for reducing stress and strain concentrations, leading to a smooth local strain distribution. Additionally, the better integration of the collagen matrix with the bone plug resulting from the partial demineralization contributes to the smooth local strain distribution. These findings support the recapitulation of continuous gradients in collagen fiber organization within tissue-engineered interfaces for the physiological functions.

Uniaxial tension tests revealed that the toughness and strain at failure of the partially demineralized constructs increased by 48% and 42%, respectively, as compared to constructs made with fully mineralized bone plugs (Figure 3.9). These improved toughness and strain at failure are attributed to the enhanced integration of collagen fibers, consistent with the microscale local strain distribution (Figure 3.6). However, although the differences were not significant, the ultimate tensile stress and tensile modulus appeared to be greater in the non-demineralized enthesis constructs, suggesting the need of additional biochemical or biomechanical stimuli or prolonged maturation of the constructs.

One of the limitations of this study is that bone plugs were not seeded with either osteoblasts or mesenchymal stem cells. We have previously demonstrated that the local mineral contents have a profound effect on the osteogenic differentiation of mesenchymal stem cells and that these osteogenic effects can be further enhanced using media with osteogenic biochemical molecules[29]. Moreover, we also showed that chemical and cellular gradients allow for mimicking spatial distribution of collagen molecules and enhancing tensile modulus, ultimate tensile stress, and toughness of tissue-engineered enthesis constructs[20]. As such, we anticipate that the incorporation of mesenchymal stem cells with osteogenic media will result in better integration and further improve mechanical properties of tissue-engineered enthesis constructs to a native tissue-like level, which can further improve this body of work.

This work investigated the influences of biochemical and biomechanical stimuli on structure and mechanics of tissue-engineered enthesis constructs along with the incorporation of mineral gradients. In this study, we demonstrate that appropriate

biochemical and biomechanical stimuli and scaffold materials are critical for recapitulating native tissue-like structure and mechanics in tissue-engineered enthesis constructs. These findings can be further applied to other interfacial tissue engineering fields.

Reference

(1) Hino, T.; Furumatsu, T.; Miyazawa, S.; Fujii, M.; Kodama, Y.; Kamatsuki, Y.; Okazaki, Y.; Masuda, S.; Okazaki, Y.; Ozaki, T. A Histological Study of the Medial Meniscus Posterior Root Tibial Insertion. *Connect. Tissue Res.* 2020, *61* (6), 546–553.

(2) Boys, A. J.; McCorry, M. C.; Rodeo, S.; Bonassar, L. J.; Estroff, L. A. Next Generation Tissue Engineering of Orthopedic Soft Tissue-to-Bone Interfaces. *MRS Commun.* 2017, *7* (3), 289–308.

(3) Boys, A. J.; Kunitake, J. A. M. R.; Henak, C. R.; Cohen, I.; Estroff, L. A.; Bonassar, L. J. Understanding the Stiff-to-Compliant Transition of the Meniscal Attachments by Spatial Correlation of Composition, Structure, and Mechanics. *ACS Appl. Mater. Interfaces* 2019, *11* (30), 26559–26570.

(4) Zhu, C.; Qiu, J.; Thomopoulos, S.; Xia, Y. Augmenting Tendon-to-Bone Repair with Functionally Graded Scaffolds. *Adv. Healthc. Mater.* 2021, *10* (9).

(5) Dang, A.; Davies, M. Rotator Cuff Disease: Treatment Options and Considerations. *Sports Med. Arthrosc.* 2018, *26* (3), 129–133.

(6) Ma, J.; Smietana, M. J.; Kostrominova, T. Y.; Wojtys, E. M.; Larkin, L. M.; Arruda, E. M. Three-Dimensional Engineered Bone-Ligament-Bone Constructs

for Anterior Cruciate Ligament Replacement. *Tissue Eng. - Part A* 2012, *18* (1–2), 103–116.

(7) Shiroud Heidari, B.; Ruan, R.; De-Juan-Pardo, E. M.; Zheng, M.; Doyle, B. Biofabrication and Signaling Strategies for Tendon/Ligament Interfacial Tissue Engineering. *ACS Biomater. Sci. Eng.* 2021, *7* (2), 383–399.

(8) Ambra, L. F.; Mestriner, A. B.; Ackermann, J.; Phan, A. T.; Farr, J.; Gomoll, A. H. Bone-Plug Versus Soft Tissue Fixation of Medial Meniscal Allograft Transplants: A Biomechanical Study. *Am. J. Sports Med.* 2019, *47* (12), 2960–2965.

(9) Horner, C. B.; Maldonado, M.; Tai, Y.; Rony, R. M. I. K.; Nam, J. Spatially Regulated Multiphenotypic Differentiation of Stem Cells in 3D via Engineered Mechanical Gradient. *ACS Appl. Mater. Interfaces* 2019, *11* (49), 45479–45488.

(10) Nie, T.; Xue, L.; Ge, M.; Ma, H.; Zhang, J. Fabrication of Poly(L-Lactic Acid) Tissue Engineering Scaffolds with Precisely Controlled Gradient Structure. *Mater. Lett.* 2016, *176*, 25–28.

(11) Wang, Y.; Xu, R.; Luo, G.; Lei, Q.; Shu, Q.; Yao, Z.; Li, H.; Zhou, J.; Tan, J.; Yang, S.; Zhan, R.; He, W.; Wu, J. Biomimetic Fibroblast-Loaded Artificial Dermis with “Sandwich” Structure and Designed Gradient Pore Sizes Promotes Wound Healing by Favoring Granulation Tissue Formation and Wound Re-Epithelialization. *Acta Biomater.* 2016, *30*, 246–257.

(12) Mosher, C. Z.; Spalazzi, J. P.; Lu, H. H. Stratified Scaffold Design for Engineering Composite Tissues. *Methods* 2015, *84*, 99–102.

(13) Li, C.; Ouyang, L.; Armstrong, J. P. K.; Stevens, M. M. Advances in the

Fabrication of Biomaterials for Gradient Tissue Engineering. *Trends Biotechnol.* 2021, *39* (2), 150–164.

(14) Killian, M. L. Growth and Mechanobiology of the Tendon-Bone Enthesis. *Semin. Cell Dev. Biol.* 2022, *123*, 64–73.

(15) Kim, H. M.; Galatz, L. M.; Patel, N.; Das, R.; Thomopoulos, S. Recovery Potential after Postnatal Shoulder Paralysis: An Animal Model of Neonatal Brachial Plexus Palsy. *J. Bone Jt. Surg. - Ser. A* 2009, *91* (4), 879–891.

(16) Thomopoulos, S.; Genin, G. M.; Galatz, L. M. The Development and Morphogenesis of the Tendon-to-Bone Insertion - What Development Can Teach Us about Healing. *J. Musculoskelet. Neuronal Interact.* 2010, *10* (1), 35–45.

(17) McCorry, M. C.; Kim, J.; Springer, N. L.; Sandy, J.; Plaas, A.; Bonassar, L. J. Regulation of Proteoglycan Production by Varying Glucose Concentrations Controls Fiber Formation in Tissue Engineered Menisci. *Acta Biomater.* 2019, *100*, 173–183.

(18) Kim, J.; Boys, A. J.; Estroff, L. A.; Bonassar, L. J. Combining TGF-B1 and Mechanical Anchoring to Enhance Collagen Fiber Formation and Alignment in Tissue-Engineered Menisci. *ACS Biomater. Sci. Eng.* 2021, *7* (4), 1608–1620.

(19) McCorry, M. C.; Mansfield, M. M.; Sha, X.; Coppola, D. J.; Lee, J. W.; Bonassar, L. J. A Model System for Developing a Tissue Engineered Meniscal Enthesis. *Acta Biomater.* 2017, *56*, 110–117.

(20) Iannucci, L. E.; Boys, A. J.; Mccorry, M. C.; Estroff, L. A.; Bonassar, L. J. Cellular and Chemical Gradients to Engineer the Meniscus-to-Bone Insertion. *Adv. Healthc. Mater.* 2018, *1800806*, 1–10.

(21) Boys, A. J.; Zhou, H.; Harrod, J. B.; McCorry, M. C.; Estroff, L. A.; Bonassar, L. J. Top-Down Fabrication of Spatially Controlled Mineral-Gradient Scaffolds for Interfacial Tissue Engineering. *ACS Biomater. Sci. Eng.* 2019.

(22) Blaber, J.; Adair, B.; Antoniou, A. Ncorr: Open-Source 2D Digital Image Correlation Matlab Software. *Exp. Mech.* 2015, *55* (6), 1105–1122.

(23) Yang, P. J.; Temenoff, J. S. Engineering Orthopedic Tissue Interfaces. *Tissue Eng. Part B Rev.* 2009, *15* (2), 127–141.

(24) Brophy, R. H.; Matava, M. J. Surgical Options for Meniscal Replacement. *J. Am. Acad. Orthop. Surg.* 2012, *20* (5), 265–272.

(25) Fox, A. J. S.; Wanivenhaus, F.; Burge, A. J.; Warren, R. F.; Rodeo, S. A. The Human Meniscus: A Review of Anatomy, Function, Injury, and Advances in Treatment. *Clin. Anat.* 2015, *28* (2), 269–287.

(26) Puetzer, J. L.; Koo, E.; Bonassar, L. J. Induction of Fiber Alignment and Mechanical Anisotropy in Tissue Engineered Menisci with Mechanical Anchoring. *J. Biomech.* 2015, *48* (8), 1436–1443.

(27) Abraham, A. C.; Haut Donahue, T. L. From Meniscus to Bone: A Quantitative Evaluation of Structure and Function of the Human Meniscal Attachments. *Acta Biomater.* 2013, *9* (5), 6322–6329.

(28) Yaylaci, S. U.; Sen, M.; Bulut, O.; Arslan, E.; Guler, M. O.; Tekinay, A. B. Chondrogenic Differentiation of Mesenchymal Stem Cells on Glycosaminoglycan-Mimetic Peptide Nanofibers. *ACS Biomater. Sci. Eng.* 2016, *2* (5), 871–878.

(29) Zhou, H.; Boys, A. J.; Harrod, J. B.; Bonassar, L. J.; Estroff, L. A. Mineral

Distribution Spatially Patterns Bone Marrow Stromal Cell Behavior on Monolithic Bone Scaffolds. *Acta Biomater.* 2020, *112*, 274–285.

CHAPTER 4

Controlling Collagen Gelation pH to Enhance Biochemical, Structural, and Biomechanical Properties of Tissue-Engineered Menisci

Abstract

Collagen-based hydrogels have been widely used in biomedical applications due to their biocompatibility. Enhancing mechanical properties of collagen gels remains challenging while maintaining biocompatibility. Here, we demonstrate that gelation pH has profound effects on cellular activity, collagen fibril structure, and mechanical properties of the fibrochondrocyte-seeded collagen gels in both short- and long-terms. Acidic and basic gelation pH, below pH 7.0 and above 8.5, resulted in dramatic cell death. Gelation pH ranging from 7.0 to 8.5 showed a relatively high cell viability. Further, physiologic gelation pH 7.5 showed the greatest hydroxyproline deposition while glycosaminoglycan deposition appeared independent of gelation pH. Scanning electron microscopy showed that neutral and physiologic gelation pH, 7.0 and 7.5, exhibited well-aligned collagen fibril structure on day 0 and enhanced collagen fibril structure with laterally joined fibrils on day 30. However, basic pH, 8.0 and 8.5, displayed a densely packed collagen fibril structure on day 0, which was also persistent on day 30. Initial equilibrium modulus increased with increasing gelation pH. Notably, after 30 days of culture, gelation pH of 7.5 and 8.0 showed the highest equilibrium modulus, reaching 150-160 kPa. While controlling gelation pH is simply achieved compared to other strategies to improve mechanical properties, its influences on biochemical and biomechanical properties of the collagen gel are vigorous and long-lasting. As such, gelation pH is a useful means to modulate both biochemical and

biomechanical properties of the collagen-based hydrogels and can be utilized for diverse types of tissue engineering due to its simple application.

Kim, J. and Bonassar, L. J. Controlling Collagen Gelation pH to Enhance Biochemical, Structural, and Biomechanical Properties of Tissue-Engineered Menisci. Submitted.

Introduction

Collagen is the major structural component of connective tissues in vertebrates, such as bones, tendons, ligaments, cartilage, skin, blood vessels, and menisci.[1] Thus, collagen has been widely used as a scaffold material for diverse tissue engineering applications.[2] Although collagen-based biomaterials have shown promising outcomes due to their excellent biocompatibility, several drawbacks including inferior mechanical properties compared to native tissue pose limitations in their clinical application.[3]

There have been significant efforts to enhance the mechanical properties of collagen-based biomaterials. A variety of strategies using chemical or photochemical cross-linking agents or incorporating other stiff materials have been investigated.[4–7] Additionally, gelation factors, such as collagen concentration,[8,9] temperature,[8,10,11] ionic strength,[8,12,13] and pH,[9–11,14] have been reported to affect collagen fibrillogenesis, which is directly related to the mechanical properties of collagen gels. Among these factors, gelation pH influences hydrophobic and electrostatic interactions,[15] major driving forces of collagen self-assembly, and kinetics of fibrillogenesis.[11,16] These influences subsequently affect fibril size and morphology of the collagen gels.[11,16,17] Notably, optimal pH for mechanical properties has been observed to be in the range of basic pH,[11,18,19] which is higher than is typically used for formulating collagen-based hydrogels.[7,20,21] Given that changes in collagen fibril architecture result in changes in mechanical properties, gelation pH can be a useful tool to tune mechanical properties of collagen-based biomaterials.

Although the aforementioned studies have demonstrated the effects of gelation pH on collagen fibrillogenesis and resultant mechanical properties, these studies mainly

focused on initial collagen fibril structure and mechanical properties upon gelation and also used relatively low concentrations of collagen compared to native tissue. Furthermore, it is unclear whether gelation pH has long-lasting biological effects on cells seeded in a collagen gel. Thus, the influences of gelation pH on structural, biochemical, and biomechanical properties of high-density collagen constructs in long-term culture have not yet been elucidated.

Menisci play an important role in biomechanical functions in the knee joint and are mainly composed of collagen. In multiple previous studies, we have developed tissue-engineered menisci using a fibrochondrocyte-seeded high-density collagen gel and cultured them up to 8 weeks.[22–25] We have also showed that collagen fiber structure can be remodeled by seeded fibrochondrocytes, leading to changes in mechanical properties. Therefore, tissue-engineered menisci represent a useful platform to investigate the short- and long-term effects of gelation pH on cellular activities of fibrochondrocytes, cell-mediated remodeling, and mechanical properties of collagen gels.

In this study, we investigated the effects of gelation pH on cell viability, fibrochondrocyte proliferation, glycosaminoglycan (GAG) and collagen deposition, collagen microstructure, and mechanical properties of tissue-engineered menisci. We hypothesize that gelation pH regulates biochemical, structural, and mechanical properties of tissue-engineered menisci, and that there exists an optimal gelation pH that results in both increased extracellular matrix production and improved mechanical properties of tissue-engineered menisci after extended culture. These results are useful for developing an optimal culture condition for enhancing functionality of tissue-

engineered menisci and facilitating the transition of tissue-engineered menisci to clinical use.

Materials and Methods

Cell Isolation. Fibrochondrocytes were harvested from the menisci of 1-3 day old bovids using a 0.3% (wt/vol) collagenase (Worthington Biochemical Corporation, Lakewood, NJ) in Dulbecco's Modified Eagle Medium (DMEM) with 100 μg/mL penicillin and 100 μg/mL streptomycin for 18 hours as previously described.[26] After digestion, the cells were filtered through a 100 μm cell strainer, washed, counted, and suspended to a concentration of 150 X 10^6 cells/mL. Harvested fibrochondrocytes were pooled from all 8 menisci to minimize zone-dependent phenotypic variation.

Construct Fabrication. Collagen was extracted from Sprague-Dawley rat tails (Pel-Freez Biologicals, Rogers, AZ), solubilized, lyophilized, and reconstituted in 0.1% (vol/vol) acetic acid at a 30 mg/mL concentration as previously described.[4,27,28] The stock collagen solution was mixed with a working solution composed of 1N NaOH, 10X phosphate-buffered saline (PBS), and 1X PBS using a syringe stopcock. To achieve desired gelation pH of 6.5, 7.0, 7.5, 8.0, 8.5 and 9.0, the amounts of 1M NaOH and 1X PBS were adjusted accordingly. Subsequently, harvested fibrochondrocytes were mixed with the collagen solution to a final concentration of 25 x 10^6 cells/mL and 20 mg/mL collagen gel and injected into meniscal molds.[22] The meniscal molds were allowed to gel for 30 min at 37 °C. Constructs were cultured in DMEM at a 500 mg/L glucose concentration, which was found to be an optimal glucose concentration for collagen organization,[24] with 10% (vol/vol) fetal bovine serum (FBS), 100 μg/mL penicillin, 100

μg/mL streptomycin, 0.1 mM non-essential amino acids, 50 μg/mL ascorbic acid, and 0.4 mM L-proline at 37 °C and 5% CO_2 for up to 30 days. Culture media were collected and replenished every third day. Photographs of each 30-day cultured construct were obtained on days 0 and 30 to calculate contraction using ImageJ software (NIH, Bethesda, MD).

Cell Viability. Cell viability was assessed immediately after construct fabrication. Cross sections of each construct were harvested and stained for 30 min using 4 μM of ethidium homodimer-1 and 8 μM of calcein AM (Sigma-Aldrich, MO, USA) according to the manufacturer's instruction. After staining, each portion of the constructs was rinsed with PBS for 5 min three times and subsequently imaged on a Zeiss LSM880 confocal/multi-photon inverted microscope. Images were then imported into ImageJ to assess cell viability.

Biochemical Analysis. Biochemical analysis was performed to measure contents of DNA via a Hoechst DNA assay,[29] GAG via a modified 1,9-dimethylmethylene blue (DMMB) assay,[30] and collagen via a hydroxyproline (Hypro) assay,[31] as previously documented. Prior to the assays, portions of each construct were measured for wet weight (w.w.), lyophilized, and then digested in 1.25 mg/mL papain digestion solution (Sigma-Aldrich, MO, USA).

Histological Analysis. Circumferentially cross-sectioned samples were fixed, dehydrated, embedded in paraffin blocks, sectioned, and stained with picrosirius red. Images were taken under brightfield and polarized light with a Nikon Eclipse TE2000-S microscope (Nikon Instruments, Melville, NY) with a SPOT RT camera (Diagnostic Instruments, Sterling Heights, MI) to investigate collagen fiber structure.

Scanning Electron Microscopy (SEM). Circumferentially cross-sectioned samples were fixed, stored in 100% ethanol, and then critical point dried. The dried samples were sputter-coated with gold at a target current of 20 mA. After coating, samples were scanned using a Zeiss Gemini 500 scanning electron microscope at an accelerating voltage of 1 kV.

Mechanical Analysis. Confined compression stress relaxation test was performed using an Enduratec ElectroForce 5500 System (Bose, Eden Prairie, MN), as previously reported.[4] Samples were prepared using 4 mm diameter biopsy punches. Six steps of 5% compression each with 10 min between steps to ensure full stress relaxation were imposed on the construct samples. The resulting loads were fitted to a poroelastic model using a custom MATLAB program to calculate the equilibrium modulus.

Statistical Analysis. Normality testing was performed by Shapiro-Wilk's test using GraphPad Prism (GraphPad Prism Software Inc., San Diego, CA). To compare multiple groups, we performed one-way or two-way analysis of variance (ANOVA) with Tukey's Honestly Significant Difference (HSD) post hoc tests. All data are reported as mean ± standard deviation with at least $n = 4$ replicates. Significance was determined with $p < 0.05$.

Results

Cell Viability Analysis. Cells are known to be sensitive to their surrounding environment, such as stiffness and pH.[32,33] Thus, in order to evaluate the effects of gelation pH on fibrochondrocyte viability, live/dead staining was performed on high-density collagen constructs gelled at pH values ranging from 6.0 to 9.0 (Figure 4.1).

Neutral to slightly basic gelation pH from 7.0 to 8.5 showed high cell viability, ranging from 81% to 83%. In contrast, acidic pH and basic gelation pH, pH 6.5 and 9.0, resulted in significantly decreased cell viability, 67.7 ± 4.5% and 19.5 ± 4.2%, respectively. Interestingly, gelation pH 9.0 exhibited the lowest cell viability corresponding to one-third of viability at gelation pH 6.5 and one-fourth of that at the rest. As cell viability is strongly associated with success of tissue engineering approaches, gelation pH ranging from 7.0 to 8.5 was chosen for further experiments.

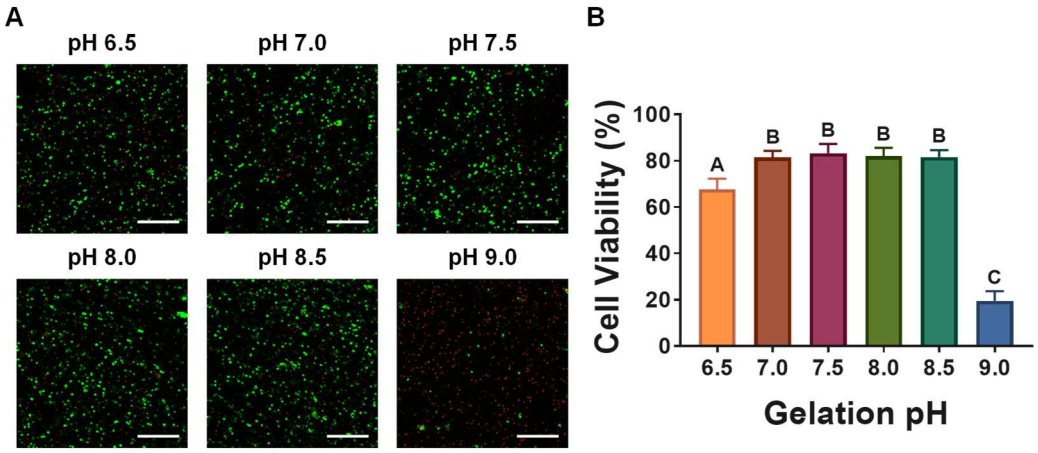

Figure 4.1. Cell viability of fibrochondrocytes seeded in high-density collagen constructs in response to various gelation pH. (A) Representative confocal fluorescent images of live/dead staining at indicated gelation pH. Live cells are stained green, and dead cells are stained red. (B) Viability of fibrochondrocytes at indicated gelation pH (n = 6-10). Different letters represent statistical significance between groups ($p < 0.05$). Scale bars are 200 μm.

Meniscal Construct Contraction Analysis. Considering that anatomic accuracy of tissue-engineered constructs is a key for successful clinical applications, it is critical to prevent dramatic construct contraction. Therefore, we examined construct

contraction over the 30-day culture period. Construct contraction appeared to be reduced with increasing gelation pH (Figure 4.2). Gelation pH 7.0 led to the greatest construct contraction, decreasing 30% from the initial size. Conversely, gelation pH 7.5 to 8.5 displayed a modest contraction to 2-20% from their initial size.

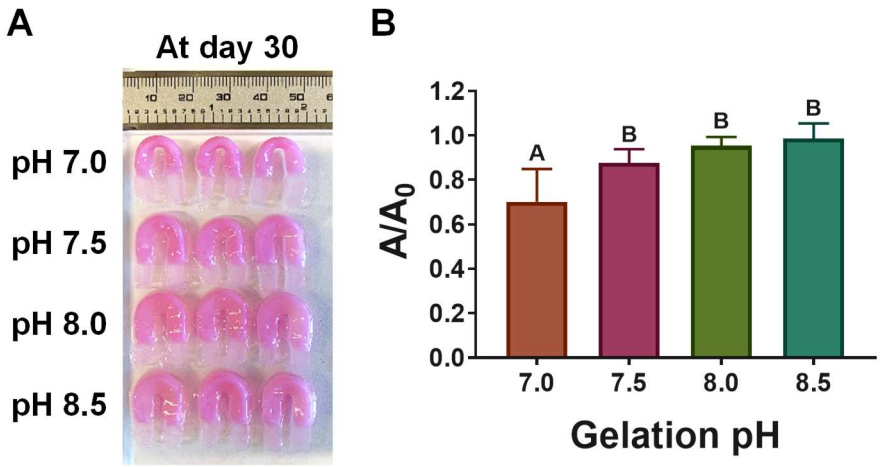

Figure 4.2. Contraction of meniscal constructs after 30 days of culture. (A) Photograph of meniscal constructs on day 30 gelled at indicated pH. (B) Ratio of construct area on day 30 over initial area (n = 6). Different letters represent statistical significance between groups ($p < 0.05$).

Cellular Activity Analysis. Next, we measured contents of DNA, GAG, and Hypro to determine the biological effects of gelation pH on fibrochondrocytes. Although gelation pH 8.5 appeared to reduce density of fibrochondrocytes over time in culture, no statistical difference was found in the DNA content between the groups (Figure 4.3A). Since constructs were made of purified type I collagen, all the constructs showed a minimal content of GAG on day 0 without significant difference between the groups (Figure 4.3B). After 30 days of culture, all meniscal constructs showed significantly increased GAG content compared to the day 0 constructs. However,

statistical difference in GAG content was not observed between the different pH conditions on day 30. Similar results were observed in GAG content normalized to dry weight and to DNA content, and total GAG content per construct (Figure 4.S1). Moreover, no statistical difference was observed in the release of GAG to media throughout the culture period (Figure 4.S2). Conversely, while Hypro content did not show significant difference between the day 0 constructs, gelation pH 7.5 resulted in the greatest Hypro content between the groups and significantly increased Hypro content compared to gelation pH 8.0 and 8.5 on day 30 (Figure 4.3C). However, gelation pH 8.0 resulted in the significantly decreased Hypro content normalized to dry weight on day 30 compared to gelation pH 7.0 on day 0 while no statistical difference was found in the other groups (Figure 4.S3A). Further, there was no significant difference in the Hypro content normalized to the DNA content and per construct (Figure 4.S3B,C) and the release of Hypro to media over time in culture between the groups (Figure 4.S4).

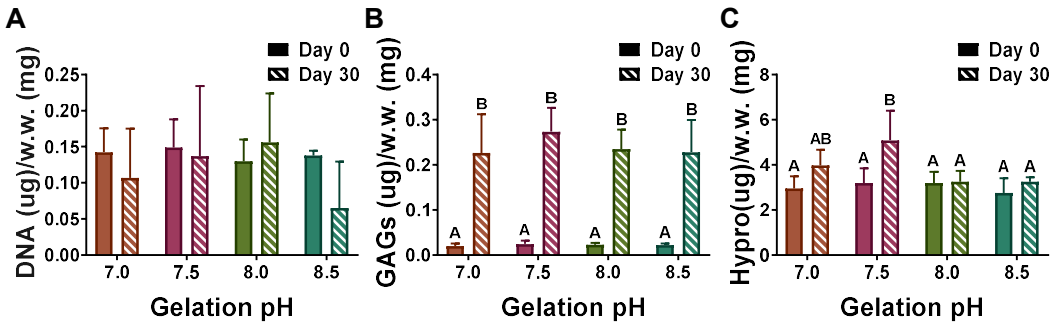

Figure 4.3. Contents of DNA, GAGs, and Hypro in high-density collagen constructs on days 0 (filled bar) and 30 (diagonal striped bar). (A) DNA content in meniscal constructs normalized to wet weight (n = 6). (B) GAG content in meniscal constructs normalized to wet weight (n = 6). (C) Hypro content in meniscal constructs normalized to wet weight (n = 6). Different letters represent statistical significance between groups (p <

0.05).

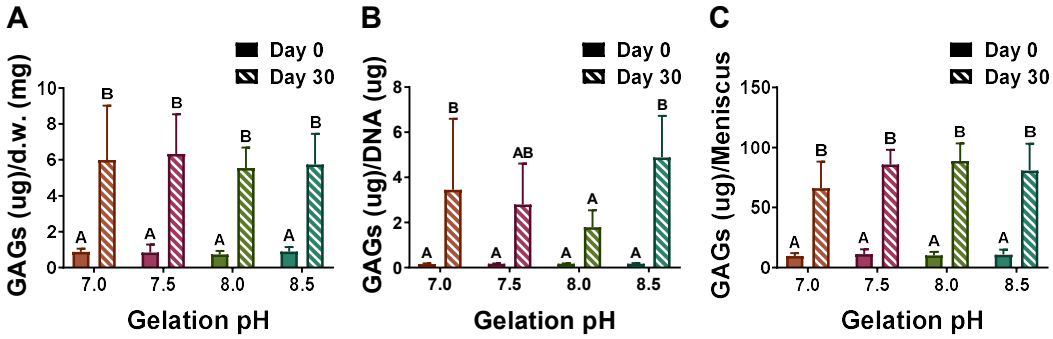

Figure 4.S1. GAG content in meniscal construct normalized to (A) dry weight and (B) DNA content on days 0 and 30. (C) Total GAG content in meniscal constructs on days 0 and 30. Different letters represent statistical significance between groups ($p < 0.05$; $n = 6$).

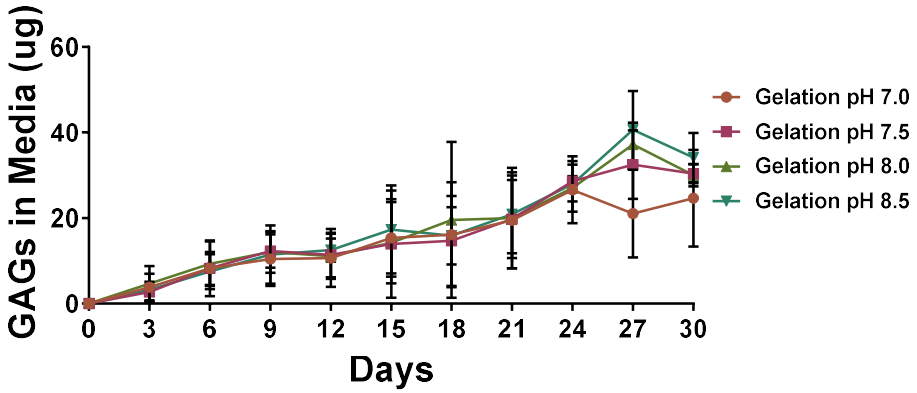

Figure 4.S2. GAG release to media over time in culture ($n = 6$). No statistical difference was observed between groups.

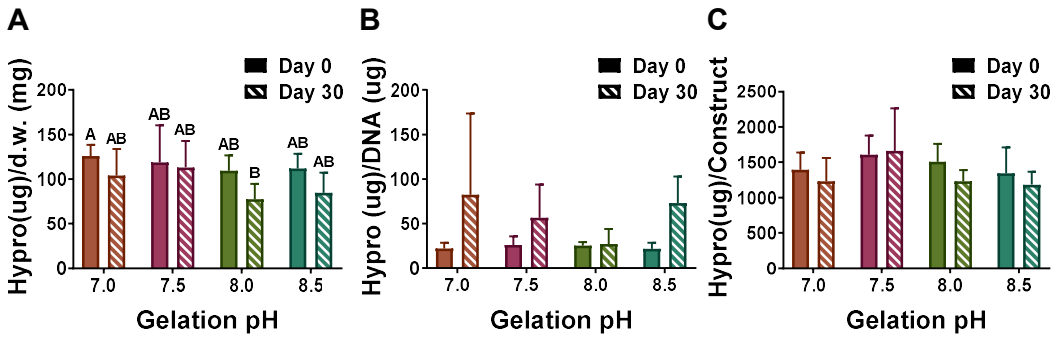

Figure 4.S3. Hypro content in meniscal construct normalized to (A) dry weight and (B) DNA content on days 0 and 30. (C) Total Hypro content in meniscal constructs on days 0 and 30. Different letters represent statistical significance between groups ($p < 0.05$; $n = 6$).

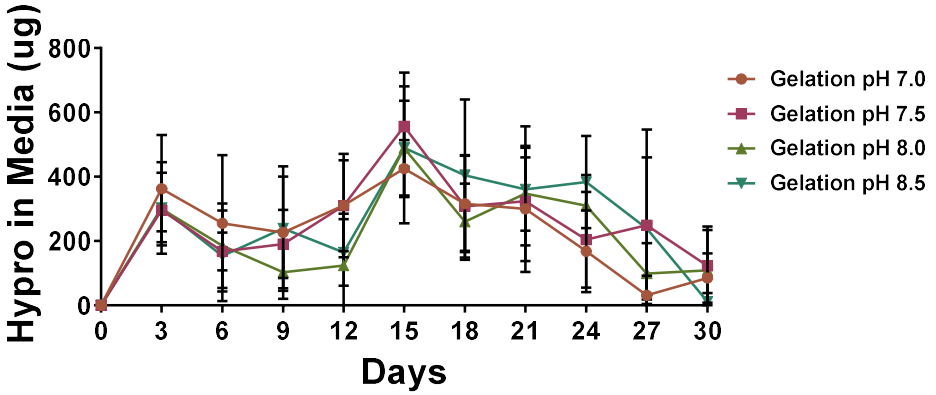

Figure 4.S4. Hypro release to media over time in culture ($n = 6$). No statistical difference was observed between groups.

Collagen Microstructure Analysis. In order to investigate how gelation pH affects collagen microstructure of meniscal constructs in the short- and long-terms, scanning electron microscope imaging was performed on meniscal constructs on days 0 and 30. Constructs gelled at basic gelation pH exhibited entangled collagen fibrils on day 0 (Figure 4.4). This collagen fibril structure was also persistent on day 30. However,

constructs gelled at pH of 7.0 and 7.5 showed aligned collagen fibrils on day 0 to some extent and more aligned collagen fibrils on day 30. Interestingly, bundles of collagen fibrils were observed at gelation pH 7.5 on day 30. Intriguingly, fibrochondrocytes were found in lacunae-like spaces surrounded by collagen fibrils at gelation pH 7.0 and 7.5 on day 30. In contrast, fibrochondrocytes within constructs gelled at pH 8.0 and 8.5 were found on the surface of collagen fibrils on day 30, similar to the day 0 groups. These observations might indicate that fibrochondrocytes were able to remodel collagen fibril structure gelled at pH 7.0 and 7.5 but not at pH 8.0 and 8.5. These findings were supported by picrosirius red staining images showing similar collagen fiber organization, enhanced collagen fiber structure at gelation pH 7.5 on day 30 compared to the other groups (Figure 4.5).

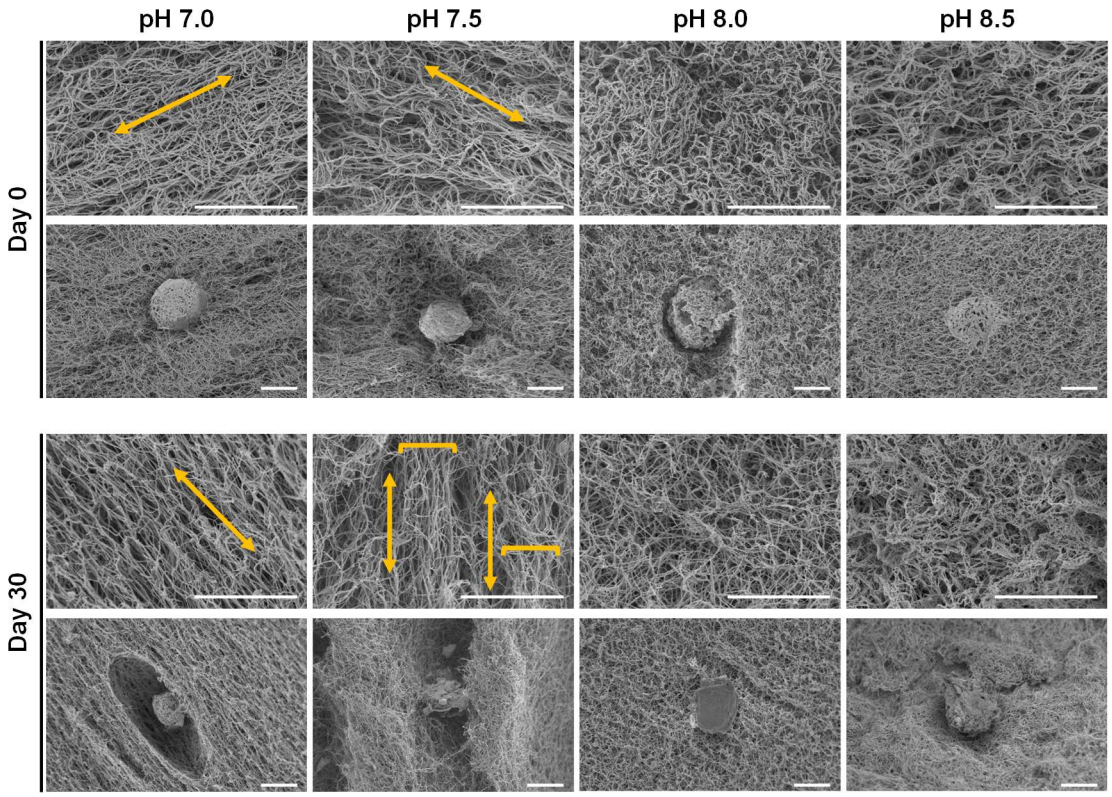

Figure 4.4. Representative scanning electron microscope images of fibril organization

of meniscal constructs after 0 and 30 days of culture. Double-headed arrows indicate a direction of collagen fibril alignment. Brackets indicate a bundle of collagen fibrils. Scale bars are 4 μm.

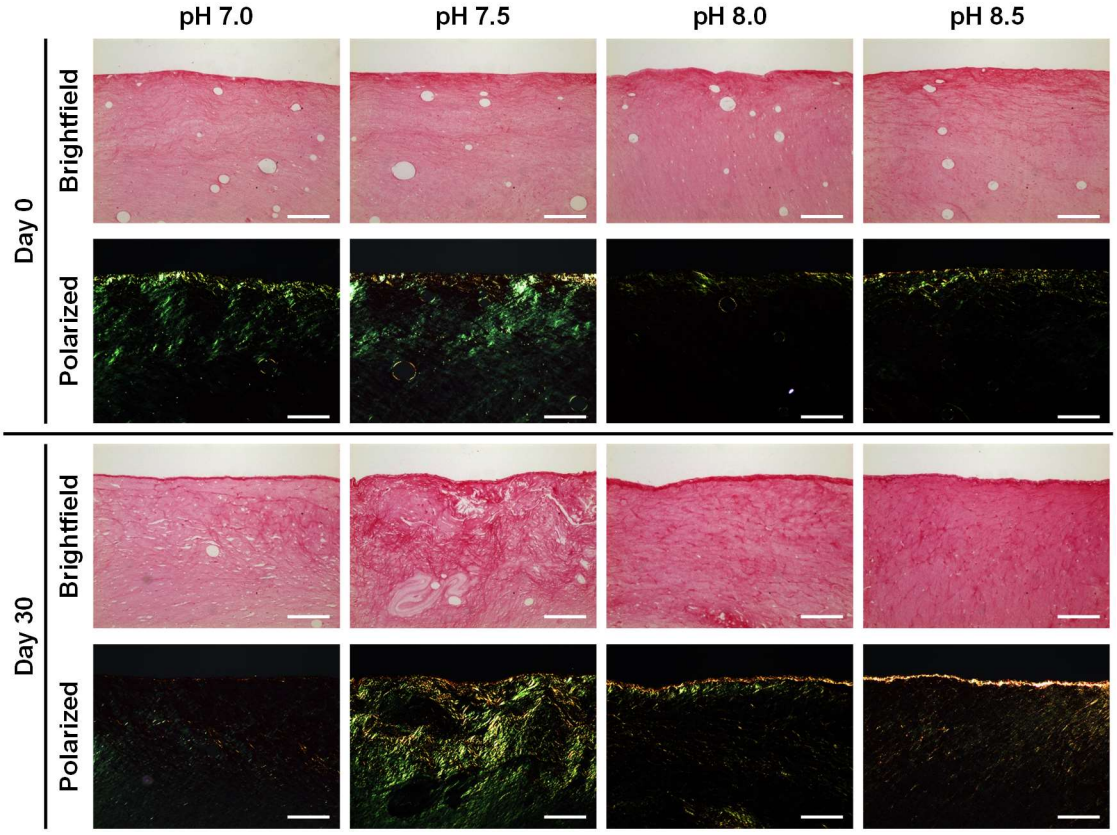

Figure 4.5. Picrosirius red stating images of collagen fiber organization of meniscal constructs under brightfield and polarized light on days 0 and 30. Scale bars are 200 μm.

Mechanical Property Analysis. It has been shown that collagen organization is critical for mechanical properties of native tissue and collagen-based biomaterials. Thus, we performed confined compression tests to obtain the equilibrium modulus, instantaneous modulus, and hydraulic permeability of meniscal constructs. For day 0 groups, the equilibrium modulus increased with increasing gelation pH with the peak

observed at gelation pH 8.5 showing a 2-fold increase relative to that of gelation pH 7.0, 111 kPa vs. 55 kPa respectively (Figure 4.6A). Interestingly, over time in culture, constructs gelled at pH 7.0 and 7.5 showed significantly enhanced equilibrium modulus compared to their day 0 groups while constructs gelled at pH 8.0 and 8.5 also showed an increase in equilibrium modulus but was not significant. The highest equilibrium modulus, ~162 kPa, was observed in gelation pH 7.5 on day 30. Instantaneous modulus also peaked at gelation pH 7.5 on day 30 while there was no difference between the other groups (Figure 4.S5). Gelation pH 7.0 and 7.5 showed significantly higher permeability than that of gelation pH 8.0 and 8.5 on day 0 but substantially decreased hydraulic permeability on day 30 comparable to that of gelation pH 8.0 and 8.5 (Figure 4.6B). On the other hand, gelation pH 8.0 and 8.5 retained hydraulic permeability throughout the culture period.

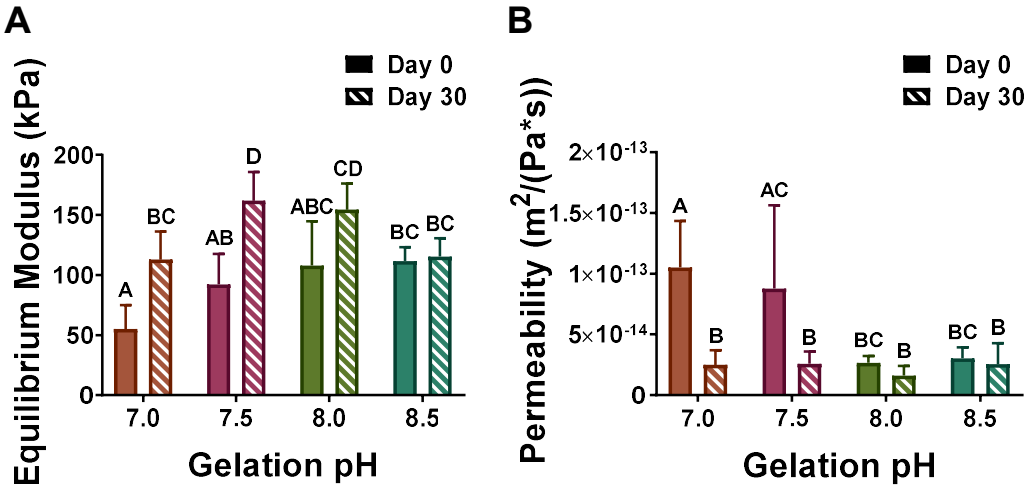

Figure 4.6. Mechanical properties of meniscal constructs on days 0 (filled bar) and 30 (diagonal striped bar). (A) Equilibrium modulus of meniscal constructs (n = 4-6). (B) Hydraulic permeability of meniscal constructs (n = 4-6). Different letters represent

statistical significance between groups ($p < 0.05$).

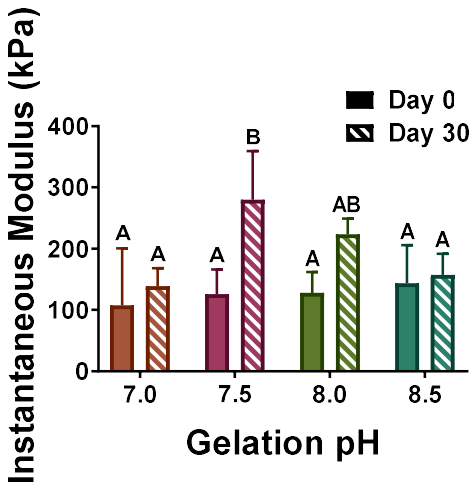

Figure 4.S5. Instantaneous modulus of meniscal constructs on days 0 and 30. Different letters represent statistical significance between groups ($p < 0.05$; $n = 4$-6).

Discussion

The goal of this study was to investigate the biological, structural, and biomechanical effects of gelation pH on high-density collagen-based constructs. In this current study, we demonstrated that gelation pH affects the biological activity of fibrochondrocytes, initial collagen fibril structure, cell-mediated collagen remodeling, and mechanical properties of the collagen gel in both short- and long-terms. We showed that gelation pH of 7.5, a physiologic condition, is beneficial for both biological and mechanical properties of the meniscal constructs, supported by enhanced Hypro deposition and equilibrium modulus after 30 days of culture.

Live/dead staining revealed that fibrochondrocytes retained a relatively high cell viability within the range of physiologic gelation pH (Figure 4.1). Interestingly, beyond

this range, substantial cytotoxicity was detected, indicating that there might exist a threshold of gelation pH that is suitable for fibrochondrocytes. Previous studies have shown that fibroblasts, keratinocytes, and stromal cells maintain a higher cell viability at physiologic pH compared to acidic and basic pH,[34,35] while chondrocytes retain a high cell viability at acidic pH comparable to physiologic pH.[36] Such data suggest that the effect of pH on cell viability is dependent on cell type and thus that the optimization of gelation pH should be taken into consideration for collagen-based biomaterials using diverse cell types.

Significant construct contraction should be avoided due to the possibility of anatomical mismatching which can lead to failure after implantation.[37] Contraction analysis demonstrated that gelation pH of 7.0 resulted in a significant contraction compared to the other groups although there was no statistical difference in cell viability between these groups (Figure 4.2). Contraction of collagen gels is attributed to weak mechanical properties and/or cell-mediated remodeling,[38] which is consistent with our findings in this study that increasing initial equilibrium modulus resulted in decreasing construct contraction (Figure 4.2B and 4.6A). These data underscore the importance of initial construct mechanics in achieving sufficient shape fidelity of implants.

It is well known that collagen and GAGs are major components of native meniscus and also give rise to the biomechanical functions of native menisci.[39,40] Cell proliferation and extracellular matrix production by cells have been shown to change in response to the surrounding environment, such as dimensionality (2D vs. 3D) or stiffness.[41,42] Biochemical analysis revealed that maintenance of cell content throughout the culture was independent of gelation pH. GAG content also did not show any

significant difference between groups on day 30. However, only gelation pH of 7.5 showed the significantly increased Hypro content compared to the day 0 groups and the groups of gelation pH of 8.0 and 8.5 on day 30. This result was consistent with increased picrosirius red staining observed at gelation pH 7.5 (Figure 4.5). These findings suggest that physiologic gelation pH is not only beneficial for cell viability but also biosynthetic activity.

Many studies have shown that collagen fibrillogenesis is mainly driven by hydrophobic and electrostatic interactions and influenced by various factors including the presence or absence of telopeptide, ionic strength, temperature, and gelation pH.[11,43] These parameters affect the kinetics of fibrillogenesis and also fibril formation. Scanning electron microscope images demonstrated that gelation pH affects collagen fibril organization of high-density collagen constructs. Whereas basic gelation pH, 8.0 and 8.5, appeared to generate compact, entangled collagen fibril structures, gelation pH of 7.0 and 7.5 resulted in focal collagen microstructures (Figure 4.5 and 4.6, top panels). This structural difference became more apparent in the constructs cultured for 30 days (Figure 4.5 and 4.6, bottom panels). Constructs gelled at pH 7.0 and 7.5 showed a lateral growth of collagen fibrils after 30 days of culture, which was not observed in those gelled at pH 8.0 and 8.5. It has been shown that gelation pH ranging from 8.5 to 10 leads to randomly interconnected collagen fibril structure due to enhanced hydrophobic interaction, while physiologic pH leads to organized collagen fibril formation mediated by thermodynamically preferred interactions.[11,16,19] Interestingly, in 12 mM NaCl or in the absence of salts, the isoelectronic point of collagen is reported to be ~9.3,[16,44] which could have a strong effect on association of fibrils. Furthermore, flexibility of collagen

molecules has been found to be greater at pH 7.4 than at pH 4.0, and such flexibility might aid in assembly of organized collagen fibril networks.[45] The exact mechanism of this structural difference is not clear, but it can be speculated that entangled and interconnected collagen fibril structure is not favorable for cell-mediated remodeling due to sterically hindered binding sites for cells or limited space between collagen fibrils. This phenomenon could explain why fibrochondrocytes were found in lacunae-like spaces only at gelation pH 7.0 and 7.5, but not at higher pH.

Confined compression testing revealed that initial equilibrium and instantaneous moduli of meniscal constructs are dependent on gelation pH since higher gelation pH led to an increasing trend of both moduli. However, equilibrium modulus on day 30 appeared to result from the interplay between collagen content and collagen fibril/fiber structure, which is consistent with previous studies showing that increased extracellular matrix molecules and enhanced collagen fiber organization are correlated with mechanical properties of collagen-based constructs.[4,22] On day 0, gelation pH 7.0 and 7.5 showed higher hydraulic permeability than the groups of gelation pH 8.0 and 8.5, suggesting collagen fibril structure determines initial permeability of the constructs. However, on day 30, all constructs presented similar permeability although they showed differing collagen fibril/fiber structure. Notably, these conditions had similar GAG content, which is known to have a strong influence on hydraulic permeability.[46,47] As such, initial mechanical properties are not likely to be a good indicator of eventual mechanical properties of collagen-based scaffolds after time in culture, which are rather accumulative effects of extracellular matrix molecule production and collagen fiber structure.

Ionic strength, as well as the types of electrolytes, has profound effects on collagen fibrillogenesis.[9,11,12] In this context, it should be noted that gelation pH was regulated by adjusting the amounts of 1M NaOH and 1X PBS, which also resulted in different ionic strength. However, the difference in ionic strength between the groups is less than 0.1%, and thus the effects of ionic strength might be negligible compared to those of gelation pH in this study.

A number of strategies have been investigated to enhance mechanical properties of collagen-based biomaterials. Chemical or photochemical crosslinking methods have been shown to increase the mechanical properties of collagen constructs[5,6]. However, these methods have several limitations, such as cytotoxicity or pigment production. Although incorporation of synthetic or natural polymers to fabricate collagen-based composites also showed promising outcomes, these methods require additional processing steps, which might limit the clinical applications. Compared to these methods, controlling gelation pH is relatively simple since it does not require any additional steps while achieving significantly enhanced extracellular matrix production and mechanical properties. We previously showed that mechanical properties and printability of bioinks can be modulated by varying gelation pH.[14] Thus, this approach can provide insight in diverse collagen-based scaffold fabrication using a mold or bioprinter.

Conclusions

Overall, this study demonstrated that gelation pH has profound effects on cellular activity, collagen fibril structure, and mechanical properties of collagen-based

hydrogels in both short- and long-terms. Notably, whereas slightly super-physiologic pH, 8.0 and 8.5, produced the highest equilibrium modulus on day 0, physiologic gelation pH showed the highest Hypro production and equilibrium modulus of the tissue-engineered constructs along with well-aligned, laterally joined fibrils after 30 days of culture. Collectively, these data highlight the importance of controlling gelation pH for collagen-based hydrogels and the versatility of gelation pH as a means to regulate biological and biomechanical properties of the collagen hydrogels.

References

(1) Holmes, D. F.; Lu, Y.; Starborg, T.; Kadler, K. E. *Collagen Fibril Assembly and Function*; 2018; Vol. 130.

(2) Nirmalanandhan, V. S.; Rao, M.; Shearn, J. T.; Juncosa-Melvin, N.; Gooch, C.; Butler, D. L. Effect of Scaffold Material, Construct Length and Mechanical Stimulation on the in Vitro Stiffness of the Engineered Tendon Construct. *J. Biomech.* 2008, *41* (4), 822–828.

(3) Lin, K.; Zhang, D.; Macedo, M. H.; Cui, W.; Sarmento, B.; Shen, G. Advanced Collagen-Based Biomaterials for Regenerative Biomedicine. *Adv. Funct. Mater.* 2019, *29* (3), 1–16.

(4) Puetzer, J. L.; Bonassar, L. J. High Density Type I Collagen Gels for Tissue Engineering of Whole Menisci. *Acta Biomater.* 2013, *9* (8), 7787–7795.

(5) Heo, J.; Koh, R. H.; Shim, W.; Kim, H. D.; Yim, H. G.; Hwang, N. S. Riboflavin-

Induced Photo-Crosslinking of Collagen Hydrogel and Its Application in Meniscus Tissue Engineering. *Drug Deliv. Transl. Res.* 2016, *6* (2), 148–158.

(6) Yoshioka, S. A.; Goissis, G. Thermal and Spectrophotometric Studies of New Crosslinking Method for Collagen Matrix with Glutaraldehyde Acetals. *J. Mater. Sci. Mater. Med.* 2008, *19* (3), 1215–1223.

(7) Fan, X.; Liang, Y.; Cui, Y.; Li, F.; Sun, Y.; Yang, J.; Song, H.; Bao, Z.; Nian, R. Development of Tilapia Collagen and Chitosan Composite Hydrogels for Nanobody Delivery. *Colloids Surfaces B Biointerfaces* 2020, *195* (189), 111261.

(8) Antoine, E. E.; Vlachos, P. P.; Rylander, M. N. Tunable Collagen I Hydrogels for Engineered Physiological Tissue Micro-Environments. *PLoS One* 2015, *10* (3), 1–18.

(9) Yan, M.; Li, B.; Zhao, X.; Qin, S. Effect of Concentration, PH and Ionic Strength on the Kinetic Self-Assembly of Acid-Soluble Collagen from Walleye Pollock (Theragra Chalcogramma) Skin. *Food Hydrocoll.* 2012, *29* (1), 199–204.

(10) Cisneros, D. A.; Hung, C.; Franz, C. M.; Muller, D. J. Observing Growth Steps of Collagen Self-Assembly by Time-Lapse High-Resolution Atomic Force Microscopy. *J. Struct. Biol.* 2006, *154* (3), 232–245.

(11) Achilli, M.; Mantovani, D. Tailoring Mechanical Properties of Collagen-Based Scaffolds for Vascular Tissue Engineering: The Effects of PH, Temperature and Ionic Strength on Gelation. *Polymers (Basel).* 2010, *2* (4), 664–680.

(12) Harris, J. R.; Soliakov, A.; Lewis, R. J. In Vitro Fibrillogenesis of Collagen Type I in Varying Ionic and PH Conditions. *Micron* 2013, *49*, 60–68.

(13) Meng, D.; Li, W.; Ura, K.; Takagi, Y. Effects of Phosphate Ion Concentration on In-Vitro Fibrillogenesis of Sturgeon Type I Collagen. *Int. J. Biol. Macromol.* 2020, *148*, 182–191.

(14) Diamantides, N.; Wang, L.; Pruiksma, T.; Siemiatkoski, J.; Dugopolski, C.; Shortkroff, S.; Kennedy, S.; Bonassar, L. J. Correlating Rheological Properties and Printability of Collagen Bioinks: The Effects of Riboflavin Photocrosslinking and PH. *Biofabrication* 2017, *9* (3).

(15) Silver, F. H.; Freeman, J. W.; Seehra, G. P. Collagen Self-Assembly and the Development of Tendon Mechanical Properties. *J. Biomech.* 2003, *36* (10), 1529–1553.

(16) Li, Y.; Asadi, A.; Monroe, M. R.; Douglas, E. P. PH Effects on Collagen Fibrillogenesis in Vitro: Electrostatic Interactions and Phosphate Binding. *Mater. Sci. Eng. C* 2009, *29* (5), 1643–1649.

(17) Noitup, P.; Morrissey, M. T. COLLAGEN : EFFECTS OF COLLAGEN CONCENTRATIONS , PH. 2005, *30* (2006), 547–555.

(18) Rosenblatt, J.; Devereux, B.; Wallace, D. G. Injectable Collagen as a PH-Sensitive Hydrogel. *Biomaterials* 1994, *15* (12), 985–995.

(19) Raub, C. B.; Unruh, J.; Suresh, V.; Krasieva, T.; Lindmo, T.; Gratton, E.;

Tromberg, B. J.; George, S. C. Image Correlation Spectroscopy of Multiphoton Images Correlates with Collagen Mechanical Properties. *Biophys. J.* 2008, *94* (6), 2361–2373.

(20) Nocera, A. D.; Comín, R.; Salvatierra, N. A.; Cid, M. P. Development of 3D Printed Fibrillar Collagen Scaffold for Tissue Engineering. *Biomed. Microdevices* 2018, *20* (2), 1–13.

(21) Wei, S.-Y.; Chen, T.-H.; Kao, F.-S.; Hsu, Y.-J.; Chen, Y.-C. Strategy for Improving Cell-Mediated Vascularized Soft Tissue Formation in a Hydrogen Peroxide-Triggered Chemically-Crosslinked Hydrogel. *J. Tissue Eng.* 2022, *13*, 204173142210840.

(22) Puetzer, J. L.; Koo, E.; Bonassar, L. J. Induction of Fiber Alignment and Mechanical Anisotropy in Tissue Engineered Menisci with Mechanical Anchoring. *J. Biomech.* 2015, *48* (8), 1436–1443.

(23) McCorry, M. C.; Bonassar, L. J. Fiber Development and Matrix Production in Tissue-Engineered Menisci Using Bovine Mesenchymal Stem Cells and Fibrochondrocytes. *Connect. Tissue Res.* 2017, *58* (3–4), 329–341.

(24) McCorry, M. C.; Kim, J.; Springer, N. L.; Sandy, J.; Plaas, A.; Bonassar, L. J. Regulation of Proteoglycan Production by Varying Glucose Concentrations Controls Fiber Formation in Tissue Engineered Menisci. *Acta Biomater.* 2019, *100*, 173–183.

(25) Kim, J.; Boys, A. J.; Estroff, L. A.; Bonassar, L. J. Combining TGF-B1 and

Mechanical Anchoring to Enhance Collagen Fiber Formation and Alignment in Tissue-Engineered Menisci. *ACS Biomater. Sci. Eng.* 2021, *7* (4), 1608–1620.

(26) Ballyns, J. J.; Wright, T. M.; Bonassar, L. J. Effect of Media Mixing on ECM Assembly and Mechanical Properties of Anatomically-Shaped Tissue Engineered Meniscus. *Biomaterials* 2010, *31* (26), 6756–6763.

(27) Bowles, R. D.; Williams, R. M.; Zipfel, W. R.; Bonassar, L. J. Self-Assembly of Aligned Tissue-Engineered Annulus Fibrosus and Intervertebral Disc Composite Via Collagen Gel Contraction. *Tissue Eng. Part A* 2010, *16* (4), 1339–1348.

(28) Cross, V. L.; Zheng, Y.; Won Choi, N.; Verbridge, S. S.; Sutermaster, B. A.; Bonassar, L. J.; Fischbach, C.; Stroock, A. D. Dense Type I Collagen Matrices That Support Cellular Remodeling and Microfabrication for Studies of Tumor Angiogenesis and Vasculogenesis in Vitro. *Biomaterials* 2010, *31* (33), 8596–8607.

(29) Kim, Y.-J.; Sah, R. L. Y.; Doong, J.-Y. H.; Grodzinsky, A. J. Fluorometric Assay of DNA in Cartilage Explants Using Hoechst 33258. *Anal. Biochem.* 1988, *174* (1), 168–176.

(30) Enobakhare, B. O.; Bader, D. L.; Lee, D. A. Quantification of Sulfated Glycosaminoglycans in Chondrocyte/Alginate Cultures, by Use of 1,9-Dimethylmethylene Blue. *Anal. Biochem.* 1996, *243* (1), 189–191.

(31) Neuman, R. E.; Logan, M. A. The Determination of Collagen and Elastin in Tissues. *J. Biol. Chem.* 1950, *186* (2), 549–556.

(32) Mao, A. S.; Shin, J. W.; Mooney, D. J. Effects of Substrate Stiffness and Cell-Cell Contact on Mesenchymal Stem Cell Differentiation. *Biomaterials* 2016, *98*, 184–191.

(33) Eagle, H. The Effect of Environmental PH on the Growth of Normal and Malignant Cells. *J. Cell. Physiol.* 1973, *82* (1), 1–8.

(34) Kruse, C. R.; Singh, M.; Targosinski, S.; Sinha, I.; Sørensen, J. A.; Eriksson, E.; Nuutila, K. The Effect of PH on Cell Viability, Cell Migration, Cell Proliferation, Wound Closure, and Wound Reepithelialization: In Vitro and in Vivo Study. *Wound Repair Regen.* 2017, *25* (2), 260–269.

(35) Stepanovska, J.; Otahal, M.; Hanzalek, K.; Supova, M.; Matejka, R. Ph Modification of High-Concentrated Collagen Bioinks as a Factor Affecting Cell Viability, Mechanical Properties, and Printability. *Gels* 2021, *7* (4).

(36) Wu, M. H.; Urban, J. P. G.; Zhan, F. C.; Cui, Z.; Xu, X. Effect of Extracellular PH on Matrix Synthesis by Chondrocytes in 3D Agarose Gel. *Biotechnol. Prog.* 2007, *23* (2), 430–434.

(37) Brophy, R. H.; Matava, M. J. Surgical Options for Meniscal Replacement. *J. Am. Acad. Orthop. Surg.* 2012, *20* (5), 265–272.

(38) Ibusuki, S.; Halbesma, G. J.; Randolph, M. A.; Redmond, R. W.; Kochevar, I. E.; Gill, T. J. Photochemically Cross-Linked Collagen Gels as Three-Dimensional Scaffolds for Tissue Engineering. *Tissue Eng.* 2007, *13* (8), 1995–2001.

(39) Fox, A. J. S.; Bedi, A.; Rodeo, S. A. The Basic Science of Human Knee Menisci: Structure, Composition, and Function. *Sports Health* 2012, *4* (4), 340–351.

(40) Vanderploeg, E. J.; Wilson, C. G.; Imler, S. M.; Ling, C. H. Y.; Levenston, M. E. Regional Variations in the Distribution and Colocalization of Extracellular Matrix Proteins in the Juvenile Bovine Meniscus. *J. Anat.* 2012, *221* (2), 174–186.

(41) McNulty, A. L.; Guilak, F. Mechanobiology of the Meniscus. *J. Biomech.* 2015, *48* (8), 1469–1478.

(42) V Thomas, L.; VG, R.; D Nair, P. Effect of Stiffness of Chitosan-Hyaluronic Acid Dialdehyde Hydrogels on the Viability and Growth of Encapsulated Chondrocytes. *Int. J. Biol. Macromol.* 2017, *104*, 1925–1935.

(43) Slyker, L.; Diamantides, N.; Kim, J.; Bonassar, L. J. Mechanical Performance of Collagen Gels Is Dependent on Purity, A1/A2 Ratio, and Telopeptides. *J. Biomed. Mater. Res. - Part A* 2022, *110* (1), 11–20.

(44) Hattori, S.; Adachi, E.; Ebihara, T.; Shirai, T.; Someki, I.; Irie, S. Alkali-Treated Collagen Retained the Triple Helical Conformation and the Ligand Activity for the Cell Adhesion via A2β1 Integrin. *J. Biochem.* 1999, *125*, 676–684.

(45) Amis, E. J.; Carriere, C. J.; Ferry, J. D.; Veis, A. Effect of PH on Collagen Flexibility Determined from Dilute Solution Viscoelastic Measurements. *Int. J. Biol. Macromol.* 1985, *7* (3), 130–134.

(46) Chang, S. C. N.; Rowley, J. A.; Tobias, G.; Genes, N. G.; Roy, A. K.; Mooney, D. J.; Vacanti, C. A.; Bonassar, L. J. Injection Molding of Chondrocyte/Alginate Constructs in the Shape of Facial Implants. *J. Biomed. Mater. Res.* 2001, *55* (4), 503–511.

(47) McCorry, M. C.; Puetzer, J. L.; Bonassar, L. J. Characterization of Mesenchymal Stem Cells and Fibrochondrocytes in Three-Dimensional Co-Culture: Analysis of Cell Shape, Matrix Production, and Mechanical Performance. *Stem Cell Res. Ther.* 2016, *7* (1), 1–10.

CHAPTER 5

Conclusions and Future Directions

Conclusions

The objective of this dissertation was to investigate strategies using biochemical and biomechanical stimuli to enhance biochemical, structural, and mechanical properties of tissue-engineered menisci and entheses. The ultimate goal of this work is to generate a full-scale, functional meniscal replacement that can be used after meniscectomy instead of allografts. To achieve this goal, there still exist several challenges to overcome although the field of tissue engineering menisci has shown great advancements. A major persistent challenge faced by most tissue engineering fields is enhancing mechanical properties of tissue-engineered constructs. Native menisci and meniscal entheses display the complexity of composition and structure including cell phenotypes, extracellular matrix molecules, collagen fiber structure, and mineral gradients, resulting in their unique mechanical functions. As such, recapitulating the complexity of native tissue in tissue-engineered menisci and entheses will create a native tissue-like functional replacement.

The complexity of native tissue is attributed to diverse interactions between cells, surrounding environments, and external stimuli, implying that a comprehensive understanding of these interactions will help generate fully functional tissue-engineered constructs. In order to recapitulate native tissue-like collagen fiber structure with physiological functions, this work employed biochemical stimuli (i.e., glucose and TGF-β1) and mechanical stimuli (i.e., mechanical anchoring). The effects of these stimuli have been investigated individually[1–4]; however, the combined effects of these

stimuli have not yet been studied. Given the complexity of native tissue and the interplay of biochemical and biomechanical cues during the development of native tissue, it is very important to understand the combined effects of these stimuli on biochemical, structural, and mechanical properties of tissue-engineered constructs. Furthermore, unlike synthetic polymers whose mechanical properties tend to become weaker over time in culture or upon implantation, mechanical properties of natural polymers, such as collagen, can be enhanced by cell-mediated remodeling due to their cell-binding sites[5,6]. Therefore, tuning appropriate conditions for cells to remodel collagen structure would be beneficial for various tissue-engineering fields using collagen-based scaffolds.

In Chapter 2, the effects of glucose and TGF-β1 in the absence and presence of mechanical stimuli on tissue-engineered menisci were investigated. Previous studies in cartilage and meniscus tissue engineering have mostly focused on maximizing extracellular matrix production using relatively high concentrations of glucose and TGF-β1[7,8]. In contrast, we aimed to enhance collagen fiber structure by optimizing concentrations of glucose and TGF-β1 resulting in balanced ECM production and cell-mediated remodeling for improved mechanical properties of tissue-engineered menisci. Compared to the traditionally used concentrations of glucose and TGF-β1, relatively lower concentrations of glucose and TGF-β1 resulted in robust, aligned collagen fiber structure, similar to native collagen fiber structure. Additionally, this phenomenon was further enhanced via mechanical anchoring. Notably, the tensile mechanical properties were strongly correlated with collagen fiber alignment, diameter, and length, indicating the importance of mimicking native tissue-like collagen fiber structure. The data in Chapter 2 suggest that enhancing mechanical properties of collagen-based constructs

cannot be achieved by utilizing a single factor but involving the interplay of various factors. These findings point to the optimization of both biochemical and biomechanical signals in the culture environment for tissue-engineered constructs should be taken into consideration.

In Chapter 3, we expanded our findings from Chapter 2 to recapitulate native enthesis collagen fiber structure. It is well-known that the interface between the soft tissue-to-bone region of native entheses contains densely interconnected collagen fibers and that the soft tissue region has nicely aligned, large collagen fibers[9]. Furthermore, the characteristic collagen fiber structure of native entheses plays a role in their mechanical functions. We know from Chapter 2 that relatively high concentrations of glucose and TGF-β1 results in dense, interconnected collagen fiber structure while relatively low concentrations of glucose and TGF-β1 lead to thicker, aligned collagen fiber structure. Therefore, we investigated the application of these two different media to corresponding regions using a tri-chamber bioreactor to recapitulate native enthesis-like collagen fiber structure. The data presented in Chapter 3 and Appendix show that we can specifically deliver two different types of media to each region of the enthesis construct using a tri-chamber bioreactor. This bioreactor also provides constructs with mechanical stimuli by anchoring the bony regions of the constructs mimicking native mechanical boundary conditions. These region-specific biochemical and mechanical stimuli resulted in native enthesis-like collagen fiber structure and mechanics, particularly less concentrated strain peak and smooth local strain distributions. These enhancements were further improved using partially demineralized bone plugs mimicking native mineral gradients, leading to smoother local strain distributions and

enhanced toughness. These findings highlight the importance of spatially controlled biochemical and biomechanical stimuli to mimic native tissue-like structure and mechanics.

In Chapter 4, the short- and long-term effects of gelation pH were investigated. Collagen-based hydrogels have gained a lot of attention due to their excellent biocompatibility. Their structure and mechanical properties can be remodeled and enhanced by cells. Moreover, it has been shown that collagen hydrogel mechanics can be modulated by collagen gelation factors, such as collagen concentration[10], temperature[11], ionic strength[12], and pH[13]. Previous studies on the gelation pH have shown that the gelation pH affects kinetics of fibrillogenesis and consequently mechanical properties of collagen hydrogels[14–16]. However, these studies investigated the short-term changes in fibrillogenesis and mechanical properties of relatively low concentrations of collagen gels. Therefore, the long-term effects of the gelation pH on tissue-engineered menisci were evaluated. High cell viability of fibrochondrocytes was observed in constructs gelled at pH ranging from 7.0 to 8.5. While slightly basic gelation pH showed greater mechanical properties at day 0, after 30 days of culture, physiologic pH 7.5 showed the greatest mechanical properties in addition to native tissue-like collagen fiber structure. The findings in Chapter 4 suggest that gelation pH is a simple, useful means to regulate biochemical and biomechanical properties of collagen-based scaffolds given that tuning the gelation pH can be simply achieved adjusting the amount of NaOH in gelation solution without adding additional steps.

Future Directions

The work presented in this dissertation investigated the combined effects of biochemical stimuli (i.e. glucose and TGF-β1) and gelation pH in combination with static mechanical stimuli on biological, structural, and mechanical properties of tissue-engineered menisci and entheses, respectively. Given that native tissues are developed over a long period of time with diverse types of interactions between cells and growth factors, this work can be further expanded with these complex interactions to create a fully functional tissue-engineered construct.

Incorporation of Stem Cells. One of the major concerns in the tissue engineering field is to find appropriate cell sources. Therefore, various cell sources have been investigated. Autologous cells, including fibrochondrocytes[17] and chondrocytes[18], produce sufficient glycosaminoglycans. However, requiring two surgical interventions and dedifferentiation of autologous cells during expansion has limited their potential as a cell source. Furthermore, obtaining enough cells for a tissue-engineered construct from autologous cell sources is unlikely to be possible due to their limited proliferative capacity.

Due to these limitations of autologous cell sources, stem cells have been considered as a promising cell source since they actively proliferate and differentiate into diverse terminally differentiated cells and show immunoregulatory effects which can facilitate the healing process[19]. Mesenchymal stem cells can be obtained from bone marrow, adipose tissue, synovium, and even urine[20]. As such, mesenchymal stem cells are attractive cell sources in tissue engineering menisci and entheses.

There are several questions that need to be addressed before utilizing

mesenchymal stem cells to create a tissue-engineered construct. First, the mechanism of fibrochondrogenic differentiation of mesenchymal stem cells should be investigated. Compared to the chondrogenic and osteogenic differentiation of mesenchymal stem cells, much less is known about fibrochondrogenic differentiation. Our lab has demonstrated that co-culture of mesenchymal stem cells and fibrochondrocytes enhances fibrochondrogenic differentiation of mesenchymal stem cells and reduces hypertrophy by mesenchymal stem cells[21]. Second, mesenchymal stem cells might respond differently to growth factors, and thus optimization of growth factors should be performed. We previously showed that mesenchymal stem cells produce more glycosaminoglycans compared to fibrochondrocytes while fibrochondrocytes produce more aligned collagen fiber structure[22]. Thus, it is important to assess whether the optimal concentrations of glucose and TGF-β1 observed in Chapter 2 result in similar effects on structural and mechanical properties of tissue-engineered menisci when mesenchymal stem cells are employed instead of fibrochondrocytes. Furthermore, additional biochemical and biomechanical stimuli might need to be investigated. If these questions can be answered, mesenchymal stem cells will be outstanding cell sources in tissue engineering menisci and entheses. Native menisci and entheses contain various cell phenotypes which can be obtained utilizing different differentiation mechanisms of mesenchymal stem cells.

Application of Additional Biochemical and Biomechanical Stimuli. A variety of growth factors, such as the TGF-β family, bone morphogenetic proteins (BMPs), basic fibroblast growth factor (bFGF), platelet-derived growth factor (PDGF)-AB, insulin-like growth factor-I (IGF-I), Connective tissue growth factor (CTGF), and

epithelial growth factor (EGF), have been widely used in tissue engineering meniscus to increase fibrochondrocyte proliferation and both collagen and glycosaminoglycan production[23]. The influences of growth factors on fibrochondrocytes depend on culture conditions and cell source regions. Interestingly, growth factors have synergistic effects which can be further enhanced through a combination of other growth factors. These synergistic effects were observed in the combination of TGF-β1 and IGF-1[24] or TGF-β3 and CTGF[25]. In this context, the TGF-β1-mediated enhancement of structural and mechanical properties observed in Chapter 2 and 3 may be further amplified by a combination of other growth factors. It should also be noted that biochemical stimuli should be applied in a spatiotemporal manner in order to achieve a more native tissue-like characteristics. The extracellular matrix components of the outer and inner regions of native meniscus are different, and cells from different regions respond differently to growth factors under same concentrations[19]. Additionally, during the development of native meniscus, the gene expression of modulators of TGF-β1 changes with age. These observations indicate that appropriate growth factors should be applied depending on the regions of tissue-engineered constructs and the stages of development. Future studies should include additional growth factors and evaluate their synergistic effects in a spatiotemporal manner.

In addition to growth factors, various types of mechanical stimuli have been applied to meniscus regeneration and tissue engineering. These stimuli include static and dynamic compressive loading, cyclic hydrostatic pressure, perfusion, or tensile loading. Similar to biochemical stimuli, mechanical stimuli can also have adverse effects if inappropriate loading regimens are applied. This suggests the importance of

optimization of the loading type and regimen. In this dissertation, static compressive loading was applied to tissue-engineered menisci and entheses. Previously, our lab has demonstrated that dynamic compressive loading significantly increases the collagen production and equilibrium modulus, compared to static compression[26]. Moreover, previous studies have shown that mechanical stimuli further increase positive effects of growth factors. Chondrogenic effects of TGF-β3 on mesenchymal stem cells are significantly enhanced in the presence of dynamic compression[27]. Similarly, the enhancement of collagen and glycosaminoglycan production and aggregate and Young's moduli was further increased in combination with TGF-β1 treatement[28], suggesting the synergistic effects of biochemical and biomechanical stimuli. As such, future studies should investigate the effects of dynamic compression or other types of mechanical stimuli on biochemical, structural, and mechanical properties of tissue-engineered constructs in combination with other biochemical stimuli.

Utilization of 3D Printing Techniques. Recapitulating microstructure and macrostructure of native menisci and entheses in tissue-engineered constructs are critical for the clinical application since these structures are closely related to physiologic functions. Native menisci and entheses exhibit zonal variations in cell phenotypes, extracellular matrix components, collagen fiber organization. Fibrochondrocytes harvested from inner zone of the meniscus are more chondrogenic than those from outer zone, supported by the greater production of type II collagen and glycosaminoglycans[29]. This dissertation utilized injection meniscal molds where zonal differences were omitted due to the limitation of the injection molding techniques. These concerns can be addressed using 3D printing techniques. 3D printing techniques

can provide two important approaches: 1) fabrication of scaffolds with native-like heterogeneity and 2) development of bioreactors enabling multiple biochemical and biomechanical stimuli. Furthermore, the findings in this dissertation can be simultaneously employed using the 3D bioprinting techniques, which are likely to be a potential next step of tissue engineering menisci and entheses. Aforementioned zonal differences in cell phenotypes, ECM compositions, and collagen fiber structure could be easily obtained using a bioprinter. For example, a bioprinter equipped with multiple syringes containing fibrochondrocytes from inner or outer zones can generate native tissue-like cell distribution within tissue-engineered menisci, which can be further used as a model to investigate the development of menisci or the effects of diverse growth factors in a zone dependent manner. Moreover, the bioprinter can be used to recapitulate gradients of native collagen fiber structure within meniscal entheses. With multiple syringes of a bioprinter, collagen solution mixed with chondrocyte-like cells at slightly basic pH can be utilized for creating the interface while collagen solution mixed with fibroblast-like cells at physiological pH for the ligamentous region. Additionally, a bioreactor capable of spatiotemporally applying biochemical stimuli (i.e. zone-specific growth factor treatment with multi-chambers) and biomechanical stimuli (i.e. compressive loading for a meniscal body and tensile loading for an enthesis) can be developed using the 3D printing technique. One of the drawbacks traditional bioreactors have is the reliance on simple diffusion of nutrients or growth factors. This drawback can be also addressed by incorporating microspheres containing specific growth factors of interest during the scaffold fabrication stage to avoid the limitation of simple diffusion. This advancement in fabrication of scaffolds and bioreactors might facilitate

clinical translation. It has also been shown that the print path of collagen influences the direction of collagen fiber alignment[30]. This would maximize the effects of biochemical and biomechanical stimuli on collagen fiber alignment and fasten the maturation of tissue-engineered constructs. Furthermore, 3D printing will enable the automation of the entire fabrication process, which is critical for scalable manufacturing of tissue-engineered constructs. Considering the versatility of 3D printing techniques, the use of 3D bioprinter will be imperative in the near future.

Significance

Meniscal injuries affect more than millions of people in the United States annually. Treatment options for meniscal injuries are limited, especially for injuries requiring total meniscectomy. Meniscus allograft transplantation is the only treatment option for total meniscectomy. Therefore, there is a need for the development of tissue-engineered menisci which can replace the entire damaged meniscus, including the enthesis. The work presented in this dissertation demonstrates that optimized biochemical and biomechanical stimuli result in native tissue-like biochemical, structural, and mechanical properties of tissue-engineered menisci and entheses. This dissertation furthers our understanding of meniscus and enthesis tissue engineering regarding biochemical, structural, and mechanical properties and eventually the translation of tissue-engineered menisci and entheses as a full-scale replacement.

References

(1) McCorry, M. C.; Kim, J.; Springer, N. L.; Sandy, J.; Plaas, A.; Bonassar, L. J.

Regulation of Proteoglycan Production by Varying Glucose Concentrations Controls Fiber Formation in Tissue Engineered Menisci. *Acta Biomater.* 2019, *100*, 173–183.

(2) Imler SM; Doshi, A. N.; Levenston, M. E. Effects of Anabolic Cytokines and Static Compression on Meniscus Tissue Explants. *Trans Orthop Res Soc* 2004, *50* (2), 633.

(3) MacBarb, R. F.; Makris, E. A.; Hu, J. C.; Athanasiou, K. A. A Chondroitinase-ABC and TGF-B1 Treatment Regimen for Enhancing the Mechanical Properties of Tissue-Engineered Fibrocartilage. *Acta Biomater.* 2013, *9* (1), 4626–4634.

(4) Hidalgo Perea, S.; Lyons, L. P.; Nishimuta, J. F.; Weinberg, J. B.; McNulty, A. L. Evaluation of Culture Conditions for in Vitro Meniscus Repair Model Systems Using Bone Marrow-Derived Mesenchymal Stem Cells. *Connect. Tissue Res.* 2020, *61* (3–4), 322–337.

(5) Puetzer, J. L.; Koo, E.; Bonassar, L. J. Induction of Fiber Alignment and Mechanical Anisotropy in Tissue Engineered Menisci with Mechanical Anchoring. *J. Biomech.* 2015, *48* (8), 1436–1443.

(6) Iannucci, L. E.; Boys, A. J.; Mccorry, M. C.; Estroff, L. A.; Bonassar, L. J. Cellular and Chemical Gradients to Engineer the Meniscus-to-Bone Insertion. *Adv. Healthc. Mater.* 2018, *1800806*, 1–10.

(7) Freed, L. E.; Marquis, J. C.; Langer, R.; Vunjak-Novakovic, G. Kinetics of Chondrocyte Growth in Cell-polymer Implants. *Biotechnol. Bioeng.* 1994, *43* (7), 597–604.

(8) Ragetly, G. R.; Griffon, D. J.; Lee, H. B.; Fredericks, L. P.; Gordon-Evans, W.;

Chung, Y. S. Effect of Chitosan Scaffold Microstructure on Mesenchymal Stem Cell Chondrogenesis. *Acta Biomater.* 2010, *6* (4), 1430–1436.

(9) Abraham, A. C.; Haut Donahue, T. L. From Meniscus to Bone: A Quantitative Evaluation of Structure and Function of the Human Meniscal Attachments. *Acta Biomater.* 2013, *9* (5), 6322–6329.

(10) Antoine, E. E.; Vlachos, P. P.; Rylander, M. N. Tunable Collagen I Hydrogels for Engineered Physiological Tissue Micro-Environments. *PLoS One* 2015, *10* (3), 1–18.

(11) Cisneros, D. A.; Hung, C.; Franz, C. M.; Muller, D. J. Observing Growth Steps of Collagen Self-Assembly by Time-Lapse High-Resolution Atomic Force Microscopy. *J. Struct. Biol.* 2006, *154* (3), 232–245.

(12) Harris, J. R.; Soliakov, A.; Lewis, R. J. In Vitro Fibrillogenesis of Collagen Type I in Varying Ionic and PH Conditions. *Micron* 2013, *49*, 60–68.

(13) Yan, M.; Li, B.; Zhao, X.; Qin, S. Effect of Concentration, PH and Ionic Strength on the Kinetic Self-Assembly of Acid-Soluble Collagen from Walleye Pollock (Theragra Chalcogramma) Skin. *Food Hydrocoll.* 2012, *29* (1), 199–204.

(14) Achilli, M.; Mantovani, D. Tailoring Mechanical Properties of Collagen-Based Scaffolds for Vascular Tissue Engineering: The Effects of PH, Temperature and Ionic Strength on Gelation. *Polymers (Basel).* 2010, *2* (4), 664–680.

(15) Li, Y.; Asadi, A.; Monroe, M. R.; Douglas, E. P. PH Effects on Collagen Fibrillogenesis in Vitro: Electrostatic Interactions and Phosphate Binding. *Mater. Sci. Eng. C* 2009, *29* (5), 1643–1649.

(16) Noitup, P.; Morrissey, M. T. COLLAGEN : EFFECTS OF COLLAGEN

CONCENTRATIONS , PH. 2005, *30* (2006), 547–555.

(17) Gunja, N. J.; Athanasiou, K. A. Passage and Reversal Effects on Gene Expression of Bovine Meniscal Fibrochondrocytes. *Arthritis Res. Ther.* 2007, *9* (5), 1–12.

(18) Peretti, G. M.; Caruso, E. M.; Randolph, M. A.; Zaleske, D. J. Meniscal Repair Using Engineered Tissue. *J. Orthop. Res.* 2001, *19* (2), 278–285.

(19) Makris, E. A.; Hadidi, P.; Athanasiou, K. A. The Knee Meniscus: Structure-Function, Pathophysiology, Current Repair Techniques, and Prospects for Regeneration. *Biomaterials* 2011, *32* (30), 7411–7431.

(20) Ji, X.; Wang, M.; Chen, F.; Zhou, J. Urine-Derived Stem Cells: The Present and the Future. *Stem Cells Int.* 2017, *2017*.

(21) McCorry, M. C.; Puetzer, J. L.; Bonassar, L. J. Characterization of Mesenchymal Stem Cells and Fibrochondrocytes in Three-Dimensional Co-Culture: Analysis of Cell Shape, Matrix Production, and Mechanical Performance. *Stem Cell Res. Ther.* 2016, *7* (1), 1–10.

(22) McCorry, M. C.; Bonassar, L. J. Fiber Development and Matrix Production in Tissue-Engineered Menisci Using Bovine Mesenchymal Stem Cells and Fibrochondrocytes. *Connect. Tissue Res.* 2017, *58* (3–4), 329–341.

(23) Chen, M.; Guo, W.; Gao, S.; Hao, C.; Shen, S.; Zhang, Z.; Wang, Z.; Wang, Z.; Li, X.; Jing, X.; Zhang, X.; Yuan, Z.; Wang, M.; Zhang, Y.; Peng, J.; Wang, A.; Wang, Y.; Sui, X.; Liu, S.; Guo, Q. Biochemical Stimulus-Based Strategies for Meniscus Tissue Engineering and Regeneration. *Biomed Res. Int.* 2018, *2018*.

(24) Izal, I.; Ripalda, P.; Acosta, C. a; Forriol, F. In Vitro Healing of Avascular Meniscal Injuries with Fresh and Frozen Plugs Treated with TGF-Beta1 and IGF-

1 in Sheep. *Int. J. Clin. Exp. Pathol.* 2008, *1* (5), 426–434.

(25) Lee, C. H.; Rodeo, S. A.; Fortier, L. A.; Lu, C.; Erisken, C.; Mao, J. J. Protein-Releasing Polymeric Scaffolds Induce Fibrochondrocytic Differentiation of Endogenous Cells for Knee Meniscus Regeneration in Sheep. *Sci. Transl. Med.* 2014, *6* (266).

(26) Puetzer, J. L.; Ballyns, J. J.; Bonassar, L. J. The Effect of the Duration of Mechanical Stimulation and Post-Stimulation Culture on the Structure and Properties of Dynamically Compressed Tissue-Engineered Menisci. *Tissue Eng. - Part A* 2012, *18* (13–14), 1365–1375.

(27) Huang, A. H.; Farrell, M. J.; Kim, M.; Mauck, R. L. Long-Term Dynamic Loading Improves the Mechanical Properties of Chondrogenic Mesenchymal Stem Cell-Laden Hydrogels. *Eur. Cells Mater.* 2010, *19* (215), 72–85.

(28) Elder, B. D.; Athanasiou, K. A. Synergistic and Additive Effects of Hydrostatic Pressure and Growth Factors on Tissue Formation. *PLoS One* 2008, *3* (6).

(29) Furumatsu, T.; Kanazawa, T.; Yokoyama, Y.; Abe, N.; Ozaki, T. Inner Meniscus Cells Maintain Higher Chondrogenic Phenotype Compared with Outer Meniscus Cells. *Connect. Tissue Res.* 2011, *52* (6), 459–465.

(30) Moncal, K. K.; Ozbolat, V.; Datta, P.; Heo, D. N.; Ozbolat, I. T. Thermally-Controlled Extrusion-Based Bioprinting of Collagen. *J. Mater. Sci. Mater. Med.* 2019, *30* (5).

APPENDIX A

Diffusion of Biochemical Molecules in a Tri-chamber Bioreactor

Introduction

Bioreactors have been extensively used in the tissue engineering field as they allow for specific biochemical or biomechanical stimuli[1–3]. Since native entheses display gradients in cell phenotypes, biochemical components, and collagen fiber organization, bioreactors are imperative to mimic native enthesis gradients in tissue-engineered enthesis constructs. In order to apply appropriate biochemical stimuli, the diffusion behavior of biochemical molecule within a bioreactor should be addressed.

Reactive Orange 16 belongs to the class of azo dyes and reacts with primary and secondary amine of proteins under alkaline conditions, leading to colorimetric labeling of proteins[4]. Therefore, we conjugated trypsin inhibitor, whose molecular weight is similar to TGF-β1, with Reactive Orange 16 to mimic and investigate the diffusion behavior of TGF-β1 in a simple, cost-effective manner.

Materials and Methods

Trypsin Inhibitor Labeling. 2 mg of trypsin inhibitor (MilliporeSigma, St. Louis, MO) was mixed with 5 mg of Reactive Orange 16 (MilliporeSigma, St. Louis, MO) in 15 mL of HEPES buffer for 24 hours at 4 °C. After the conjugation, the mixture of trypsin inhibitor and Reactive Orange 16 was dialyzed using a Slide-a-Lyzer dialysis cassette (10K MWCO, MilliporeSigma, St. Louis, MO) in 2L of 1X PBS for 24 hours three times.

Conjugation Efficiency. After three rounds of dialysis, conjugation efficiency

was assessed using QuickDrop Spectrophotometer (Molecular Devices, LLC., MA, USA). Known concentrations of trypsin inhibitor and Reactive Orange 16 were used as standards to calculate extinction coefficients at 230 and 494 nm.

Diffusion of TGF-β1 in a Bioreactor. Acellular tissue-engineered enthesis constructs were fabricated and located in a tri-chamber bioreactor. 15 mL of dye solution was applied to the outer chambers of the bioreactor, and 30 mL of PBS was applied to the center chamber of the bioreactor. Then, the bioreactor with constructs was placed in an incubator for 3 days. After 3 days, constructs were removed from the bioreactor and axially cut in half. Cut plane of constructs was imaged and further analyzed using ImageJ software (NIH, Bethesda, MD).

Results and Discussion

First, the conjugation efficiency was measured to evaluate the effectiveness of this labeling method. After 1 day of conjugation and 3 days of dialysis, a 8.5% loss of trypsin inhibitor was detected. Furthermore, the ratio of Reactive Orange 16 to trypsin inhibitor was found to be ~0.6.

Photographs of the bioreactor were taken upon the application of dye solution and 72 hours later. We were not able to see any noticeable leakage as each chamber appeared to maintain their initial colors of each solution, suggesting that different media components were specifically applied to each region and that molecular diffusion likely occurred mainly via bone-to-collagen interfaces (Figure A1 and A2a). Image analysis revealed the sigmoidal shape of dye intensity across the construct, following Fick's 1st law (Figure A2b). These results indicate that we can specifically apply biochemical stimuli and mimic gradients in native enthesis using a tri-chamber bioreactor.

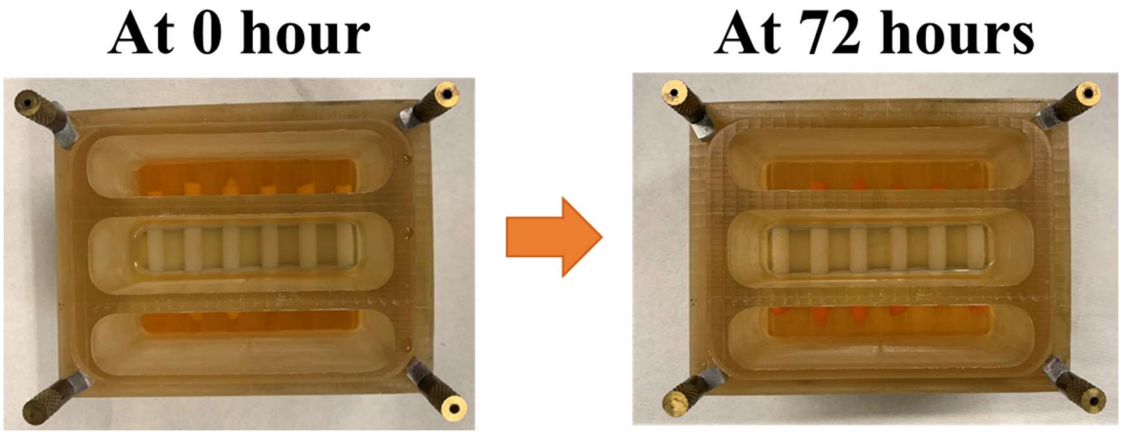

Figure A1. Photographs of a bioreactor upon and 72 hours after the application of dye solution and PBS.

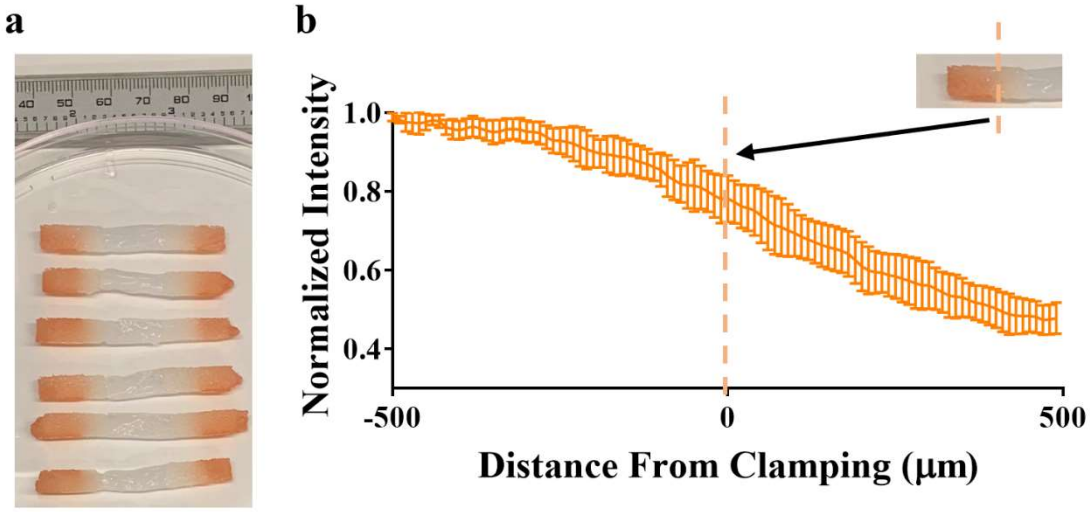

Figure A2. Diffusion of Reactive Orange 16 conjugated trypsin inhibitor across the enthesis construct. (a) Cross-sectional image of enthesis constructs 72 hours after incubation with dye-solution. (b) Quantitative analysis of dye intensity across the constructs.

References

(1) Selden, C.; Fuller, B. Role of Bioreactor Technology in Tissue Engineering for Clinical Use and Therapeutic Target Design. *Bioengineering* 2018, *5* (2), 1–10.

(2) Ahmed, S.; Chauhan, V. M.; Ghaemmaghami, A. M.; Aylott, J. W. New Generation of Bioreactors That Advance Extracellular Matrix Modelling and Tissue Engineering. *Biotechnol. Lett.* 2019, *41* (1), 1–25.

(3) Fu, L.; Li, P.; Li, H.; Gao, C.; Yang, Z.; Zhao, T.; Chen, W.; Liao, Z.; Peng, Y.; Cao, F.; Sui, X.; Liu, S.; Guo, Q. The Application of Bioreactors for Cartilage Tissue Engineering: Advances, Limitations, and Future Perspectives. *Stem Cells Int.* 2021, *2021*.

(4) Compton, M. M.; Lapp, S. A.; Pedemonte, R. Generation of Multicolored, Prestained Molecular Weight Markers for Gel Electrophoresis. *Electrophoresis* 2002, *23* (19), 3262–3265.